Structural and Functional Analysis of Bestrophin

Dissertation zur Erlangung des
Naturwissenschaftlichen Doktorgrades
der Bayerischen Julius-Maximilians-Universität Würzburg

vorgelegt von

Vladimir M. Milenkovic

aus Belgrad

Würzburg, Juli 2006

Eingereicht am: .....

Bei der Fakultät für Biologie

Mitglieder der Promotionskommission

Vorsitzender:

Gutachter: Prof. Dr. Bernhard H.F. Weber

Gutachter: Prof. Dr. R. Benavente

Tag des Promotionskolloquiums: .....

Doktorurkunde ausgehändigt am: .....

Erklärung gemäß §4, Absatz 3 der Promotionsordnung für die Fakultät für Biologie der Universität Würzburg:

Hiermit erkläre ich, dass ich die vorliegende Dissertation selbständig durchgeführt und verfasst habe.
Andere Quellen als die angegebenen Hilfsmittel und Quellen wurden nicht verwendet.
Die Dissertation wurde weder in gleicher noch in ähnlicher Form in einem anderen Prüfungsverfahren vorgelegt.
Es wurde zuvor kein anderer akademischer Grad erworben.

Die vorliegende Arbeit wurde am Institut für Humangenetik der Universität Würzburg unter der Leitung von Prof. Bernhard H.F. Weber angefertigt.

Würzburg, den

“Nothing in biology makes sense except in the light of evolution”

Theodosius Dobzhansky (1900-1975)

Acknowledgements

This study was performed at the Institute of Human Genetics, University of Würzburg. First of all I would like to thank my supervisor Prof. Bernhard Weber for giving me the opportunity to work with a very interesting subject, for his help and support during the course of the thesis.

I am grateful to Prof. Ricardo Benavente for accepting to be a member of the thesis committee and for reviewing this work.

I want to thank Dr. Heidi Stöhr for being always helpful, for interesting discussions and technical tips.

My special thanks goes to the all members of the AG Weber for the friendly atmosphere: Andrea Gehrig, Birgit Geis, Claudia Berger, Nicole Mohr, Jelena Stojic, Heidi Schulz, Franziska Krämer, Andreras Jansen, Barbara Batke, Peter Benz, Florian Rauscher, Johanna Forster, Lars Fritche and many others.

I would also like to extend my special thanks to all at the Institute of Human Genetics in Würzburg: Prof. Höhn, Ilse Neumann, Jörg Schroeder, and especially Birgit Halliger for never ending supply of cakes and chocolates. A big thank you to: Wolfgang "Carlos" for superb sequencing and Indrajit for discussing various scientific topics.

I am very thankful to my family and to my wife Andrea for love, care, and for believing in me.

This thesis is dedicated to my mother and father, with love and thanks for all they have done for me throughout my life.

Table of Contents

I Summary **1**

II Zusammenfassung **3**

III Introduction **6**

1. The retina and the retinal pigment epithelium (RPE) 6
2. Vitelliform macular dystrophy (BMD) 7
3 Clinical description of BMD 7
4. Genetics of BMD 10
5. Aims of the thesis 11

IV Materials and Methods **13**

1. Reagents and chemicals **13**

2. General methods of microbiology **13**

2.1 Bacterial culture and storage 13
2.2 Preparation of electrocompetent E.coli cells 13
2.3 Transformation in E. coli 14

3. Molecular biology techniques **14**

3.1 RNA isolation 14
3.2 First-strand cDNA synthesis 14
3.3 Isolation of plasmid DNA 15
3.4 Restriction Endonuclease Digestion 15
3.5 Polymerase chain reaction (PCR) 15
3.6 Agarose gel electrophoresis 16
3.7 Purification of PCR products 16
3.8 Cloning of PCR products 16
3.8.1 T-overhang cloning 16
3.8.2 Cloning by introducing new restriction sites 16
3.8.3 Selection and screening of recombinant bacterial clones 17
3.9 Ligation reaction 17
3.10 Site-directed mutagenesis 17
3.11 DNA sequencing 18
3.12 Phenol/chlorophorm purification of DNA 18

4. Protein biochemistry **18**

4.1 Preparation of protein extracts 18
4.2 Estimation of protein concentration 19
4.3 Protein expression in bacteria 19
4.3.1 Purification of GST and MBP tagged proteins from bacteria 19

4.4 GST pull down assay 20
4.5 Subcellular fractionation of protein 20
4.6 Sodium dodecyl sulphate polyacrylamide gel electrophoresis (SDS-PAGE) 21
4.7 Immunoblotting 21
4.8 Immunoprecipitation 22
4.9 Staining of PAA gels 22
4.10 Protein precipitation 22
4.10.1 Ammonium sulphate precipitation 22
4.10.2 TCA precipitation 22
4.11 Immunocytochemistry 23

5. Mammalian cell culture 23

5.1 Culturing Conditions 23
5.2 Mammalian cell lines 24
5.2.1 ARPE-19 24
5.2.2 EBNA-293 24
5.2.3 COS-7 24
5.2.4 CHO-K1 24
5.3 Transient transfection 25
5.4 Establishing stable cell lines 25
5.5 Cryopreservation of cells 25

6. In Vitro Transcription/Translation in Reticulocyte Lysate 25

7. Cysteine scanning mutagenesis 26

8. MATCHMAKER Yeast Two-Hybrid System 27

8.1 Yeast Two-Hybrid System 27
8.2 Bait constructs of bestrophin 28
8.3 Construction of a bovine RPE cDNA Y2H library 28
8.4 Lithium-acetate (LiAc) transformation 29
8.5 Isolation of plasmid DNA from yeast 30
8.6 β-galactosidase reporter assay 30
8.6.1 β-galactosidase colony-lift filter assay 30
8.6.2 Semiquantitative β-galactosidase assay using ONPG as a substrate 31
8.7 Yeast protein extracts 31

9. CytoTrap Yeast Two-Hybrid System 31

9.1 Bait constructs 32
9.2 Re-cloning of a bovine RPE cDNA Y2H library 32
9.3 Screening of cDNA library and verification of putative positive clones 33

10. Bioinformatic tools 33

V Results **35**

1. Searching for interacting partners of bestrophin **35**

1.1 MATCHMAKER GAL4 Y2H System 35
1.1.1 Full length and truncated bestrophin baits 36
1.1.2 Construction of a bovine RPE cDNA Y2H library 37
1.1.3 Y2H screen to identify interacting partners of bestrophin 38
1.1.4 Verification of putative positive clones 39

1.2 CytoTrap™ Yeast Two-Hybrid System 42
1.2.1 Truncated bestrophin baits 43
1.2.2 Screening of cDNA library and verification of putative positive clones 44

2. Functional analysis of bestrophin domains **46**

2.1 Bestrophin proteins, orthologous and paralogous 46
2.2 RFP protein family and subfamilies 47
2.3 Identification of conserved motifs 48

3. Topology of normal and mutated bestrophin 50

3.1 Potential transmembrane domains of bestrophin 51
3.2 Leader peptidase as insertion vehicle 52
3.3 SA (signal anchor) potential of individual putative TMDs of bestrophin 54
3.4 SA and ST (stop transfer) function of adjacent bestrophin fragments 55
3.5 SA and ST function of three consecutive TMDs of bestrophin 56
3.6 SA and ST function of COOH-terminally truncated bestrophin fragments 56
3.7 Effect of BMD-related mutations on bestrophin topology 59
3.8 Cysteine scanning mutagenesis 61

VI Discussion **65**

1. Search for interacting partners of bestrophin **65**

1.1 Advantages of GAL4 based Y2H system 65
1.2 Screening of the RPE cDNA library 66
1.3 Limitations of the Y2H system 68

2. Functional analysis of bestrophin domains **68**

2.1 Phylogenetic analysis of the bestrophin family 69
2.2 Bestrophin orthologous and paralogous 69
2.3 Conserved motifs of bestrophin 70

3. Topology of normal and mutant bestrophin **72**

3.1 Putative TMDs of bestrophin 73

3.2 Insertion of individual TMDs of bestrophin in the ER membrane 73
3.3 Insertion of multiple TMDs of bestrophin into the ER membrane 74
3.4 Effect of the BMD mutations on the topology of bestrophin 76

VII References **77**

VIII Appendix **85**

IX Curriculum Vitae **92**

X List of publications **93**

1. Summary

Best disease, also termed vitelliform macular dystrophy type 2, VMD2, (OMIM #153700), is an autosomal dominant, early onset macular dystrophy associated with a remarkable accumulation of lipofuscin-like material within and beneath the retinal pigment epithelium (RPE). The VMD2 gene mutated in Best disease encodes a 585 amino acid putative transmembrane protein named bestrophin, and is preferentially expressed in the RPE. The protein has a complex membrane topology with 4-6 putative transmembrane domains (TMDs) and is presumably involved in Ca^{2+}-dependent transport of chloride ions across the membrane.

The vast majority of known disease-associated alterations are missense mutations non-randomly distributed across the highly conserved N-terminal half of the protein with clusters near the predicted TMDs. The mechanism connecting Best disease pathology with the identified mutations or the Cl^- channel function is not yet clear. To further elucidate the biological function of the bestrophin protein and to identify the molecular mechanisms underlying the disease, a search for interacting partners of bestrophin was performed using the GAL4-based yeast two hybrid system (Y2H). Screening of a bovine RPE cDNA library with various truncated bestrophin baits resulted in the identification of 53 putative interacting partners of bestrophin. However, verification of the interaction has excluded all candidate clones. Our comprehensive Y2H analyses suggest that bestrophin may not be suitable for traditional yeast two hybrid screens likely due to the fact that the protein is integral to the membrane and even fragments thereof may not be transported to the nucleus which is, however a prerequisite for protein interaction in the yeast system.

Bestrophin belongs to a large family of integral membrane proteins with more than 100 members identified to date originating from evolutionarily diverse organisms such as mammals, insects and worms. The most distinctive feature of the bestrophin family, besides the invariant RFP (arginine-phenylalanine-proline) domain, is an evolutionarily highly conserved N-terminal region. To clarify the phylogenetic relationship among bestrophin homologues and to identify structural and functional motifs conserved across family members, a bioinformatics/phylogenetic study of the conserved N-terminal region was conducted. Phylogenetic analysis of the bestrophin homologues reveals existence of four evolutionary conserved family members in mammals, with high homology to the human VMD2, VMD2-L1 to L3 proteins. The significant level of protein sequence similarity between divergent species suggests that each of the bestrophin family members has a unique,

evolutionarily conserved function and that the divergence of bestrophin into several family members occurred before the divergence of individual mammalian species.

Multiple amino acid sequence alignments of 10 selected orthologous bestrophins revealed conserved motifs that might be important for structure and function of the protein: (i) a conserved glycophorin A-like dimerization motif positioned in the second TMD, (ii) dileucine lysosomal sorting signals and (iii) several putative TMDs. Presumptive TMDs of bestrophin were functionally characterized using various molecular, cell biological and biochemical assays.

Resolving the membrane topology of bestrophin will be of importance to understand the mechanism underlying BMD etiology. In order to examine bestrophin topology and to assess consequences of point mutations on membrane integration, we have investigated its insertion into the endoplasmic reticulum (ER) membrane. One objective of this study was to identify insertion signals of bestrophin and to determine whether interaction with downstream or upstream topogenic signals can affect their ability to insert into the membrane. Comprehensive topological analyses provide evidence for a model of bestrophin with 4 TMDs, and one large cytoplasmatic loop between TMD2 and 5. Accordingly, the relatively hydrophobic segments of putative TMD3 and TMD4 (aa 130-149 and aa 179-201 respectively) are likely located within the cytoplasm.

A considerable number of Best disease-associated mutations are located within the six putative TMDs of bestrophin-1. To elucidate the mechanism by which a single amino acid change may lead to disease, we tested the effect of disease-associated alterations on signal anchor (SA) activity of various truncated constructs of bestrophin. Eighteen mutations located in the putative transmembrane segments or the immediate flanking regions of TMD1 and TMD6 were examined. We found that some mutations involving polar and charged residues significantly diminished the ability of the TMDs to insert into the membrane. These results correlate well with the general finding suggesting that a high proportion of disease-associated mutations which occur in TMDs of membrane proteins are found to involve gain or loss of polar residues. In turn, this may result in decreased folding efficiency and loss of stability of the mutated proteins.

2. Zusammenfassung

Morbus Best (OMIM 153700), auch als vitelliforme Makuladystrophie Typ 2 (VMD2) bezeichnet, ist eine autosomal dominant vererbte Makuladystrophie mit juvenilem Beginn. Die Erkrankung geht einher mit einer Ansammlung von Lipofuscin-ähnlichem Material im sowie unterhalb des retinalen Pigmentepithels (RPE). Das bei Morbus Best mutierte VMD2-Gen kodiert für ein 585 Aminosäuren langes Transmembranprotein, genannt Bestrophin, und wird vorwiegend im RPE exprimiert. Das Protein hat eine komplexe Membrantopologie mit 4-6 putativen Transmembrandomänen (TMD) und ist vermutlich in den Ca^{2+}-abhängigen Transport von Chloridionen durch die Plasmamembran involviert.

Die überwiegende Mehrheit der krankheitsassoziierten Veränderungen bei M. Best Patienten sind Missense-Mutationen, die innerhalb der hochkonservierten N-terminalen Hälfte des Proteins nahe der mutmaßlichen Transmembrandomänen akkumulieren. Der Zusammenhang zwischen Pathologie und identifizierter Mutationen bzw. der Chloridkanal-Funktion von Bestrophin-1 ist noch unklar. Um die biologische Funktion von Bestrohin-1 weiter aufzuklären und die zugrunde liegenden molekularen Mechanismen der BMD besser zu verstehen, wurde mit Hilfe des GAL4-basierenden Hefe-Zwei-Hybridsystems (Y2H) nach interagierenden Partnern von Bestrophin-1 gesucht. Ein Screen in einer bovinen RPE cDNA-Bank mit verschiedenen verkürzten Fragmenten von Bestrophin-1 ergab 53 mögliche interagierende Partner. Allerdings schlossen anschließende Verifikationsexperimente die Kandidatengene aus. Somit deuten die Resultate dieser umfangreichen YH2-Studie daraufhin, dass Bestrophin für das herkömmliche Zwei-Hybrid-System nicht geeignet ist. Zum einen könnte dies daran liegen, dass das Protein ein integraler Bestandteil der Membran ist und zum anderen, dass möglicherweise der Transport der gewählten Bestrophin-Fragmente zum Nukleus nicht stattfindet. Dies gilt jedoch als Grundvoraussetzung für eine Proteininteraktion im Hefe-2-Hybridsystem.

Bestrophin gehört zu einer großen Familie von integralen Membranproteinen, von der bis heute bereits über 100 Mitglieder bei verschiedenen Organismengruppen wie denSäugern, Insekten und Würmern identifiziert werden konnten. Als auffälligste Besonderheit in der Familie der Bestrophine zeigt sich neben einer nicht-variablen RFP-Domäne (Arginin-Phenylalanin-Prolin) eine evolutionär hochkonservierte N-terminale Region. Um die phylogenetische Beziehung der Bestrophine zu untersuchen sowie den Aufbau und die Funktion von konservierten Motiven innerhalb der Familienmitglieder zu identifizieren, wurde diese konservierte N-terminale Region sowohl bioinformatisch wie auch

phylogenetisch weiter untersucht. Die phylogenetische Analyse der Bestrophin Homologen brachte vier evolutionär konservierte Familienmitglieder in Säugern hervor, die jeweils eine starke Homologie zu den Proteinen VMD2, VMD2-L1 bis VMD2-L3 des Menschen zeigen. Die signifikante Ähnlichkeit der Proteinsequenz innerhalb der vier Familienmitglieder lässt die Schlussfolgerungen zu, dass zum einen jedes einzelne Familienmitglied ihre eigene evolutionär konservierte Funktion hat und zum anderen dass die Divergenz des Bestrophins in verschiedene Familienmitglieder zeitlich vor der Divergenz der verschiedenen Säugerspezien erfolgt sein muss.

Mit Hilfe eines multiplen Aminosäure-Sequenzvergleichs von 10 ausgewählten orthologen Bestrophinproteinen konnten mehrere konservierte Motive entdeckt werden, die für die Struktur und Funktion von Bestrophin wichtig sein könnten: (i) Ein in der zweiten Transmembrandomäne liegendes konserviertes Glycophorin A-ähnliches Dimerisationsmotiv, (ii) ein putatives Dileucin Sortingsignale für die Lysosomen und (iii) mehrere putative TMDs. Die hypothetischen TMDs von Bestrophin wurden mit verschiedenen molekularen, zellbiologischen und biochemischen Methoden funktionell weitere charakterisiert.

Die Aufklärung der Membrantopologie von Bestrophin ist für das Verständnis des zugrunde liegenden Mechanismus der Krankheitsentstehung bei Morbus Best von enormer Wichtigkeit. Um die räumliche Struktur und die Auswirkungen von Punktmutationen in den Membraneinbau von Bestrophin aufzuklären, wurde das Integrationspotential des Proteins in die Membran des Endoplasmatischen Retikulums (ER) untersucht. Gegenstand dieser Studie war es, zunächst die entsprechenden Insertionssignale zu identifizieren. Im nachfolgenden Schritt sollte dann bestimmt werden, ob eine Interaktion mit den davor oder danach liegenden topologischen Signalen die Integration in die Membran beeinflussen kann. Die umfassende topologische Analyse dieser Arbeit deutet darauf hin, dass Bestrophin vier Transmembrandomänen und eine große zytoplasmatische Schleife zwischen TMD2 und 5 besitzt. Dementsprechend orientieren sich die hydrophoben Segmente der putativen TMDs3 und 4 (AS 130-149 bzw. AS 179-201) wahrscheinlich zur zytoplasmatischen Seite der Membran.

Eine beträchtliche Anzahl von krankheitsbezogenen Mutationen ist innerhalb der sechs möglichen TMDs lokalisiert. Um zu beleuchten, wie ein Austausch einer einzigen Aminosäure im Protein zur Erkrankung führen könnte, untersuchten wir die Auswirkung von krankheitsbezogenen Veränderungen auf die „Signal Anchor“ (SA)-Aktivität mit Hilfe verschiedener verkürzter Bestrophinkonstrukte. Achtzehn Mutationen, die in den sechs putativen TMDs und den angrenzenden Regionen liegen, wurden untersucht. Es wurden

einige Mutationen entdeckt, die die Polarität bzw. die Ladung der Aminosäurereste veränderten und somit die Fähigkeit der entsprechenden TMDs zur Membranintergration beeinflußten. Diese Ergebnisse korrelieren sehr gut mit bisher veröffentlichen Daten, die davon ausgehen, dass viel der krankheitsbezogenen Mutationen in den TMDs von Membranproteinen die Polarität von Aminosäureresten verändern.. Letztendlich führt dies zu einer verminderten Faltungsfähigkeit und somit zum Stabilitätsverlust des Proteins.

3. Introduction

1. The retina and the retinal pigment epithelium (RPE)

The human eye is a photosensitive, highly complex sensory organ composed of three layers (Fig.1A). The outer layer comprises the sclera and the cornea, the intermediate layer is formed by the choroid including the iris and ciliary body and it contains most of the vasculature of the eye. The neuronal retina represents the inner layer of the eye involved in signal transduction and contains rod and cone photoreceptors. The retina itself is composed of ten histologically identifiable layers (Fig. 1B). The rod photoreceptors which are responsible for peripheral and night vision are distributed throughout the retina, and the cone photoreceptors are predominantly located in the macula. The macula is a small area of about 5-6 mm in diameter in the centre of the retina,

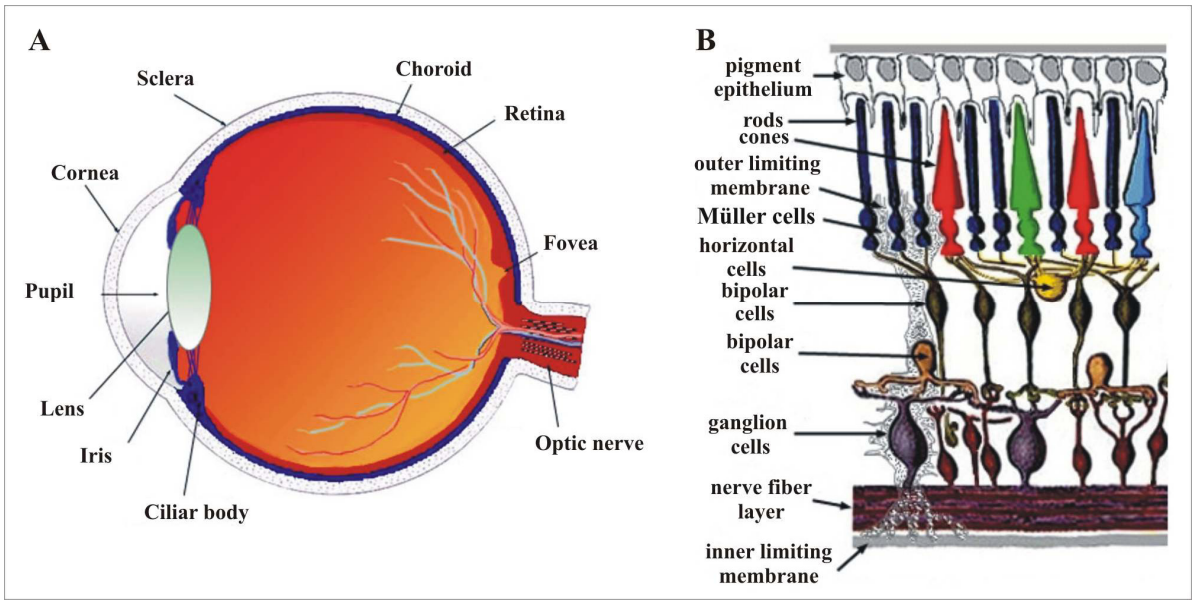

Fig. 1 A cross-section through the human eye A, and schematic representation of the ten layers of the retina B. Figure is taken from http://webvision.med.utah.edu/

with highest concentration of cone photoreceptors, which are responsible for color and visual acuity. The outer segments of the photoreceptor cells are engulfed by the microvilli of the RPE, a single cellular layer that lies between the retina and the choroid that performs various physical and metabolic functions required for the proper function of the retina. The most important functions of the RPE cells are: (i) the phagocytosis of the photoreceptor outer segment membranes, (ii) transport of metabolites, (iii) recycling of the visual pigment, (iv) absorption of excess light by melanin granules, and (v) maintenance of the blood-retinal barrier. A number of different retinal degenerations such as: Stargardt disease, Best disease

and adult-onset vitelliform dystrophy involve the RPE as the primary cellular site of disease origin

2. Vitelliform macular dystrophy (BMD)

Best disease, also termed Best macular dystrophy (BMD) or vitelliform macular dystrophy type 2 (VMD2, OMIM1 #153700), is an autosomal dominant, early onset macular degeneration with reduced penetrance and considerably variable expressivity (Weber et al. 1994a). BMD was first identified in 1905 by the German ophthalmologist Friedrich Best who described a first familial situation (Best, 1905). The disease is associated with striking accumulation of lipofuscin-like material within and underneath the central retinal pigment epithelium (RPE). The disease is characterized by progressive loss of central vision and with variable age of onset and severity. Peripheral vision usually remains unaffected. BMD is a rare disorder with a prevalence estimated to be 2-4 per 10 000 in the Swedish population (Nordstrom, 1974). Best disease is diagnosed by its typical fundus appearance (Fig. 2), an abnormal electrooculogram (EOG) and by a positive family history.

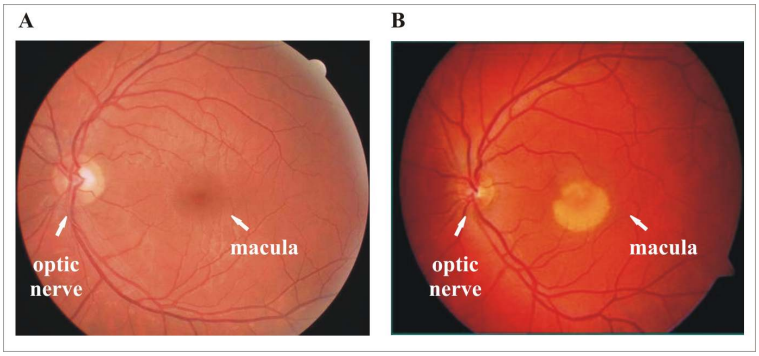

Fig. 2 Fundus photograph of (A) a healthy retina, and (B) of a retina from a patient with BMD, Note the central positioned reddish pigmentated macula in the nonaffected eye on the left. Classic "egg-yolk" appearance is evident in the second (vitelliform) stage of vitelliform macular dystrophy. The 0.5-6 mm diameter yellow or orange lesion results from an accumulation of lipofuscin beneath and within the RPE**.**

3. Clinical description of BMD

Best disease is clinically characterized by typical vitelliform, yellowish yolk-like macular lesions, which are usually bilateral. Multifocal lesions and the lesions outside the macula have also been reported (Godel et al. 1986). The disease is typically diagnosed within the first two decades of life although the prognosis for Best disease patients is extremely variable, ranging from full functional vision in adulthood to central blindness even in young children. Several stages of Best disease progression are known (Deutmann 1971; Mohler and Fine 1981) but not all patients progress beyond the early stages, and some patients may not reveal all consecutive stages. In early disease, a yellowish lipofuscin-containing cyst is formed under the RPE in the area of the fovea. In Best disease, lipofuscin accumulates within

macrophages in the subretinal space, in RPE cells, and between RPE cells and photoreceptors (O´Gorman et al. 1988). Despite the presence of the egg-yolk cyst many patients experience only temporary decline in vision during the vitelliform and pseudohypopyon stages.

Fig.3 Stages of disease progression in BMD

Stage 1 (previtelliform) - At the previtelliform stage, fundus appears normal or with a subtle pigmentation of the RPE. Vision is nonaffected with abnormal EOG.

Stage 2 (vitelliform) - Circular, well-circumscribed, 0.5-5 mm in diameter, yellow cyst is typical for the vitelliform stage. The cyst is usually centered on the fovea and it can be multifocal. Vision is usualy normal or slightly reduced (20/40).

Stage 3 (pseudohypopyon) - In the pseudohyopyon stage cyst is partially reabsorbed. The yellowish material from the lipofuscin containing cyst can break through the RPE and accumulate in the subretinal space. Visual acuity can degrade moderately.

Stage 4 (vitelliruptive) - For the vitelliruptive stage characteristic scrambled egg appearance is due to rupture of the vitelliform lesion. Pigment clumping occurs and early atrophic changes can be observed. Visual acuity is often not affected.

Stage 5 (atrophic) - The yellow material disappears over time, leaving an area of RPE atrophy in the region of the macula which can be difficult to differentiate from other macular degeneration. Subretinal neovascularization may develop, leading to a fibrous scar.

Diagnostic methods to assess BMD pathology

The diagnosis of Best disease is based on a distinct fundus appearance, a characteristic electrooculogram (EOG), family history of BMD and molecular genetic testing. An abnormal EOG which reflects RPE function is the critical diagnostic test for evaluating vitelliform macular dystrophy. In some cases multifocal electroretinogram (ERG), concentrating on macular function was found to be abnormal (Scholl et al. 2002), although full field ERG is relatively normal with a reduced C-wave (Deutmann 1971).

The EOG measures indirectly the potential which is present between the cornea and Bruch's membrane at the back of the eye (Arden et al. 1962). Even though the EOG response originates in the RPE, the light rise of the potential requires both a normal RPE and retinal function. The EOG recording from a healthy and BMD-affected person (Fig. 4) shows the change in voltage in the eye during 15 minutes of dark adaptation and 15 minutes of exposure to bright light. Characteristically the voltage decreases during a dark adaptation (the dark trough) reaching its lowest potential after about 8-12 minutes.

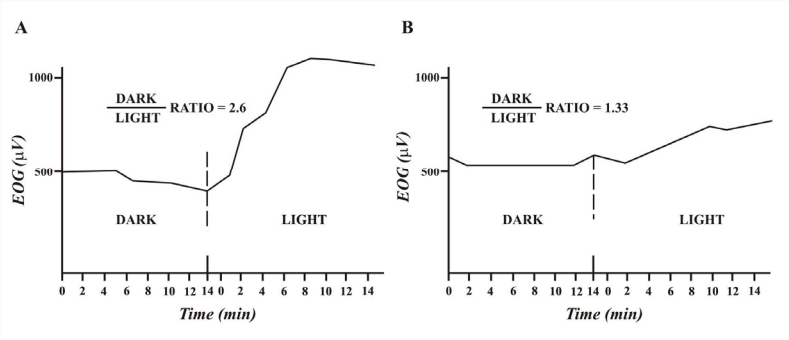

Fig. 4 Electrooculogram (EOG) recording from the healthy A, and BMD affected person, B
The EOG measures indirectly the standing potential that exists between the cornea and Bruch's membrane at the back of the eye. The light/dark (Arden) ratio in the patient with BMD was severely depressed, **B,** as compared with healthy control, **A.**

After switching on the light, potential rises reaching its peak in about 10 minutes (the light peak, LP). A normal light peak/dark trough ratio (Arden ratio) is usually greater then 1.7 (Fig. 4A). In the patients with BMD pathology and in asymptomatic carriers of the mutated VMD2 gene, the EOG is generally abnormal with a reduced light peak/dark trough ratio (Fig. 4B) (Pinckers et al. 1996). No association exists between EOG response and disease stage or visual acuity. The abnormal EOG in BMD is also useful to distinguish clinically BMD from adult vitelliform macular dystrophy (AVMD) which has a similar phenotype to BMD.

4. Genetics of BMD

Originally the locus for BMD was mapped to chromosome 11q13 by genetic linkage analysis (Forsman et al. 1992; Stone et al. 1992). Localization of the disease gene was further refined to the pericentromeric region of chromosome 11, between the microsatelite marker D11S4076 and the uteroglobin gene (Graf et al. 1994; Graf et al. 1997; Hou et al. 1996; Nichols et al. 1994; Stöhr and Weber 1995; Weber et al. 1994b; Weber et al. 1994c). Following the assembly of a primary transcript map (Stöhr et al. 1998), 19 candidate genes were identified within the critical region for the Best disease gene. One of the novel genes cloned in the lab of Dr. Bernhard Weber, subsequently identified as the VMD2 gene, is preferentially expressed in the RPE and was found to be responsible for Best disease (Marquardt et al. 1998, Petrukhin et al. 1998).

The VMD2 gene spans a 14.1 kb of genomic DNA and contains 11 exons. The protein encoded by the VMD2 is designated bestrophin and comprises 585-amino acids with an approximate mass of 68 kDa. Bestrophin belongs to the RFP (arginine-phenylalanine-proline) family (Stöhr et al. 2002, Kramer et al. 2004) which appears to have four closely related members in mammals. According to immunocytochemical studies of macaque and porcine eyes, bestrophin localizes to the basolateral plasma membrane of the RPE (Marmorstein et al. 2000), suggesting that bestrophin may be responsible for the EOG alterations in BMD.

Whole cell patch clamp experiments of bestrophin and its paralogous family members after heterologous expression in cultured mammalian cells suggests involvement of bestrophin in Ca^{+2}- dependant transport of chloride ions across the basolateral membrane of the RPE (Sun et al. 2002, Tsunenari et al. 2003, Qu et al. 2003, Qu and Hartzell 2004, Qu et al. 2004, Fischmeister and Hartzell 2005).

To date 94 distinct mutations are identified in the VMD2 gene (VMD2 Mutation Database at http://www.uni-wuerzburg.de/humangenetics/vmd2.html). The vast majority of the known disease-associated alterationas are missense mutations located in four clusters near the predicted transmembrane domains (TMDs). Mutations in the VMD2 gene are additionally associated with two other retinal diseases: adult onset vitelliform macular dystrophy (AVMD, OMIM #608161) and autosomal dominant vitreo-retino-choroidopathy (ADVIRC, OMIM #193220). All diseases caused by mutations in the VMD2 gene exhibit a dominant pattern of inheritance.

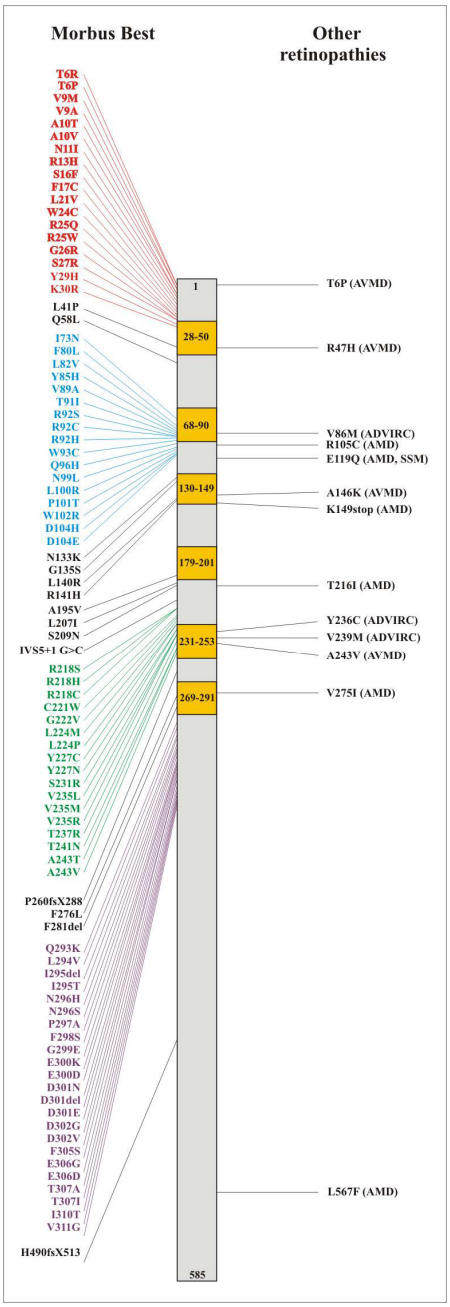

Fig. 5 Position of the mutations found in the VMD2 gene

Six predicted TMD´s and mutational hotspots are color coded. AVMD: adult onset vitelliform macular dystrophy, ADVIRC: autosomal dominant vitreo-retino-choroidopathy, AMD: age-related macular degeneration, SSM: superficial spreading melanoma

From the 94 mutations identified in the VMD2 gene, 88 are missense mutations, three are in frame deletion of a single amino acid, two are frameshift mutations and one disease associated alteration is splice site mutation. Mutations are found in four clusters near the predicted TMD´s indicating functional importance of these regions. Some amino acid residues have been affected by three different amino acid substitutions. Dominant pattern of inheritance and overabundance of missense mutations suggests that disease mechanism appears to be dominant negative rather then haploinsufficiency.

5. Aims of the thesis

The main objective of the present thesis was to functionally and structurally characterize bestrophin. Toward this goal a search for interacting protein partners of bestrophin was performed using the GAL4-based yeast two hybrid (Y2H) system. Identification of the potential interacting partners will lead to a better understanding of the function of the bestrophin.

Bestrophin is highly homologous to more then 100 members of the RFP (arginine-phenylalanine-proline) protein family identified to date from evolutionary diverse organisms. A comprehensive bionformatic/phylogenetic study of the bestrophin family was performed

with the purpose to clarify their phylogenetic origin but also to identify conserved regions and motifs likely suggesting common functional properties.

Another project was focused on clarifying the topology of bestrophin. Insertion of the bestrophin into the endoplasmic reticulum (ER) membranes was examined using the in vitro translation of various truncated bestrophin constructs in the presence of dog pancreas microsomes. In particular, the aim was to identify and verify insertion signals in the bestrophin peptide sequence, and to examine their ability to insert into the membrane. To elucidate the mechanism by which disease-associated single amino acid changes may lead to disease, effects of the point mutations on bestrophin membrane topology was investigated in a cell free in vitro translation/translocation system.

4. Materials and Methods

1. Reagents and Chemicals

All routinely used chemicals were of the highest grade available and, unless otherwise specified, were purchased from Sigma-Aldrich (Taufkirchen, Germany), Merck (Darmstadt, Germany) and Invitrogen (Karlsruhe, Germany). Restriction enzymes were mostly purchased from New England Biolabs (Frankfurt am Main, Germany). Radioisotopes were supplied by Amersham Biosciences (Freiburg, Germany). Buffers and solutions were prepared in double deionized water (ddH_2O) and sterilized by autoclaving or filtering, as described in Sambrook et al. (1989).

2. General methods of microbiology

2.1 Bacterial culture and storage

DH10B, DH5α (Invitrogen, Karlsruhe, Germany), JM110 and BL21-CodonPlus(DE3)-RIL *E. coli* strains (Stratagene, Heidelberg, Germany) were cultured in Luria Bertani (LB) medium (10 g tryptone, 5 g yeast extract, 5 g NaCl and 2g $MgSO_4$ per liter), with appropriate selection antibiotics at 37^{o}C using vigorous shaking (200-250 rpm). For long-term storage of recombinant clones, overnight cultures were combined with glycerol at a final concentration of 15% (v/v) and stored at -80^{o}C.

2.2 Preparation of electrocompetent *E.coli* cells

One single colony of *E. coli* was streaked out from a glycerol stock onto a LB plate with appropriate antibiotics and incubated overnight at 37^{o}C. Following overnight incubation, a single colony was picked and inoculated into 10 ml of LB which was again incubated overnight. On the third day, a log phase culture was obtained by inoculating 10 ml of the overnight culture into 400 ml of LB medium and incubating it at 37^{o}C in an orbital shaker. When OD_{600} reached 0.5-.07 the bacterial culture was cooled on ice for 15 minutes and kept cold from this time on. The bacteria were collected by centrifugation at 2600 x g and washed 3 times with 150 ml ice-cold 10% (v/v) glycerol. The bacteria were resuspended in 2 ml 10% glycerol and 50 µl aliquots were snap frozen using a dry-ice/alcohol bath and stored at -80^{o}C.

2.3 Transformation in *E. coli*

Approximately 20-50 ng of ligation products or 5-20 ng of plasmid DNA were added to 50 µl of electrocompetent *E. coli* cells and the cell mixture was transferred to a pre-chilled electroporation cuvette (BioRad, München, Germany). After a brief incubation on ice, the cells were exposed to a voltage of 1.8 kV (for cuvettes with 0.1 mm width) using the BioRad Gene Pulser electroporation device (BioRad, München, Germany). Subsequently, cells were transferred to 500 µl of SOC medium (2% tryptone, 0.5% yeast extract, 10 mM NaCl, 10 mM MgCl2, 10 mM MgSO4, 20 mM glucose) and incubated for 45 min at 37^{o}C with shaking (150-200 rpm). After incubation, 100 µl of the transformed bacteria were plated on a LB plates with appropriate antibiotics and incubated overnight at 37^{o}C.

3. Molecular Biology Techniques

3.1 RNA isolation

Total RNA was isolated from cell culture or fresh/frozen tissue using the RNeasy Mini Kit (Qiagen, Hilden, Germany) following the instructions of the manufacturer. Briefly, the frozen tissue was homogenized in the provided highly denaturing guanidine isothiocyanate (GITC)-containing buffer, which immediately inactivates RNases to ensure isolation of intact RNA. 75% ethanol was then added to provide appropriate binding conditions, and the sample was loaded to an RNeasy Mini column where the total RNA bound to the membrane and contaminants were washed away. The RNA was then eluted with 30 µl of RNase free water and stored at -80°C.

3.2 First-strand cDNA synthesis

The synthesis of first strand cDNA was carried out by reverse transcriptase (RT) enzyme SuperscriptII (Invitrogen, Karlsruhe, Germany) in a total volume of 20 µl. In the first step, 1-2µg poly(A)+ RNA were mixed with 10 pmol 3'-RACE AP primer (GGC CAC GCG TCG ACT AGT ACD(T)25(A,G,C), 1µl dNTPs (10mM of dATP, dTTP, dGTP, dCTP) and RNase free water. RNA was denatured at 70°C for 10 min and the mixture was immediately transferred to ice. In the second step, 4µl of 5 X first strand buffer (250mM Tris-HCl, pH 8.3; 30 mM $MgCl_2$; 375mM KCl), 2 µl of 0.1M DTT and 1µl of SuperscriptII (200 U/µl) were added and the reaction is incubated for 50 min at 42^{o}C. After incubation the enzyme was

inactivated by heating to 70^{o}C for 15 min. The quality of synthesized cDNA was subsequently assayed by PCR using the exonic primers of the glyceraldehyde-3-phosphate dehydrogenase (Table 1, Appendix).

3.3 Isolation of plasmid DNA

Plasmid DNA was isolated from bacterial overnight cultures in LB media supplemented with appropriate antibiotics using the commercially available kits which are based on the alkaline lysis method (Sambrook et al.1989). Depending on the amount of plasmid DNA needed, plasmid DNA was obtained from 1-5 ml of saturated *E. coli* culture (NucleoSpin Plasmid kit, Macherey-Nagel, Düren, Germany) or from 25-100 ml (QIAfilter Plasmid Midi/Maxi, Qiagen, Hilden, Germany). Plasmid DNA yield was quantified with NanoDrop spectrophotometer (NanoDrop Technologies, Wilmington, USA) and in addition quality of the purified DNA was analyzed by agarose gel electrophoresis (see Materials and Methods, section 3.6).

3.4 Restriction Endonuclease Digestion

Restriction digestions of DNA were generally performed in a final volume of 50µl, containing 0.2-5 µg of DNA, 5µl of 10 X restriction enzyme buffer, 1µl of restriction enzyme (10-20U) and ddH_2O. The reaction mixture was incubated at the recommended temperature for 1-2 hours. Following incubation, the digestion products were electrophoresed on agarose gels (see Materials and Methods, section 3.6) either to check for completeness of digestion or for gel extraction (see Materials and Methods, section 3.7).

3.5 Polymerase chain reaction (PCR)

Typically a polymerase chain reaction (PCR) would contain 20-50 ng DNA template, 1-1.5 mM $MgCl_2$, 50 mM dNTPs (Peqlab, Erlangen, Germany), 10 pmol of each primer and 0.2 µl Taq polymerase (house made) in a volume of 25 µl in the 1xPCR buffer (50mM KCl, 10 mM Tris-HCl pH 8.3, 0.01% gelatine). DNA fragments were amplified by a three-step PCR. In the first step DNA was denatured by heating reactions to 95^{o}C for 2 min, and in the second step, primers were annealed at approximately 5^{o}C above their melting temperature and finally DNA was elongated at 72^{o}C for 1 min per kilobase of DNA. Generally 30 cycles were completed and obtained PCR products were analyzed by agarose gel electrophoresis. For the

amplification of long PCR products for cloning PfuTurbo and PfuUltra DNA polymerase (Stratagene, Heidelberg, Germany) were used.

3.6 Agarose gel electrophoresis

The separation of nucleic acids by agarose gel electrophoresis was performed using a 0.6-2% agarose/ethidium bromide gel. The used buffer was 1x TBE (89 mM Tris-HCl, 89 mM borate acid, 2 mM Na_2EDTA - pH 8.3). Prior to loading, the DNA was mixed with a 10x gel-loading buffer (0.25% bromophenol blue, 40% sucrose) to an approximate final concentration of 1x. The electrophoresis was done for 20-30 min at 100-160 volts and DNA fragments were visualized on a UV transilluminator and photographed. The size of the DNA fragments was estimated by comparison with the 1 kb Plus DNA Ladder (Invitrogen, Karlsruhe, Germany).

3.7 Purification of PCR products

To directly purify PCR products and to isolate DNA fragments from agarose gels, the NucleoSpin Extract kit (Macherey-Nagel, Düren, Germany) was used, following the instructions of the manufacturer.

3.8 Cloning of PCR products

3.8.1 T-overhang cloning

The fact that many Taq polymerases leave an adenine overhang at the end of replicated molecules was used to clone PCR products into a vector with thymine overhangs. The pGEM-T vector system (Promega, Mannheim, Germany) based on this principle was used according to the manufacturer's instructions. The PCR products amplified with PfuTurbo and PfuUltra DNA polymerase (Stratagene, Heidelberg, Germany), which generate blunt-ended fragments had to be modified by adenine-tailing for cloning into pGEM-T vector. Briefly, 7.8 µl of purified PCR product was incubated with 0.2 µl in-house Taq, 1 µl 2 mM dATP and 1 µl 15 mM $MgCl_2$ at 70^{o}C for 30 min and up to 3 µl of the adenine-tailed PCR product were used for ligation (see Materials and Methods, section 3.9).

3.8.2 Cloning by the introduction of new restriction sites

In this protocol, oligonucleotide primers incorporating new unique restriction sites are used to amplify a region of DNA to be subcloned into a vector containing compatible restriction sites. Usually two different restriction sites are used to ensure directional cloning of the PCR product into the predigested vector. The amplified DNA fragment is purified, subjected to enzymatic digestion at the new restriction sites, and then ligated (see Materials and Methods, section 3.9) into the vector.

3.8.3 Selection and screening of recombinant bacterial clones

Following the transformation of competent E. coli with products of a ligation reaction, bacteria transformed with recombinant plasmid form colonies overnight on the selection plate. From this, well defined colonies were picked and used as a template in a standard PCR with a pair of appropriate primers (Table 1, Appendix) annealing to both sites of the polylinker region of the vector. The positive clones identified were then verified by DNA sequencing (see Materials and Methods, section 3.12).

3.9 Ligation reaction

Ligation reactions were performed in a reaction volume of 10 µl containing vector and insert DNA, 1 µl of 10x ligase buffer (500 mM Tris-pH 7.5, 100 mM MgCl2, 100 mM DTT, 250 µg/ml BSA and 10 mM ATP) and 1 µl of T4 DNA ligase (New England Biolabs, Frankfurt am Main, Germany). The amount of vector and insert DNA used ranges from equimolar concentrations to a molar ratio of 1:10 (vector: insert) depending on the relative size of the insert to the vector DNA. The ligation reaction was incubated at 14^{o}C for 1-2 hours.

3.10 Site-directed mutagenesis

For site directed mutagenesis, the desired mutation was inserted into sense and antisense oligonucleotide primers complementary to the region of interest, with the mutation in the middle of the primer containing an additional 15 bp on either side of the mutation. For amino acid substitutions, the codon from disease related missense mutations was selected as the mutation site. The oligonucleotide primers (Table 2, Appendix), with full length cDNA of human *VMD2* cloned into vector pCDNA3.1 as a template, are extended during temperature cycling by PfuUltra DNA polymerase (Stratagene, Heidelberg, Germany). Incorporation of

the oligonucleotide primers generates a mutated dsDNA containing nicks. Following temperature cycling, the product is treated with Dpn I. The Dpn I endonuclease is specific for methylated and hemy-methylated DNA and is used to digest the parental DNA template. The nicked dsDNA containing the desired mutations is then transformed into DH10B competent cells (Invitrogen, Karlsruhe, Germany) by electroporation. The coding sequence of manipulated *VMD2* was then verified by DNA sequencing (see Materials and Methods, section 3.11).

3.11 DNA sequencing

DNA sequencing was performed with a Beckman CEQ 2000 automated sequencer using the Dye Terminator Cycle Sequencing (DTCS) quick start kit (Beckman Coulter, München, Germany). Prior to the cycle sequencing reaction, PCR products were treated with shrimp alkaline phosphatase (USB, Cleveland, USA) and exonuclease I (USB, Cleveland, USA) to remove ssDNA and unincorporated dNTPs, respectively. After amplifications following the cycling conditions of the manufacturer, the product was purified by ethanol precipitation with 0.1 vol 3 M sodium acetate (pH 4.6) and 2.5 vol 100% ethanol. The sequences were viewed and analyzed using the Chromas software (Technelysium Pty Ltd, Helensvale, Australia).

3.12 Phenol/chlorophorm purification of DNA

To a DNA sample to be purified, an equal volume of phenol:chloroform:isoamyl alcohol (25:24:1) was added and the mixture was vigorously vortexed. After centrifugation for 1 min at 14 000 x g, the top aqueous layer was transferred into fresh tube and 1 volume of chloroform:isoamyl alcohol (24:1) was added to the DNA solution. After mixing and centrifugation, the top layer was again transferred to a fresh tube and the DNA was precipitated by ethanol. This was used as a general method of purifying plasmid DNA from proteins such as restriction endonucleases before subsequent treatments.

4. Protein Biochemistry

4.1 Preparation of protein extracts

Total protein lysate from bacterial and mammalian cells were prepared by resuspending cells in 1x Laemmli sample buffer [62.5 mM Tris-HCl (pH 6.8), 2 % SDS, 10 %

glycerol, 5 % β-mercaptoethanol, 0.001 % bromphenol blue] containing a proteinase inhibitor cocktail, Complete Mini-EDTA-free (Roche, Mainheim, Germany). Soluble and insoluble protein fractions from the transfected mammalian cells were obtained by incubating 1 x 10^7 cells in 1 ml lysis buffer (1 % TX-100, 10 % glycerol, 1 x PBS pH 7.4), with stirring for 30 minutes on ice. After 30 minutes centrifugation at 16 000 x g, 4^{o}C, supernatant resembling soluble fraction was collected and used for subsequent experiments or stored at 4^{o}C.

4.2 Estimation of protein concentration

The protein extracts isolated from bacterial culture, mammalian cells and tissues were quantified using the Bradford Protein Assay (BioRad, München, Germany), according to the manufacturer's instructions. Briefly, protein samples of unknown concentration were incubated with 1x Bradford dye reagent at RT for 5 min, and extinction at 595 nm was measured. Protein concentration was estimated from the standard curve.

4.3 Protein expression in bacteria

For expression of recombinant proteins in E. coli, the open reading frame of the desired gene was cloned into pGEX (Amersham Biosciences, Freiburg, Germany) or pMAL (New England Biolabs, Frankfurt am Main, Germany) expression vectors. Expression of GST (Glutathione-S-Transferase) and MBP (Maltose Binding Protein) recombinant fusion proteins is under the control of the *tac* promoter, which can be induced by the lactose analog, isopropyl b-D thiogalactoside (IPTG). Plasmid constructs were introduced into BL21-CodonPlus(DE3)-RIL *E. coli* strain (Stratagene, Heidelberg, Germany) and bacteria were cultivated in LB medium supplemented with chloramphenicol and ampicillin. Protein overexpression was induced by the addition of IPTG in a final concentration of 0.5 mM. After 4 hours of growth at 30^{o}C under vigorous shaking, bacteria cells were harvested by centrifugation at 6000 x g for 15 min and stored at -20^{o}C.

4.3.1 Purification of GST and MBP tagged proteins from bacteria

Recombinant fusion proteins containing GST and MBP tags, respectively, were purified by affinity chromatography using Glutathione Sepharose 4B (Amersham Biosciences, Freiburg, Germany) and amylose resin beads (New England Biolabs, Frankfurt am Main, Germany), respectively, following the instructions of the manufacturer. Briefly,

cells were lysed by passing through a French Press using a pressure of about 12 000 PSI (SLM Instruments, Rochester, USA), centrifuged and supernatant was applied to the column packed with Glutathione Sepharose 4B beads for GST fusion proteins or with amylose resin for MBP fusion proteins. The column was washed extensively and then eluted with appropriate elution buffer. Elution fractions were collected and the protein quantity and quality were determined by SDS-PAGE and Bradford assay.

4.4 GST pull down

The GST pull-down assay is used to detect interaction of GST-fusion proteins bound to glutathione coupled beads to proteins of interest in a cell lysate. Soluble fraction of the cell lysate prepared in lysis buffer (1 % TX-100, 10 % glycerol, 1 x PBS pH 7.4) from the transiently transfected mammalian cells was incubated with 10 µg of appropriate GST fusion protein, overnight at 4^{o}C with agitation. The following day, 50 µl of glutathione sepharose 50% slurry was added and incubated for 1 hour, at 4^{o}C with agitation. The beads were washed three times in lysis buffer and boiled in Laemmli sample before SDS-PAGE and Western blot analysis.

4.5 Subcellular fractionation of protein

To separate cytoplasmic and nuclear compartments, cells were washed with ice cold PBS, scraped and centrifuged at 1000 x g for 5 min. The cell pellet was resuspended in hypotonic buffer (20 mM Tris-HCl, pH 7.4, 1 mM EDTA, 1 mM DTT, supplemented with complete set of protease inhibitors (Roche, Mainheim, Germany), and incubated on ice for 20 min. Cells were Dounce homogenized and nuclei were pelleted by centrifugation at 1000 x g for 5 min. The supernatant was centrifuged at 100 000 x g for 1 h to obtain the cytoplasmic fraction.

Lysosomes were isolated from non-transfected and transfected EBNA-293 cells. Cells from four 50 cm^2 tissue culture dishes were washed twice with cold PBS and once with cold buffer HB (250 mM sucrose, 3 mM imidazole-HCl, pH 7.4). They were scraped in 3 ml of buffer HB, centrifuged for 5 min at 800 x g, and resuspended in 1.6 ml of buffer HB. The cells were homogenized with a Dounce tissue grinder and nuclei were pelleted by centrifugation at 1000 x g for 10 min. The supernatant was layered on top of a following step gradient (from bottom to top): (i) 2M sucrose in 10 mM triethanolamine, (ii) buffer A (10 mM acetic acid, 250 mM sucrose + 10 mM EDTA, ph 7.2), (iii) Percoll (Amersham Biosciences,

Freiburg, Germany) in buffer A adjusted to density 1.090 g/ml and (iv) Percoll in buffer A with density 1.075 g/ml. The gradient was centrifuged in a Beckman SW 60 Ti rotor (Beckman Coulter, München, Germany) at 42 000 x g for 40 min and stopped without braking. Immediately after collection of the fractions, 25 µl aliquots were assayed for β-hexosaminidase activity by incubation with 0.3 mM methylumbelliferone in acetate buffer (100 mM sodium acetate and 0.1 % Triton X-100) at 37^{o}C for 1 hour in the dark. Trichloroacetic acid was added to a final concentration of 10 % to stop the reactions. Samples were diluted 1:20 with 0.5 M glycine and 0.5 M sodium carbonate buffer and then read at an excitation of 356 nm and emission of 450 nm on a POLARstar OPTIMA plate reader (BMG Labtech, Offenburg, Germany).

4.6 Sodium dodecyl sulphate polyacrylamide gel electrophoresis (SDS-PAGE)

SDS-PAGE was performed on a Hoefer SE 600 gel electrophoresis unit (Amersham Biosciences, Freiburg, Germany). Separating gels contained 7-15 % acrylamide (acrylamide: bisacrylamide 37.5 : 1, Aplichem, Darmstadt, Germany), 375 mM Tris-HCl, pH 8.8, 0.1 % (w/v) SDS. Stacking gels contained 5 % acrylamide, 125 mM Tris-HCl, pH 6.8, 0.1 % (w/v) SDS. Polymerization of the gels were mediated by the addition of 0.07 % (w/v) ammonium persulfate and 0.2 % (v/v) N,N,N´N,N´- tetramethylenediamine (TEMED). Electrophoresis was performed at room temperature (170 volts, 2h) in running buffer [25 mM Tris, 192 mM glycine and 0.1 % (w/v) SDS].

4.7 Immunoblotting

For Western blotting, proteins were transferred to a polyvinylidene fluoride (PVDF) membrane (Millipore, Eschborn, Germany) in a transfer buffer (2.5 mM Tris, 192 mM glycine, 15 % methanol) using semi dry transfer unit PerfectBlue (Peqlab, Erlangen, Germany). The PVDF membranes were blocked for 30 min with 5 % fat free milk/PBS. Primary antibodies diluted in 0.5 % fat free milk/PBS were added to the membranes for 1 h at room temperature. Blots were washed (3 times for 15 min each) in PBS supplemented with 0.05 % (v/v) Tween 20 prior to addition of horseradish peroxidase conjugated anti IgG antibodies (Calbiochem, San Diego, USA). Membranes were washed as before and developed using SuperSignal West Pico Chemiluminescent Substrate (Pierce Biotechnology Inc, Rockford, USA). The membranes were then exposed to X-ray film (Fotochemische Werke, Berlin, Germany).

4.8 Immunoprecipitation

Prior to addition of 1-5 µg of the primary antibody, protein lysates (see Materials and methods, section 4.1) were precleared with protein A/G agarose beads (Sigma-Aldrich, Taufkirchen, Germany). Incubation of the precleared protein lysates with primary antibodies was performed for at least 1 hour or overnight at 4^{o}C with gentle shaking, and the protein-antibody complex was immobilized with addition of 10 µl of 50 % slurry of protein A/G agarose beads for 1 hour at 4^{o}C. The beads were washed three times in lysis buffer (see Materials and Methods, section 4.1), and after the last washing step beads were boiled in 1 x Laemmli sample buffer and analyzed by SDS-PAGE and immunoblotting. The following antibodies were used: rabbit pAB-334, which specifically detects bovine and human VMD2 and mouse mAb anti-Rho-1D4, directed against Rho-tag which was cloned into a modified pCEP4 expression vector (see Table 7, Appendix).

4.9 Staining of PAA gels

The polyacrylamide gels containing proteins were subsequently stained with Coomassie brilliant blue [25 % (v/v) isopropyl alcohol, 10 % (v/v) acetic acid and 0.025 % (w/v) Coomassie brilliant blue R250]. Gels were destained overnight in 30 % (v/v) methanol and 10 % (v/v) acetic acid and air dried for long time storage using cellophane (BioRad, München, Germany).

4.10 Protein precipitation

4.10.1 Ammonium sulphate precipitation

To concentrate protein samples, two volumes of saturated ammonium sulfate were added into reaction containing proteins to be precipitated and incubated on ice for 30 minutes. Precipitated proteins were pelleted, washed with ice-cold 96% ethanol and subsequently resuspended in 1x Laemmli sample buffer, before loading on a gel.

4.10.2 TCA precipitation

To precipitate protein, equal volumes of protein sample and 20% ice cold (trichloroacetic acid) TCA were mixed and incubated on ice for 30 minutes. Precipitated

proteins were centrifuged and washed with ice cold acetone and protein pellet was resuspended in 1x Laemmli sample buffer before loading on a gel.

4.11 Immunocytochemistry

For the immunocytochemical studies, transiently transfected mammalian cells were grown on a sterile glass cover slip. 24-48 hours after the transfection cells were washed with 1 x PBS, and fixed for 30 min at room temperature with 4 % (w/v) para-formaldehyde. After three additional washing steps with 1 x PBS, cells were permeabilized with blocking/permeabilization solution [10 % (v/v) normal goat serum, 0.5 % (v/v) Triton X-100 in 1 x PBS) for 30 min. Cells were then labeled for 1 hour with appropriate primary antibody diluted typically 1:1000 in 2 % normal goat serum, 0.1 % Triton X-100 in 1 x PBS. After three additional washing steps cells were incubated for 1 hour with appropriate Alexa Fluor secondary antibody (Molecular Probes, Leiden, Netherlands). Cellular nuclei were additionally labeled with DAPI (Aplichem, Darmstadt, Germany) at a final concentration of 0.1 µg/ml in 1 x PBS. Cells were mounted in confocal matrix (Micro Tech Lab, Graz, Austria) and examined on an Axioskop 2 (Zeiss, Göttingen, Germany) fluorescence microscope.

5. Mammalian cell culture

5.1 Culturing Conditions

Mammalian cells were grown and maintained according to standard procedures (Freshney, 2000), using sterile equipment and solutions while working in a laminar flow hood. Cells were cultured in cell culture dishes (Greiner, Frickenhausen, Germany) at 37^{o}C/5% CO_2. Cultures were passaged when 80-90% confluency was reached. Trypsin-EDTA (0.05% trypsin, 0.53 mM EDTA, Invitrogen, Karlsruhe, Germany) was used to detach cells from the culture dish. Counting of viable cells in culture was performed on a Fuchs-Rosenthal chamber. Prior to counting, cells were mixed briefly to ensure uniform suspension density. A 1:1 solution of resuspended cells and 0.4% (w/v) trypan blue (Applichem, Darmstadt, Germany) was then loaded onto the assembled Fuchs-Rosenthal chamber and cells were counted using phase-contrast microscopy.

5.2 Mammalian cell lines

5.2.1 ARPE-19

ARPE-19 is a spontaneously-immortalized RPE cell line from the normal eye of a 19 year-old head trauma patient. The cells form stable monolayers and exhibit morphological and functional polarity. They also express the RPE-specific markers CRALBP and RPE 65 (Dunn et al. 1996). Cells were cultured in Dulbecco's Modified Eagle's Medium, DMEM/F12 (1:1) (Sigma-Aldrich, Taufkirchen, Germany) supplemented with 42 mM $NaHCO_3$, 100.000 units/l penicillin and 100 mg/l streptomycin (Invitrogen, Karlsruhe, Germany), and 10% fetal calf serum, FCS (PAN Biotech, Aidenbach, Germany).

5.2.2 EBNA-293

The EBNA-293 cell line was generated by modifications of the parental human embryonic kidney cell line HEK-293 (Young et al. 1988). The cells were cultured in DMEM medium containing L-glutamine, 4500 mg/l glucose and 110 mg/l sodium pyruvate, supplemented with 10% FCS, 100.000 units/l penicillin, 100 mg/l streptomycin and 250 mg/l geneticin (G418 sulphate, Calbiochem, San Diego, USA)

5.2.3 COS-7

The COS-7 cell line is an African green monkey kidney cell line derived from CV-1 simian cells. It is suitable for transfection by vectors requiring expression of SV40 T antigen. COS-7 cells are cultured in DMEM medium supplemented with 10% FCS, 100.000 units/l penicillin and 100 mg/l streptomycin.

5.2.4 CHO-K1

The CHO-K1 cell line was derived as a subclone from the parental CHO cell line established from the excised tissue of adult Chinese hamster ovary (Puck et al. 1958). Unlike the original CHO line, CHO-K1 cells require proline in the medium for growth in culture. Epithelial cells, which grows in a monolayer were cultured in DMEM/F12 (1:1) supplemented with 10% FCS, 100.000 units/l penicillin and 100 mg/l streptomycin.

5.3 Transient transfection

Depending on the cell type and the specific experimental requirements transient transfection of cells was performed according to the calcium phosphate precipitation method (Chen et al. 1987) or with cationic lipid transfection reagent (Transfectin, BioRad, Munchen, Germany).

5.4 Establishing stable cell lines

To generate the stable cell line, EBNA-293 cells were transiently transfected with appropriate constructs. The following day, standard media was replaced with selection media containing 150 μg/ml hygromycin B, which will select for cells that have stably incorporated the plasmid into their genomic DNA. During 1-2 weeks of selection, media with dead cells was carefully changed every day leaving colonies of stable transfected cells behind. Cells with stably integrated plasmid DNA were consequently subcloned and the selected clones were maintained in media with 50 μg/ml hygromycin B.

5.5 Cryopreservation of cells

For long-term storage, cells were concentrated by centrifugation at 1000 x g, and resuspended to 2-5 x 10^6 cells/ml in appropriate freezing medium (DMEM or F-12 containing 20% FCS, and 10% DMSO). Cells were gradually cooled to -80^{o}C using a 1.8 ml Nunc cryo vial, before stored in liquid nitrogen.

6. In Vitro Transcription/Translation in Reticulocyte Lysate

Recombinant constructs were PCR amplified with forward primer containing the T7 promotor sequence (5'-TAATACGACTCACTATAGGGAGACCACC-3') and with the respective gene-specific reverse primers (Table 3, Appendix). In vitro transcription/translation of [S^{35}] methionine labeled proteins from the PCR amplified products was performed in TnT reticulocyte lysate (Promega, Mannheim, Germany) in the presence or absence of canine pancreas microsomes (Promega, Mannheim, Germany) according to the manufacturer's instructions. Translation reactions were carried out at 30^{o}C for 90 min in a final volume of 10 μl. All samples were analyzed by SDS-PAGE using 12.5 or 15% polyacrylamide gels. To confirm identity of glycosylated and unglycosylated bands, translated products were treated with EndoH (New England Biolabs, Frankfurt am Main, Germany). The gels were scanned in

a Typhoon 9200 Phosphorimaging plate scanner and analyzed using the ImageQuant TL software (Amersham Biosciences, Freiburg, Germany). Glycosylation efficiency was calculated as the ratio between the intensity of the glycosylated band and the sum of the glycosylated and non-glycosylated bands. All assays were performed at least three times. Student's t-test was applied to identify statistically significant variation between different constructs. Values of significance were taken as *P<0.05, **P<0.01, and ***P<0.001.

7. Cysteine scanning mutagenesis

For the analysis of bestrophin topology, individual cysteine residues are inserted into each of the predicted extracellular and intracellular loops of human bestrophin, and the orientation with respect to the membrane is evaluated using membrane permeable and membrane impermeable sulfhydryl reagents.

EBNA-293 cells grown in 50 cm^2 tissue culture dishes were transfected with wild type (wt) or mutant hVMD2 constructs (Table 4, Appendix). Thirty-six hours after transfection cells were harvested by incubation with 1 mg/ml trypsin in PBS (140 mM NaCl, 3 mM KCl, 6.5 mM Na_2HPO4, and 1.5 mM KH_2PO4) for 5 min at 37^oC. Cells were scraped from the plate, centrifuged for 5 min at 800 x g and washed with PBS. Cells were then resuspended in 2 ml of PBSCM (PBS buffer containing 0.1 mM $CaCl_2$ and 1 mM $MgCl_2$, pH 7.0) and divided into two equal samples. To the one sample, 30 µl of 17 mM lucifer yellow iodacetamide (LYIA) (Invitrogen, Karlsruhe, Germany) was added, and the sample was incubated for 20 min at room temperature, in the dark with occasional mixing. After that, 10 µl of 20 mM biotin maleimide (Invitrogen, Karlsruhe, Germany) was added to both samples and the samples were incubated with occasional mixing for 15 min at room temperature. Labeling was stopped by the addition of 0.5 ml of 2 % (v/v) 2-mercaptoethanol in DMEM and incubated at room temperature for 10 min. After washing with PBSCM, cells were lysed in lysis buffer (see Materials and Methods, section 4.1), and the bestrophin protein was immunoprecipitated with antibodies pAB334 or mAB1D4. Following SDS-PAGE and transfer to PVDF membrane, biotinylated proteins were detected by incubation of the blot with 10 ml of 1:2500 diluted streptavidin-biotinylated horseradish peroxidase (Amersham Biosciences (Freiburg, Germany). After 1 hour incubation and subsequent washing steps, blots were visualized using SuperSignal West Pico Chemiluminescent Substrate (Pierce Biotechnology Inc, Rockford, USA) and X-ray film (Fotochemische Werke, Berlin, Germany).

8. MATCHMAKER Yeast Two-Hybrid System (Y2H)

8.1 Yeast Two-Hybrid System

The MATCHMAKER Yeast Two-Hybrid System 3 (BD Biosciences Clontech, Heidelberg, Germany) was used in this study. In this system, two different sets of vectors were employed to assess protein-protein interaction. One set of vectors includes the Gal4 DNA-binding domain (DBD), pGBKT7 in which full length and truncated bestrophin constructs were cloned as bait and another set of vectors contain Gal4 DNA-activation domain (AD), pGADT7 which was used for cloning of the bovine RPE cDNA library. Two *S. cerevisiae* strains AH109 and Y187 (Table 1) and additional control vectors (pGBKT7-53, pGADT7-T, pGBKT7-LamC and pCL1) were provided with the system. Yeast AH109 strain

Strain	Genotype	Reporters
AH109	MATa**,** trp1-901, leu2-3, 112, ura3-52, his3-200, gal4Δ, gal80Δ, LYS2 : : $GAL1_{UAS}$-$GAL1_{TATA}$ -HIS3, -$GAL2_{UAS}GAL2_{TATA}$-ADE2, URA3 : : $MEL1_{UAS}$-$MEL1_{TATA}$-lacZ	HIS3, ADE2, MEL1, lacZ
Y187	MATα**,** ura3-52, his3-200, trp1, leu2, ade2-101, trp1-901, leu2-3, 112, gal4Δ, gal80Δ, met^-, URA3 : : $GAL1_{UAS}$-$GAL1_{TATA}$-lacZ	MEL1, lacZ

Table 1 Yeast host strain genotypes used in this study

utilizes two nutritional markers ADE2 and HIS3 to control the stringency of selection: the ADE2 gene reduces the number of false positives, while the HIS3 gene, under the control of the GAL1 promotor, provides sensitive growth selection. Yeast cells were cultured at 30^{o}C in a rich YPD medium or in a synthetic dextrose (SD) medium. YPD is a standard, complex medium composed of 1% yeast extract, 2% tryptone and 2% glucose. SD medium is used for selective growth of yeast auxotrophs. It contains 0.67% yeast nitrogen base without amino acids, 2% glucose, and addition of any necessary auxotrophic supplements. The necessary auxotrophic supplements includes 30 mg/L L-isoleucine, 150 mg/L L-valine, 20 mg/L adenine hemisulfate salt, 20 mg/L arginine HCl, 20 mg/L L-histidine HCl monohydrate, 100 mg/L L-leucine, 30 mg/L lysine HCl, 20 mg/L L-methionine, 50 mg/L L-phenylalanine, 200 mg/L L-threonine, 20 mg/L L-tryptophan, 30 mg/L L-tyrosine, 20 mg/L L-uracil. Any of the above auxotrophic supplements can be omitted to provide a selection media for yeast transformation. The auxotrophic supplements were made in 10 x stocks and added into media prior to autoclaving. To make plates, 2% agar was added to either YPD or SD medium prior

to autoclaving. Yeast cells can be stored for up to four months on plates sealed with parafilm at 4C. For long term storage, yeast cells were grown in appropriate liquid medium (rich or 48 minimal media) at 30^{o}C overnight. 0.7 ml of the culture was added into 0.3 ml of 50% sterile glycerol and then stored at -70^{o}C.

8.2 Bait constructs of bestrophin used in this study

The full length sequence and a series of truncated bovine bestrophin fragments were fused to the GAL4 DNA binding domain (DBD) pGBKT7 vector and used as baits in the Y2H screening (Table 2). Bestrophin fragments were PCR amplified, digested with EcoRI/BamHI and cloned into the appropriate restriction sites of the pGBKT7 vector. All constructs were confirmed by DNA sequencing.

Construct name	aa-aa
GBK-flbVMD2	1-585
GBK-Nter	1-30
GBK-loop	91-234
GBK-Cter1	291-367
GBK-Cter2	291-320
GBK-Cter3	368-584

Table 2 Bestrophin baits used for Y2H screen

8.3 Construction of a bovine RPE cDNA Y2H library

Two bovine RPE suppression subtractive hybridization (SSH) cDNA/GAL4-AD fusion libraries, one oligo(dT) primed and an additional one random primed were available (Schulz et al. 2004). RPE was collected from 30 bovine eye balls after removal of the retinal layer by gently shedding the cells in PBS buffer with a soft brush. PolyA(+) RNA was isolated from bovine RPE, heart and liver with the Oligotex mRNA Mini Kit (Qiagen, Hilden, Germany). cDNA was then synthesized using Superscript II reverse transcriptase (Invitrogen, Karlsruhe, Germany) and with cDNA synthesis (CDS) primer 5`-AAG CAG TGG TAA CAA CGC AGA GTA $CT_{(30)}N_{-1}$ N-3`provided in the SMART PCR cDNA Synthesis Kit (BD Biosciences Clontech, Heidelberg, Germany) or random primer 5`-AGC AGT GGT AAC AAC GCA GAG TAC NNN NNN TGT GG-3`. The cDNA was then subtracted with PCR-

Select cDNA Subtraction Kit (BD Biosciences Clontech, Heidelberg, Germany) and cloned into pGADT7 vector. The libraries were validated and analyzed for complexity and average insert size by PCR amplification using pGADT7 vector sequencing primers.

8.4 LiAc transformation of yeast

Transformation of yeast cells was performed using modified polyethylene glycol/lithium acetate (PEG/LiAc) transformation protocol (Gietz et al, 1992). Transformation of yeast was used for introduction of bait and prey plasmids intended for interaction assays and for transformation of control plasmids. A fresh (1 to 3 week old) colony with 2-3 mm in diameter was scraped into 1 ml of YPDA medium or appropriate SD medium and vortexed vigorously to disperse any clumps. After transfer into a flask containing 50 ml of the appropriate medium, the culture was incubated at 30^{o}C overnight. The following day, sufficient volume of the overnight culture was transferred to a flask containing 100 ml of medium to give OD_{600} up to 0.2. The secondary culture was then incubated at 30^{o}C for further 3-5 h at 200 rpm to an OD_{600} of 0.6 The cells were centrifuged at 1000 x g for 5 min at room temperature, the supernatant was discarded and the cells were washed by resuspending and vortexing in 25-50 ml of sterile TE buffer (10mM Tris-HCl, pH 7.5, 1mM EDTA). The washed cells were combined in one falcon and centrifuged at 1000 x g for 5 min at room temperature and the supernatant was discarded. The cells were then resuspended in 1 ml of freshly prepared sterile TE/LiAc (10mM Tris-HCl, 1mM EDTA, 100 mM LiAc; pH 7.5). 0.1-0.5 µg of the appropriate plasmid DNA, 50 µg of herring testes carrier DNA and 100 µl of the freshly prepared yeast competent cells are mixed in 2.0 ml Eppendorf tubes. 600 µl of freshly made sterile PEG/LiAc [40% (w/v) PEG 4000, 10 mM Tris-HCl, 1 mM EDTA, 100 mM LiAc; pH 7.5] solution was added to each tube and vortexed at high speed for 10 sec. Then the mixture was incubated at 30^{o}C for 30 min with shaking at 200 rpm. After incubation, 70 µl of DMSO was added and mixed by gentle inversion only. The cells were heat shocked for 15 min in a 42^{o}C water bath then chilled on ice for 1-2 min. The supernatant was carefully removed after centrifuging cells at 14 000 x g for 5 sec and the transformed cells were resuspended in 150 µl of TE buffer and 30-50µl of the transformation mixture was plated on an appropriate SD plate. For the library scale transformation amounts of plasmid DNA, buffers and yeast competent cells were scaled up. For the low stringency assay transformed yeast cells were plated on SD/-Trp-Leu plates and subsequently stamped on SD/-His-Ade-Leu-Trp + 5 mM 3AT plates. For the high stringency assay, yeast transformants were plated

directly onto SD/-His-Ade-Leu-Trp + 5 mM 3AT plates. The plates were incubated at 30°C for 3-14 days until colonies form.

8.5 Plasmid isolation from yeast

Putative positive clones were picked from the SD/-His-Ade-Leu-Trp + 5mM 3AT plates and resuspended in 200 µl of lysis buffer (100 mM NaCl, 100 mM Tris-HCl pH8.0, 1 mM EDTA, 0.1 % SDS). The same volume of glass beads, 425-600 µm, (Sigma-Aldrich, Taufkirchen, Germany) was added and vortexed at high speed for 1 min. After addition of equal volume of phenol:chloroform:isoamyl alcohol (25:24:1), the sample was centrifuged at 14.000 g at 4°C for 10 min and supernatant was transferred into a fresh Eppendorf tube. Plasmid DNA was then ethanol precipitated and used to transform E.coli.

8.6 β-galactosidase reporter assay

The expression level of the lacZ reporter gene was measured using two different β-galactosidase assays: the colony-lift filter assay and the semiquantitative β-galactosidase assay using ONPG (o-nitrophenol β-D-galactopyranoside) as a substrate.

8.6.1 β-galactosidase colony-lift filter assay

The β-galactosidase colony-lift filter assay was used primarily to screen the large number of putative positive clones that survived the nutritional selection (Bartel and Fields, 1995). Yeast two-hybrid strain AH109 was transformed simultaneously with different combinations of bait and prey constructs. For each combination, 3 independent clones were resuspended in sterile ddH_2O, spotted onto SD-Leu/-Trp plates and allowed to grow for 3 days. Cells were transferred to a Whatman No.1 filter paper, immersed in liquid nitrogen for 10 seconds to permeabilize cells, and placed on top of another filter which was presoaked with a mixture of 1.8 ml Z-buffer (16.1 g/L Na_2HPO_4 x $7H_2O$, 5.50 g/L NaH_2PO_4 x H_2O, 0.75 g/L KCl and 0.246 g/L MgSO4 x $7H_2O$, pH 7.0) containing 5 µl β-mercaptoethanol and 45 µl of 20 mg/ml X-gal dissolved in N,N-dimethylformamide (DMF). Plates were sealed with parafilm and incubated at 30°C. Color development was monitored during 8 hours of incubation.

8.6.2 Semiquantitative β-galactosidase assay using ONPG as a substrate

The semiquantitative β-galactosidase assay using ONPG (o-nitrophenol β-D-galactopyranoside) as a substrate can be used to verify and quantify β-galactosidase activity in the yeast two-hybrid assay. The yeast cells cotransformed with plasmid DNA from the putative positive clones and the corresponding bait were plated on SD/-Leu-Trp plates and incubated at 30°C until colonies grew to a size of 2-3 mm in diameter. Overnight cultures in appropriate SD selection medium were prepared and incubated 1:5 in YPD medium at 30°C until the cells are in mid-log phase (OD_{600}=0.5-0.8). Cells were placed in triplicate into 1.5 ml Eppendorf tubes and centrifuged at 14.000g for 30 sec. After washing with Z buffer, cells were resuspended in 300 µl of Z buffer and permeabilized by three freeze/thaw cycles in liquid nitrogen. After addition of 700 µl Z buffer with β-mercaptoethanol and 160 µl of ONPG (4mg/ml in Z buffer), time was measured until a yellow color developed. The reaction was stopped with 1M Na_2HCO_3 and the OD_{420} was measured. Activity of the β-galactosidase was calculated from the formula: β-galactosidase activity in Miller Units = [1000 x OD 420] / [V(ml) x T(min) x OD600], where t stand for elapsed time in min and V represents the concentration factor (Miller, 1972).

8.7 Yeast protein extracts

AH109 cells transformed with a two-hybrid construct were grown in 10 ml SD-Trp-Leu liquid media at 30°C overnight, subcultured in fresh SD-Trp-Leu media and allowed to grow at 30°C until a cell density of OD600 = 0.8 was reached. Yeast cells were harvested by centrifugation at 3000x g for 10 minutes at 4°C. Yeast crude cell extract was prepared by resuspending the cell pellet in urea/SDS lysis buffer (1% SDS, 8M Urea, 10mM MOPS, pH 6.8, 10mM EDTA, 0.01% bromophenol blue), with addition of glass beads and vigorous vortexing for 2 min. Probes were incubated for 10 min at 70°C and clarified by centrifugation. Supernatants were subsequently analyzed by SDS-PAGE and immunoblotting (see Materials and Methods, section 4.6).

9. CytoTrap Yeast Two-Hybrid System

The CytoTrap membrane based yeast two-hybrid system (Stratagene, Heidelberg, Germany) was developed to significantly increase the prospect for finding unique protein-protein interactions with integral membrane proteins. The CytoTrap system uses the yeast

S.cerevisiae cdc25H temperature sensitive strain, and two sets of vectors for cloning bait (pSos), and prey (pMyr) constructs. Combination of the control plasmids pMyr-MAFB and pSos-MAFB serves as a positive control and pairwise combination of pMyr-SB with pSos-MAFB as a negative control in the assay.

9.1 Bait constructs used in this study

Truncated fragments of the bovine bestrophin transcript were fused to the hSos gene encoding a guanyl nucleotide exchange factor, and were used as baits in the Y2H screening (Table 3). Bestrophin fragments were PCR amplified, digested with BamHI and cloned into the predigested pSos vector. All constructs were confirmed by DNA sequencing.

Construct name	aa-aa
Sos-Nter	1-30
Sos-loop	91-234
Sos-Cter1	291-367
Sos-Cter2	291-320
Sos-Cter3	368-584

Table 3 Bestrophin bait constructs used for CytoTrap Y2H screen

9.2 Recloning of a bovine RPE cDNA Y2H library

The bovine RPE cDNA library (see Materials and Methods, section 8.3) was recloned into the pMyr vector which is designed for cDNA library construction. The pMyr vector was modified with the oligonucleotide linker shown bellow.

EcoRI SmaI Xho I EagI **SalI**
5´-G/AATTCCCGGGCTCGAGCGGCCG/**TCGAC -3´**

The oligonucleotide linker was designed so that after annealing, the 5´overhangs corresponding to the restriction enzymes EcoRI and SalI will be generated. The annealed oligonucleotide linker was ligated with ExoRI/SalI digested pMyr vector, which was subsequently digested with SmaI/EagI restriction enzymes and ligated with the bovine cDNA RPE library digested with the same combination of restriction enzymes. The ligation reactions were transformed in DH10B competent cells (Invitrogen, Karlsruhe, Germany) and plated on

LB plates containing chloramphenicol. The colonies were scraped from the LB plates and combined. Plasmid DNA was isolated using the maxi-prep kit (Qiagen, Hilden, Germany).

9.3 Screening of cDNA library and verification of putative protein-protein interactions

Prior to the Y2H screen the bestrophin bait constructs were tested for self activation. Bait construct plasmid DNA was cotransformed with empty prey vector pMyr, and/or pMyr-LamC and then plated onto SD/Glucose/–Ura-Leu plates. After 3-4 days incubation at RT they were streaked out on SD/Galactose/–Ura-Leu plates and incubated at 37^{o}C. Only growth of the positive control should be observed after 3-5 days at 37^{o}C.

The bovine RPE/pMyr cDNA library was screened against pSos bait constructs of bestrophin. Double transformants were selected on SD/Glucose/–Ura-Leu plates at RT. After incubation for 3-5 days, colonies were stamped onto SD/Galactose/–Ura-Leu plates and incubated at 37^{o}C for several days. Putative positive clones were verified by plating the yeast colonies onto SD/Glucose/–Ura-Leu plates. After incubation for two days at RT, galactose dependant growth at 37^{o}C was assessed by growing putative positive clones on SD/Galactose/–Ura-Leu plates.

2.10 Bioinformatic tools

Bioinformatic analyses of the nucleotide and protein sequences (Table 5, Appendix) were carried out using a number of bioinformatics tools. DNA and protein sequences were obtained from the public databases, hosted by the National Center of Biotechnology Information - NCBI (http://www.ncbi.nlm.nih.gov/) and unfinished genome projects at the Human Genome Browser at the University of California, Santa Cruz (USCS Genome Browser at http://genome.ucsc.edu/). Various bioinformatic tools and programs were used to analyze DNA and protein sequences (Table 4).

Name	URL	Application
NCBI-BLAST	http://www.ncbi.nlm.nih.gov/blast/	DNA and amino acid sequence homology searches
TOPPRED2	http://bioweb.pasteur.fr/seqanal/interfaces/toppred.html	Topology prediction of membrane proteins
BOXSHADE	http://www.ch.embnet.org/software/BOX_form.html	Shading of multiple-alignment files
NetPhos 2.0	http://www.cbs.dtu.dk/services/NetPhos/	Predictions for serine,

Server		threonine and tyrosine phosphorylation sites
Kyte-Doolittle hydropathy plot	http://occawlonline.pearsoned.com/bookbind/pubbooks/bc_mcampbell_genomics_1/medialib/activities/kd/kyte-doolittle.htm	Hydropathy profiles of protein sequences
TREECON	http://bioinformatics.psb.ugent.be/psb/Userman/treecon_userman.html	A software package for the construction and drawing of evolutionary distance trees
PHYLIP	http://evolution.genetics.washington.edu/phylip.html	Package of programs for inferring phylogenies
EXPASY	http://www.expasy.org/	Analysis of protein sequences
ClustalW	http://www.ebi.ac.uk/clustalw/index.html?	Multiple sequence alignment program for DNA or proteins
Phylodendron	http://iubio.bio.indiana.edu/treeapp/treeprint-form.html	Phylogenetic tree printer
PEPWINDOWALL	http://genopole.toulouse.inra.fr/bioinfo/emboss/pepwindowall.html	Displays protein hydropathy of a set of sequences
Helical wheel	http://cti.itc.virginia.edu/~cmg/Demo/wheel/wheelApp.html	Helical wheel representation of an amino acid sequence
GeneDoc	http://www.psc.edu/biomed/genedoc/	Multiple sequence alignment editor

Table 4 Bioinformatic tools and software used in this study

5. Results

1 Searching for interacting partners of bestrophin

As mentioned previously one important objective of this work was to identify interacting partners of bestrophin and to elucidate the molecular function of the protein. Toward this goal a yeast two hybrid (Y2H) screen of the bovine RPE cDNA library was performed. The Y2H system is a sensitive and powerful technique designed to identify novel, relatively weak and transient protein-protein interactions, which was previously restricted entirely to biochemical assays. The most important advantage of the Y2H is that it allows the identification of putative interacting partners and at the same time the isolation of the encoding genes.

1.1 MATCHMAKER GAL4 Y2H System

To identify proteins interacting with bestrophin, a MATCHMAKER GAL4-based Y2H system was used. The assay is performed in yeast (*S.cerevisiae*) and uses transcription of yeast reporter genes to measure protein interaction. A protein of the interest (bait) is typically expressed as a fusion to a DNA-binding domain (DBD), and the other protein (prey) is expressed as a fusion to the transcription activation domain (AD). If the fusion proteins interact, they activate transcription of the ADE2, HIS3 and lacZ reporter genes (Fig. 7).

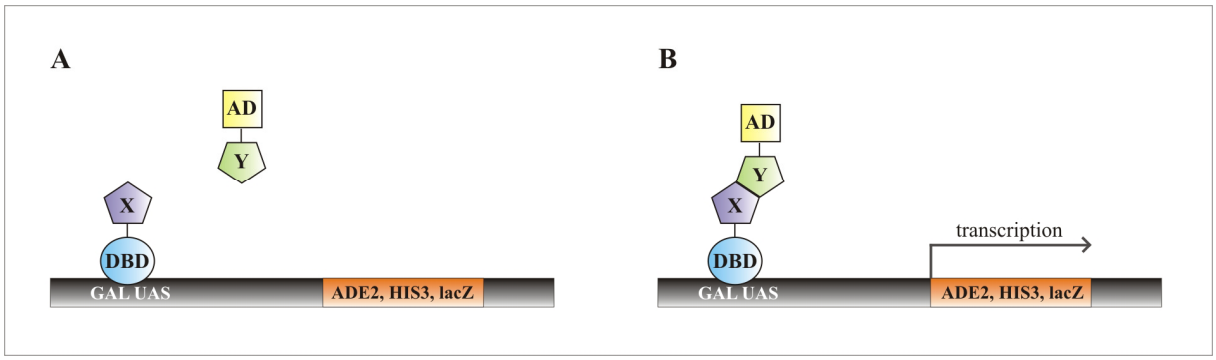

Fig. 7 Principle of the GAL4 Y2H system. A, Two proteins (X and Y) interacting with each other are cloned into pGBKT7 and pGADT7 vectors which contain the DBD and the AD of the yeast GAL4 protein, respectively. **B,** Fusions of the GAL4 DBD with protein X (bait) and the GAL4 AD with protein Y (prey) can reconstitute an active transcription factor if proteins X and Y interact with each other. This transcription factor then activates reporter genes having GAL upstream activating sequence (UAS).

1.1.1 Full length and truncated bestrophin baits

Originally the full length bovine VMD2 transcript was cloned in frame with GAL4 DBD in the pGBK-T7 vector as bait, but initial experiments showed that this construct was a strong activator of reporter genes. Therefore a series of truncated bovine VMD2 fragments fused to the GAL4 DNA binding domain pGBKT7 vector were constructed (Fig. 8).

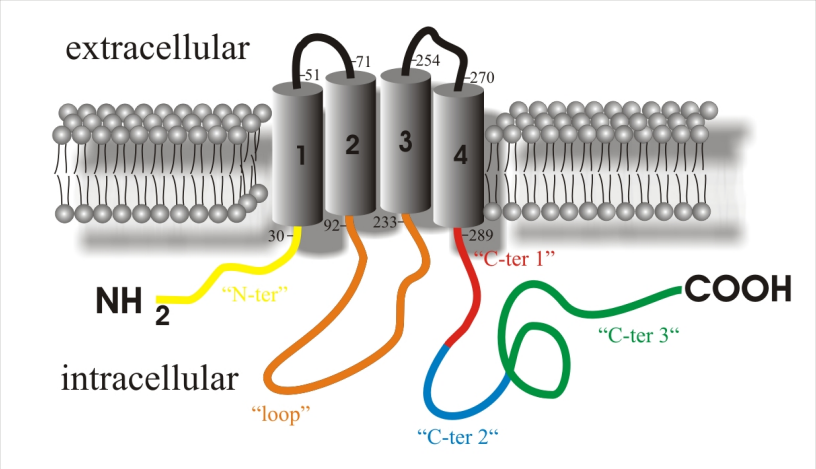

Fig. 8 Bestrophin baits used for Y2H screen.
The suggested model of the bestrophin protein with the four predicted transmembrane regions. Fusion constructs generated for the Y2H screen are shown: yellow (GBK-Nter, 1-30 aa), orange (GBK-loop, 91-234 aa), red-blue (GBK-Cter1, 291-367 aa), red (GBK-Cter2, 291-320 aa) and green (GBK-Cter3, 368-584 aa)

Because in the GAL4-based Y2H system protein-protein interaction takes place in the yeast nucleus, transmembrane domains which could interfere with proper nuclear localization of the fusion proteins, were avoided. Baits were designed to cover the entire protein, with the exception of the transmembrane domains and two short extracellular loops (51-71 aa and 254-270 aa). Before performing the Y2H screens, the yeast (AH109) cells were transformed with GBK-VMD2 fusion constructs and expression of the c-Myc tagged DBD-VMD2 fusion proteins were confirmed by western blot analysis (Fig. 9).

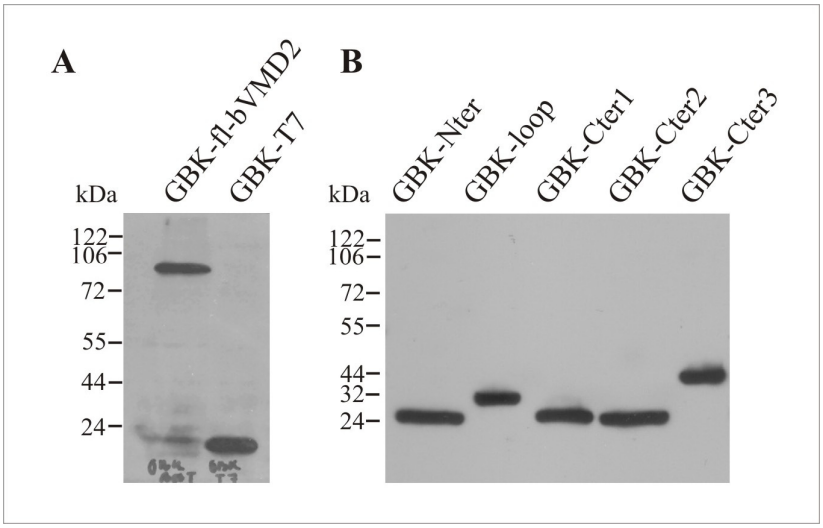

Fig. 9 Verification of bestrophin fusion proteins expression.
Western blot of bestrophin fusion proteins extracted from the yeast and probed with primary anti c-Myc antibody. Blots were visualized with HRP-conjugated secondary antibody after ECL reaction. Fusion proteins of various bestrophin fragments and DBD with their respective size in kDa are shown: **A,** full length bovine bestrophin, 88; DBD alone, 19. **B,** GBK-Nter, 24; GBK-loop, 37; GBK-Cter1, 31; GBK-Cter2, 25; GBK-Cter3, 45.

All baits were additionally tested for self activation, which is defined as ability of fusion proteins to activate transcription of the reporter genes without requiring specific prey protein. Yeast cells transformed with various bestrophin baits were streaked on selective synthetic dextrose medium lacking tryptophan, histidine and adenine (SD/-Trp-His-Ade) and containing 5 mM 3-amino-1,2,4-triazole (3AT). Interestingly, all three bestrophin C-terminal derived baits (Fig. 10 C, D and E) were self activating, and thus not suitable for interaction screening. Only the fusion proteins incapable to activate reporter genes (Fig. 10 A and B) were used in subsequent Y2H screens.

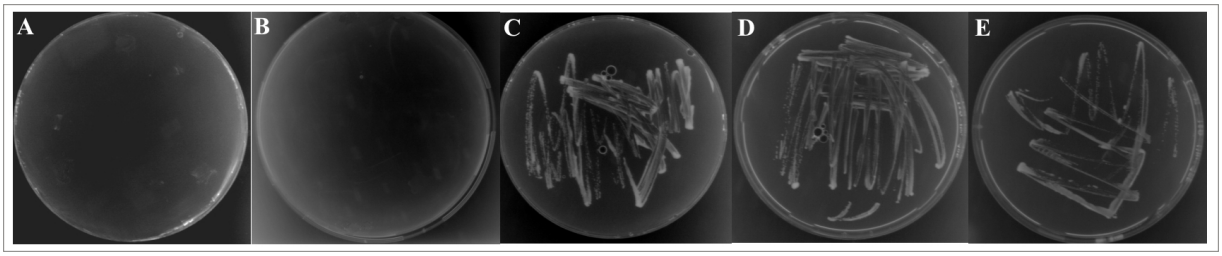

Fig. 10 Verification of bestrophin baits suitability for Y2H assay
Yeast cells of the AH109 strain transformed with the different constructs of bestrophin, were streaked out onto SD/-Trp-His-Ade +5mM 3AT and incubated for 72h at 30°C. Growth of the yeast cells indicates activation of the reporter genes. **A,** GBK-Nter; **B,** GBK-loop; **C,** GBK-Cter1; **D,** GBK-Cter2; **E,** GBK-Cter3.

1.1.2 Construction of a bovine RPE cDNA Y2H library

Since expression of bestrophin is restricted to the RPE, a Y2H library generated from RPE cDNA was used to search for interacting partners of bestrophin. Two bovine subtracted RPE cDNA/GAL4 AD fusion libraries, one oligo(dT) primed and the other randomly primed, were constructed (see Materials and Methods, section 8.3). After preparation, the libraries were validated and analyzed for complexity and average insert size (Table 5).

Library	Complexity	% of clones with insert	Average insert size	% of insert ≥ 1kb
oligo(dT)	6×10^5	95	0.83 kb	30
random primed	6×10^5	95	0.96 kb	35

Table 5 Complexity and average insert size of bovine RPE cDNA libraries

In addition, the validity of the RPE (random and oligo dT primed) libraries was assessed by evaluating tags from genes previously known to be expressed specifically in the RPE (Table 6, Appendix). Libraries were pooled together, transformed into E.coli and fifty randomly selected clones were PCR amplified with AD vector primers and subsequently sequenced. As a result, a high number of genes (11-cis-retinol dehydrogenase, bestrophin,

transthyretin, RPE65, cathepsin D, cystatin C) known to be expressed uniquely or predominantly in the RPE was found.

1.1.3 Y2H screen to identify interacting partners of bestrophin

The plasmids GBK-Nter and GBK-loop containing the truncated fragments of bestrophin fused to the GAL4 DBD were used to screen a bovine RPE cDNA (1:1 random/oligo primed) library. Screening of approximately 2.6 million independent transformants with GBK-Nter as bait resulted in isolation of 47 putative positive clones. Correspondingly, screening of about 1.6 million independent clones with GBK-loop as a bait resulted in isolation of 6 putative interacting partners of bestrophin. These putative positive clones were able to grow on interaction plates (SD/-His-Ade-Leu-Trp) in the presence of 5 mM 3AT, indicating expression of the ADE2 and HIS3 reporter genes were subsequently tested for their ability to activate the β-galactosidase (lacZ) reporter gene. Plasmid DNAs from the clones positive in the β-galactosidase filter assay were isolated and sequenced (Table 6). Sequence analysis and homology searches were performed using the BLASTN program (Altschul et al. 1997).

Table 6 Summary of the putative interacting partners of bestrophin isolated in Y2H screens

Bait	No. of clones screened	No. of positive clones	Name of positive clones, accession No.	No. of times isolated
GBK Nter	2 600 000	47	Transthyretin (TTR), NM 000371	17
			Spermidine/spermine N1-acetyltransferase (SSAT), NM 002970	10
			P-cadherin (CDH3), NM 001793	5
			Bovine retinal pigment (RPE1), M81193	4
			Coatomer protein complex, subunit alpha (COPA), NM 004371	3
			HCLS1 associated protein X-1 (HAX1), NM 006118	2
			Echinoderm microtubule associated protein-like (EMAPL), XM 590509	1
			Solute carrier family 26, member 6 (SLC26A6), NM 134426	1
			Yeast transcriptional activator GAL4, IPR005600	1
			no homology	3
GBK loop	1 560 000	6	Retinol binding protein 5, cellular (RBP5), NM 031491	1
			Bovine retinal pigment (RPE1), M81193	1
			Secreted frizzled-related protein 5 (SFRP5), NM 003015	1
			no homology	3

1.1.4 Verification of putative positive clones

Plasmid DNAs from the putative positive clones identified in the Y2H screens and the bait plasmids were cotransformed into the yeast AH109 strain to confirm the interaction. Semiquantitative β-galactosidase assay using ONPG (o-nitrophenol β-D-galactopyranoside) as a substrate was used to verify and quantify two-hybrid interactions (Fig 11). As expected, the two most frequently isolated putative positive clones (TTR and SSAT) exhibited strongest activation of the lacZ reporter gene which correlates with the strength of the protein-protein interaction.

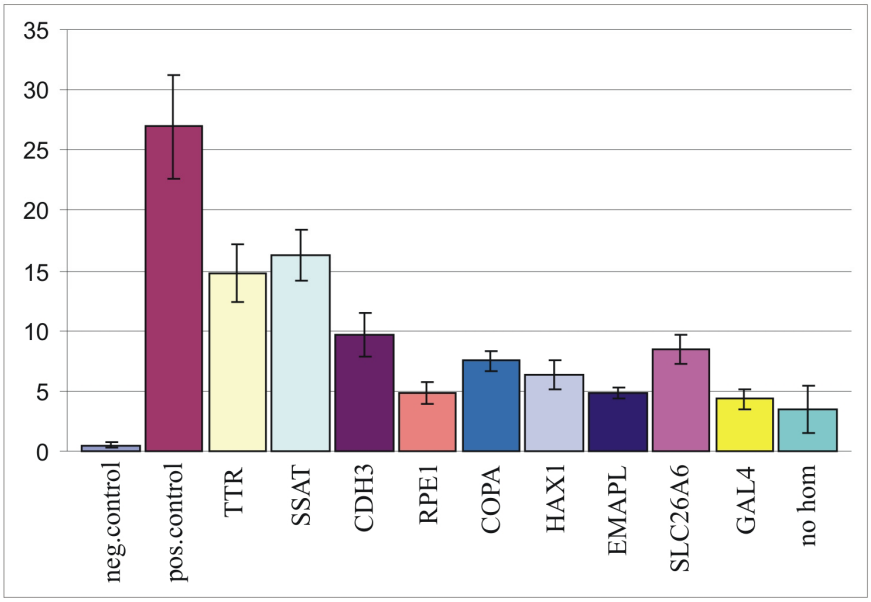

Fig. 11 Semiquantitative β-galactosidase assay using ONPG as a substrate
Putative positive clones were cotransformed with bait plasmid into the yeast cells and grown overnight at 30°C in liquid SD/-Trp-Leu selection medium. Constructs p53+T7T and p53+LamC serve as a positive and negative control, respectively. The β-galactosidase activity is given in Miller units (Miller, 1972).

Further characterization and verification of the putative positive clones included reintroduction of prey plasmids from the positive clones into the yeast cells pretransformed with (i) the empty bait vector (pGBKT7), (ii) with the bait used in initial search (pGBKT7-Nter) and (iii) with a plasmid encoding unrelated protein (pGBKT7-LamC). Transformants were spotted on the interaction plates (SD/-His-Ade-Leu-Trp) in the presence of 5 mM 3AT, and assayed for activation of ADE1 and HIS3 reporter genes (Fig. 12). False positive clones which were able to activate transcription of the reporter genes without the presence of bait vector were eliminated from further studies.

In conclusion, as a result of the Y2H screening and additional verification steps, all putative positive clones except spermidine/spermine N1-acetyltransferase (SSAT) were rejected as false positives because they demonstrated interaction with the GAL4 DBD alone and the irrelevant human lamin C protein in fusion with DBD. Sequencing of the entire insert

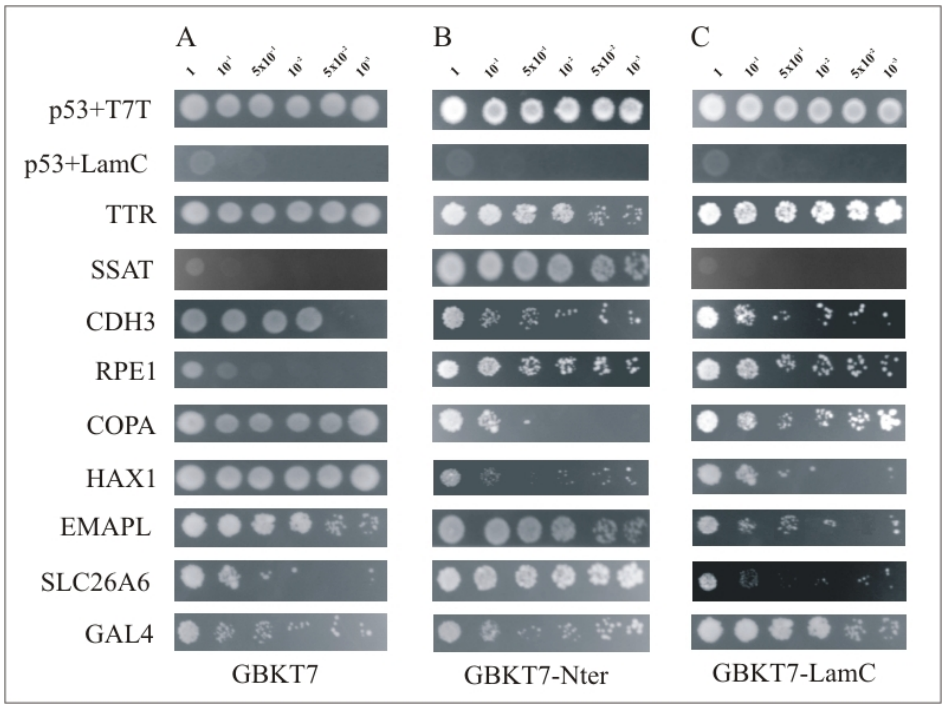

Fig. 12 Yeast two hybrid interaction test on SD/-His-Ade-Leu-Trp +3-AT plates.
All putative positive clones were tested for interaction with **A,** the empty bait vector, pGBKT7, with **B,** the bait used in an initial search pGBK-Nter, and with **C,** lamin C bait vector hybrid (pGBK-LamC). Constructs p53+T7T and p53+LamC serve as a positive and negative control, respectively. The series of dilutions of transformed cells is indicated.

of the bovine SSAT clones revealed that the C-terminal part (121-167 aa) of the protein was responsible for interaction with the N-terminal bestrophin fragment. To independently confirm the interaction between SSAT and bestrophin, a series of immunoprecipitation experiments were performed using the C-terminal portion of SSAT cloned from human RPE cDNA and the wt and mutant human bestrophin constructs transiently expressed in EBNA 293 mammalian cells (Fig. 13 and 14). The GST pull-down assays were carried out with recombinant GST-hSSAT fusion protein expressed in bacteria and Triton X-100 solubilized

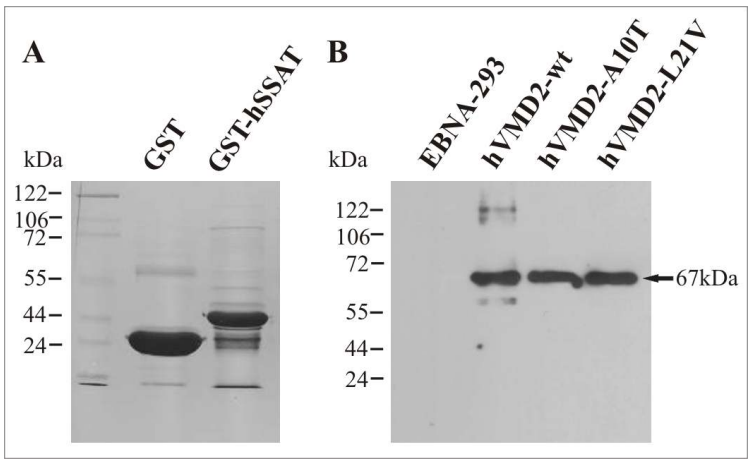

Fig. 13 Expression of recombinant human SSAT and bestrophin constructs
A, Coomassie stained gel showing empty GST and GST-hSSAT fusion proteins expressed in bacteria and purified by affinity chromatography. B, Western blot analysis of the heterologously expressed wt and mutant bestrophin constructs detected with pAb334. Bestrophin was detected in all three transiently transfected EBNA-293 cells at an expected molecular weight of 67 kDa. EBNA-293 cell lysate was used as a negative control.

wt and disease related mutant bestrophin (A10T and L21V) protein extracts. GST protein alone was used as a control, to ensure that SSAT binding was specific to bestrophin. Immunoblot analysis with pAb334 antibody directed against C-terminus of human bestrophin

demonstrates presence of the bestrophin in both the input (5% input) and not bound (NB) fractions (Fig. 14). The amount of the GST and GST-hSSAT fusion proteins used in this assay can be seen on the Ponceau-S stained membranes (Fig. 14, shown as a pink band). Although the quantity of the recombinant proteins were adequate, both GST and GST-hSSAT fusion proteins failed to immunoprecipitate bestrophin from the solution, suggesting lack of interaction between SSAT and bestrophin (Fig. 14, lanes GST-IP and GST-hSSAT-IP).

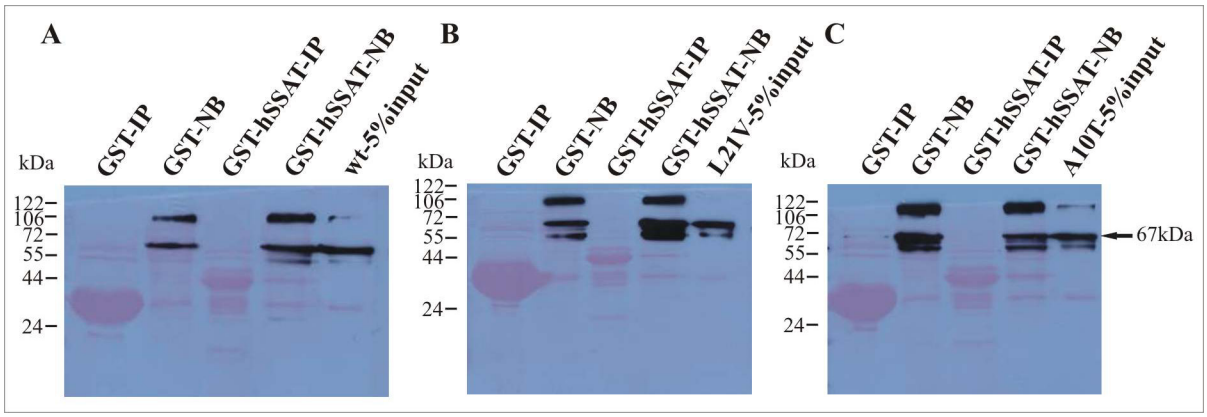

Fig. 14 GST pull-down assay
Immunoblot analysis of the GST pull-down assays using GST-hSSAT fusion protein and full length wt bestrophin A, bestrophin with L21V mutation, B, and bestrophin with A10T mutation, C. Scanned images of the Ponceau-S stained PVDF membranes demonstrating the levels of GST and GST-hSSAT fusion proteins expression were merged with the scanned X-ray films of the immunoblot. 5% of the Triton X-100 solubilized bestrophin was used as an input, GST fusion proteins immobilized on glutathione sepharose beads were designated as IP, and not bound fraction was labeled as NB. GST alone served as a negative control.

Since interactions that are dependent on post-translational modifications that are added within the endoplasmic reticulum, may not occur in the *E.coli* expression system, an hSSAT was expressed in mammalian EBNA-293 cells. Full length hSSAT tagged with Rho-1D4 tag and wt bestrophin constructs were co-transfected into EBNA-293 and expression of bestrophin and hSSAT-Rho-1D4 constructs were assessed with anti-bestrophin

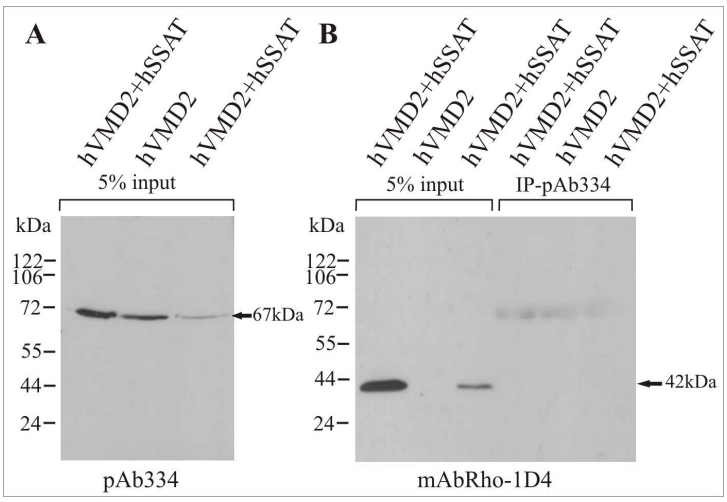

Fig. 15 Co-immunoprecipitation assay between human SSAT and bestrophin co-expressed in EBNA-293 cells
A, Immunoblot of the protein extracts from the EBNA-293 cells transfected with SSAT and bestrophin constructs probed with anti bestrophin antibody indicated a band corresponding to bestrophin at ~67kDa; **B,** same protein extracts were analyzed by antibody against Rho-1D4 tag; **C,** detection of the immunoprecipitated proteins by anti-Rho-1D4 monoclonal antibody

and anti-Rho-1D4 antibodies, respectively (Fig. 15, A, B, lines with 5% input). Immunoprecipitation was performed with anti-bestrophin antibody (pAb334), followed by immunoblot analysis with the anti-Rho-1D4 monoclonal antibody. Inability of bestrophin to immunoprecipitate SSAT despite ample expression levels of both proteins demonstrates lack of interaction between bestrophin and SSAT (Fig. 15, B, lines with IP-pAb334).

In summary, 53 interacting partners of bestrophin could be isolated after extensive screenings of Y2H RPE cDNA library with two soluble domains of bestrophin as baits. However, no genuine interaction could be confirmed. Our findings emphasize a general limitation of the yeast two hybrid system in which a high sensitivity of the system often gives rise to false positives. In addition, the fusion proteins used in the two hybrid system have to be transported to and properly folded in the nucleus. This may cause problems, because for a large variety of proteins, such as integral membrane proteins, the nucleus does not represent the appropriate organelle for folding, stability, and interaction with other partners. Thus, our result suggests that bestrophin is not suitable for the traditional yeast two hybrid screens.

1.2 CytoTrap Yeast Two-Hybrid System

The CytoTrap (Sos recruitment system, SRS) is an alternative Y2H system based on reconstitution of the Ras signaling pathway. In the CytoTrap system, the protein-protein interactions form in the cytoplasm instead of in the nucleus, as is the case in the conventional Y2H system. Therefore this system is particularly suitable for membrane

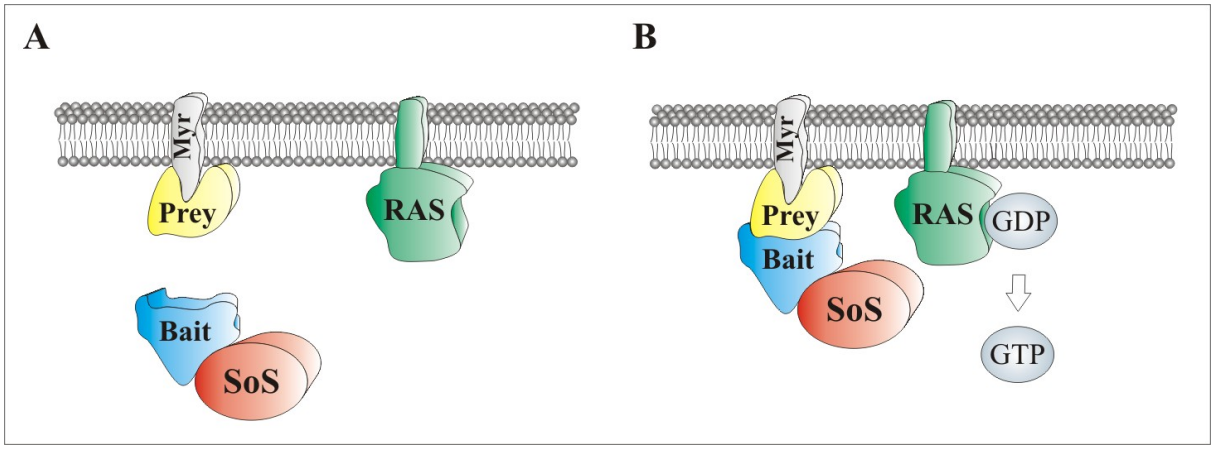

Fig. 16 Principle of SRS system
A, The prey protein or cDNA library is expressed as a fusion with the Src myristylation signal (Myr), which anchors it to the cytoplasmic surface of the cell membrane, and the bait protein is fused with hSos. **B,** After the co-transformation of the bait and prey constructs into the cdc25H yeast strain only colonies containing a specific protein-protein interaction will activate RAS signaling cascade that permits mutant yeast cdc25H to grow at 37°C.

proteins and proteins that depend on post-translational modification in cytoplasm for their proper function. The SRS uses the novel yeast (*S.cerevisiae)* temperature sensitive strain cdc25H, which contains a mutation in the guanyl nucleotide exchange factor cdc25 gene, the yeast homologue for human Sos (hSos) required for cell growth and survival. This temperature sensitive mutation can be complemented by the hSos protein, but only if the hSos is localized to the membrane as a consequence of protein-protein interaction (Fig. 16). The protein of interest is expressed as a fusion protein with the hSos protein from the pSos vector and the pMyr vector designed for cDNA library insertion. Expression of the fusion constructs is under control of a galactose dependent promotor. When the cDNA library and the bait construct are cotransformed into the cdc25H yeast strain, the only cells capable of growing at 37°C on galactose medium should be those that have been rescued by a protein-protein interaction recruiting hSos to the cell membrane.

1.2.1 Truncated bestrophin baits

The various truncated bestrophin fragments were expressed as a fusion to the hSos protein (Table 7) in the temperature sensitive yeast strain cdc25H, and were used to screen the bovine RPE/Myr fusion cDNA library. Prior to the Y2H screens bestrophin bait constructs were tested for self activation (Fig. 17, B). Interestingly, C-terminal fusion constructs of bestrophin (Sos-Cter1-3) which were unsuitable for GAL4 based Y2H screens because of unspecific activation of the reporter genes, were appropriate for the SRS system. Expression of the hSos-bestrophin fusion proteins were verified as well, however because of the lack of an antibody against hSos protein, only the expression of the hSos-Cter3 fusion protein could be confirmed. Expression of the Sos-Cter3 fusion protein which contains a fragment of bovine bestrophin from amino acids 368 to 584 was verified with the polyclonal pAb334 antibody which is directed against both bovine and human C-terminal epitopes (Fig. 17, A).

Construct name	aa-aa
Sos-Nter	1-30
Sos-loop	91-234
Sos-Cter1	291-367
Sos-Cter2	291-320
Sos-Cter3	368-584

Table 7 Truncated bestrophin baits

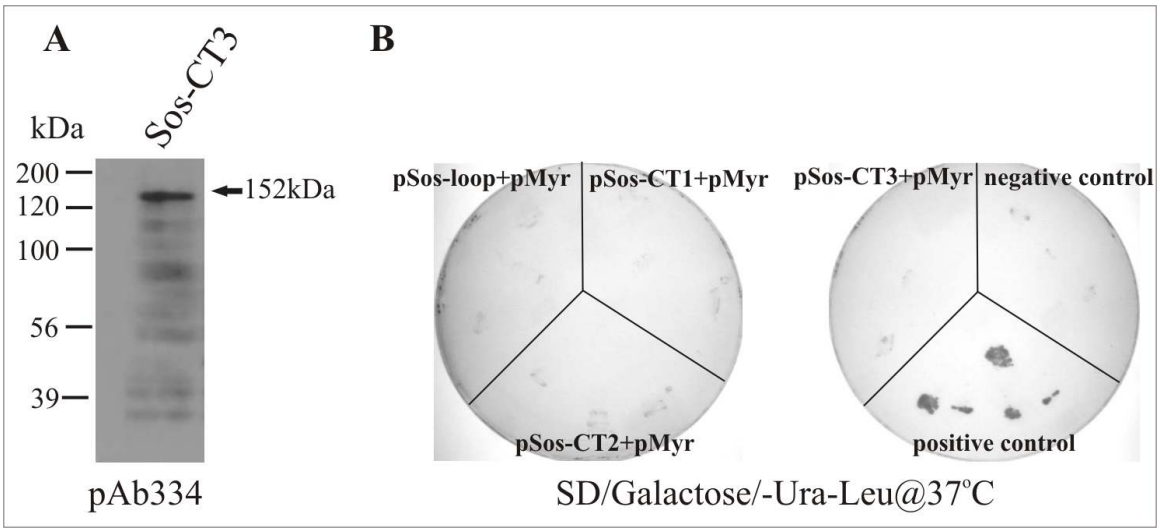

Fig. 17 Verification of bestrophin baits
A, Immunoblot of the Sos-CT3 fusion protein extracted from the yeast and detected with anti-bestrophin pAb334 antibody. **B,** plasmid DNA of bestrophin bait constructs were cotransformed with empty prey vector pMyr and then plated onto the SD/Glucose/–Ura-Leu plates. After 3-4 days incubation at RT they were streaked out on to the SD/Galactose/–Ura-Leu and incubated at 37°C. Only growth of positive control (Sos-MAFB + Myr-MAFB) should be observed after 3-5 days at 37°C.

1.2.2 Screening of cDNA library and verification of putative positive clones

The bovine RPE cDNA library (see Materials and Methods, section 8.3) was recloned into a modified pMyr vector and screened against Sos-loop and Sos-Cter3 (Table 7) bait constructs of bestrophin. Bait and prey constructs were simultaneously co-transformed into cdc25H cells and the double transformants were selected on SD/Glucose/–Ura-Leu plates at RT (>25°C). After incubation for 3-5 days at RT, colonies were stamped onto SD/Galactose/–Ura-Leu plates and incubated at 37°C until colony growth. Putative positive clones were verified by streaking yeast colonies onto SD/Glucose/–Ura-Leu plates. After incubation for two days at RT, galactose dependant growth at 37°C was assessed by growing putative positive clones on SD/Galactose/–Ura-Leu plates to exclude spontaneous revertants that would grow at 37°C. Screening of the bovine RPE/Myr cDNA library with Sos-loop and Sos-Cter3 baits resulted in isolation of 103 and 175 putative positive clones, respectively (Table 8).

Bait	No. of clones screened	No. of positive clones
Sos-loop	740 000	103
Sos-CT3	1 040 000	175

Table 8 Summary of the SRS Y2H screening

All putative positive clones were tested for galactose dependency, by replica plating onto glucose and galactose minus uracil and leucine plates and incubation at 37°C (Fig. 18).

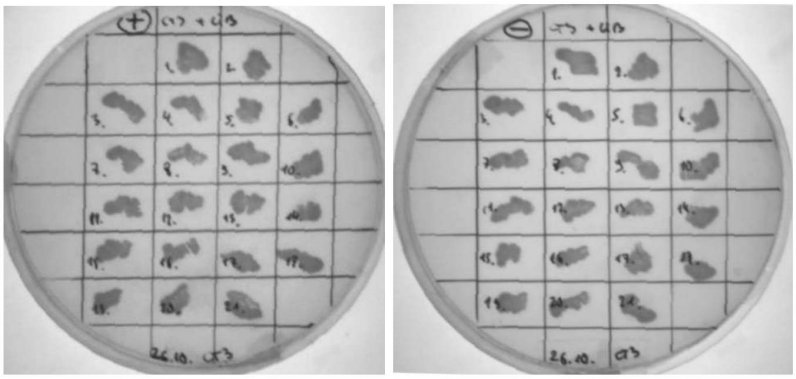

SD/Galactose/-Ura-Leu@37°C SD/Glucose/-Ura-Leu@37°C

Fig. 18 Procedure to rule out false positives in SRS screen
Verification of 21 putative positive clones from the screening of bovine RPE cDNA library with Sos-Cter3 as bait. Putative positive clones were verified by streaking out yeast colonies onto SD/Glucose/–Ura-Leu and SD/Galactose/–Ura-Leu plates to exclude spontaneous revertants that would grow on glucose plates at 37°C.

Since presence of glucose can suppress the galactose dependant expression of the fusion constructs, only those clones showing growth on galactose plates but not on glucose plates at 37°C indicate real interaction between the bait and prey fusion proteins,. Although the yeast cdc25H strain was verified for temperature-sensitive growth (not shown), and control constructs performed as expected, all putative positive clones isolated in the various Y2H screenings are apparently temperature revertants. Therefore the relatively high number of temperature revertants (false positive clones) makes Y2H screens labour intensive and little effective. In conclusion, failure of the Y2H screens to identify interacting partners of bestrophin may indicate that the selected approaches were not suitable for the putative membrane protein bestrophin. Alternatively, dissection of the bestrophin protein in distinct, partial fragments could disrupt some as yet unknown domains important for bestrophin interaction.

2. Functional analysis of bestrophin domains

Bestrophin belongs to a novel family of putative integral membrane proteins highly conserved throughout evolution. Phylogenetic studies of a protein family can be very valuable in determining conserved regions, potentially leading to prediction of protein function (Eisen 1998). To elucidate the evolutionary history of the family of bestrophin proteins and to identify novel structural and functional motifs conserved across family members, a comprehensive bioinformatics/phylogenetic analysis of the bestrophin protein family was conducted. The most distinctive feature of the bestrophin family, besides the invariant RFP (arginine-phenylalanine-proline) domain, is the evolutionary highly conserved N-terminal region from amino acid 1 to 317.

2.1 Bestrophin proteins, orthologous and paralogous

Bestrophin homologues were identified by performing similarity searches of protein sequence databases and unfinished genomic sequencing projects with the translated VMD2 mRNA sequence (GeneBank accession no. NM004183) and the BLASTP program (Altschul et al. 1997). Proteins identified by the BLASTP search program with greater than 25% identity over 200 or more amino acids were considered as potentially homologuous or orthologuous proteins. Sequences were aligned using CLUSTAL W (ver. 1.82) (Thompson et al. 1994) and alignments were refined manually in Genedoc (http://www.psc.edu/biomed/genedoc). Incomplete sequences and regions with uncertain alignments were excluded from the analysis, finally leaving 14 taxa with 41 sequences and 317 amino acid positions to be included in the study. Phylogenetic analyses were carried out using the PHYLIP (ver.3.5) (Felsenstein 1988, Felsenstein 1989) and TREECON (ver. 1.3b) (Van de Peer and De Wachter 1994) programs. The support for each phylogenetic group was tested using 1,000 bootstrap pseudoreplicates.

Phylogenetic analyses of 41 protein sequences from 14 representative invertebrate and vertebrate species (Fig.19) revealed that bestrophin orthologues and paralogues are clustering according to a defined protein category rather than to organismal type. Each of the human proteins (VMD2, VMD2L1 to L3) identified appears to be more related to the gene from other vertebrate species than to other members of the human VMD2 protein family, while invertebrate proteins tend to cluster together. Interestingly all paralogous proteins from *Xenopus laevis* appear to be related to the VMD2-L1 protein subfamily.

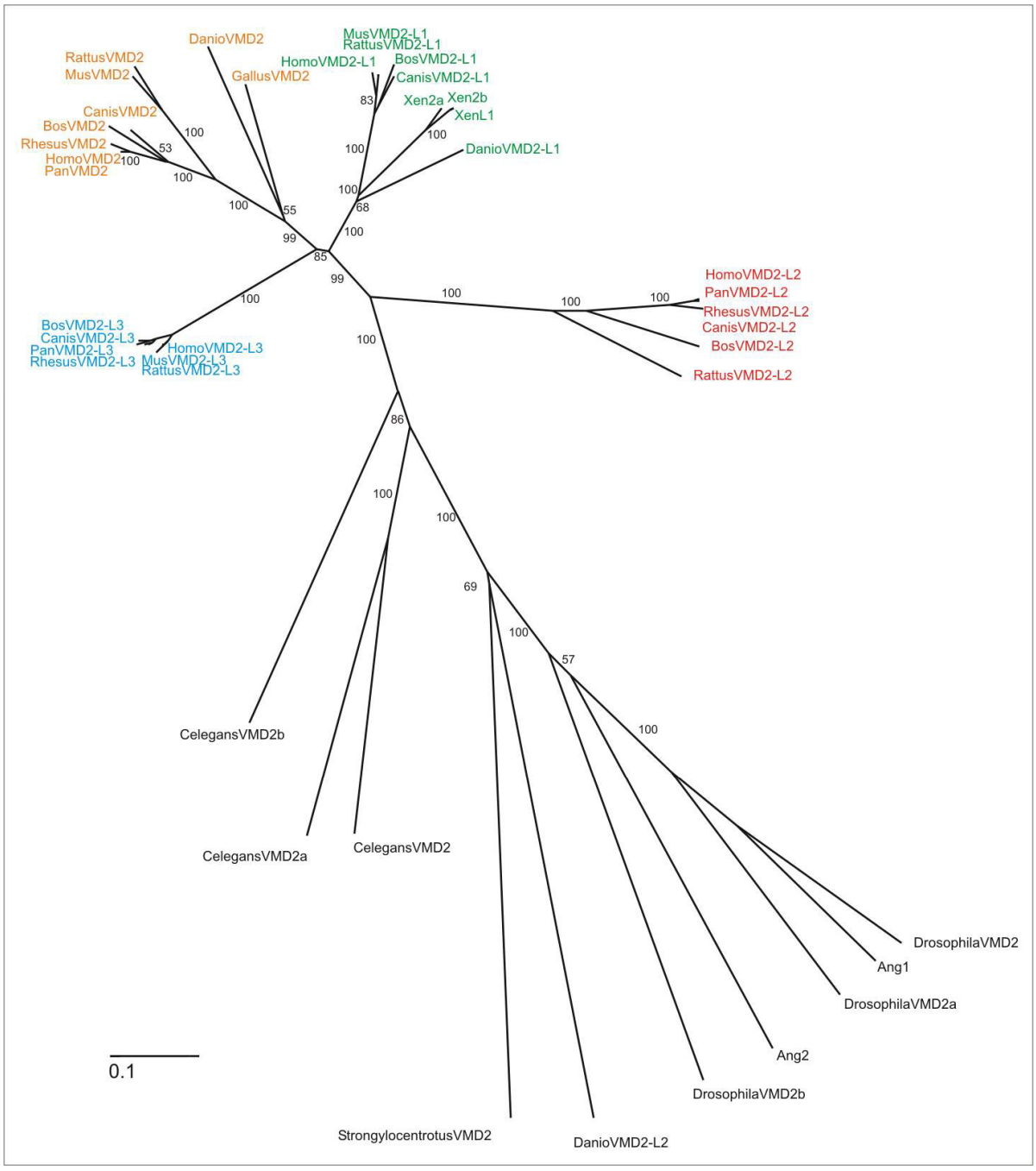

Fig. 19 Phylogenetic analysis of the bestrophin protein family
Unrooted dendrogram displaying evolutionary relationship between 41 bestrophin family members based on the alignment of partial bestrophin protein sequence (the first 317 N-terminal amino acid residues were used). Phylogenetic analysis of the aligned sequences was performed using the Neighbor-Joining (NJ) method (Saitou and Nei 1987). The support for each phylogenetic group was tested using 1,000 bootstrap pseudoreplicates. Number at the nodes represents bootstrap values. Accession numbers for the 41 full-length bestrophin sequences used in the phylogenetic analyses are listed in Table 5, Appendix.

2.2 RFP protein family and subfamilies

Phylogenetic analyses of the bestrophin homologous proteins (Fig. 19) reveal existence of four distinctive subfamilies in mammals, with high homology to the human VMD2, VMD2-L1 to L3 proteins. This significant level of protein sequence identity and

similarity between such divergent species suggest that each of the paralogous proteins has a unique, evolutionary conserved function. It also indicates that the divergence of bestrophin into subfamilies occurred before the divergence of individual mammalian species. Different channel properties of all four human bestrophin family members for which whole cell currents have been measured so far (Tsunenari et al. 2003) are further supporting the notion that the different paralogous proteins serve different functions in organism.

2.3 Identification of conserved motifs

Since human bestrophin shares significant sequence conservation with homologous proteins from numerous evolutionary divergent species, construction of a multiple alignment reveals the regions highly conserved throughout the phyla. The amino acid sequence alignment of 10 selected orthologous proteins of the bestrophin family (Fig. 20) including the N-terminal 317 amino acids was constructed. Since Zebrafish and Drosophila diverged from a common ancestor with mammals about 450 and 990 Myr ago, respectively, (Hedges 2002, Zdrobnov et al. 2002), they provide an excellent tool to distinguish conserved features from neutrally evolving elements in the protein sequence. 141 from 317 amino acids of highly conserved N-terminal sequence are identical among ten orthologous proteins sequences examined. These conserved residues tend to lie in four mutational hotspots identified in human Best disease patients, suggesting their functional importance. BMD related mutations show considerable colocalization with evolutionary conserved residues, since 42 from 65 amino acid residues affected in bestrophin are identical between all sequences surveyed (Fig. 20). The four highly conserved regions (1-30aa, 75-107aa, 217-245aa and 290-310aa) identified appear to be absolutely critical for the structure and the function of the bestrophin protein subfamily.

Comprehensive bioinformatics analysis of the bestrophin protein sequence revealed several conserved motifs which are summarized in Fig. 21. From the average hydropathy plot (Fig.29) derived from the multiple alignment of 10 orthologues of bestrophin, six putative TMDs were identified (TMD1 28-50aa, TMD2 68-90aa, TMD3 130-149aa, TMD4 179-201aa, TMD5 269-291, and TMD6 269-300aa). A putative well conserved glycophorin A like dimerization motif (Brosig and Langosch, 1998) was identified in the second TMD (^{75}LIxxSxxxGxxxT^{87}). Two potential dileucine lysosomal sorting signals (Bonifacino and Traub, 2003) were found at positions ^{119}ExxxLL^{124} and ^{203}DxxLL^{207}, however both motifs are conserved only in vertebrates. Another exceptionally well conserved site composed of four consecutive, aspartic acid residues ^{310}DDDD^{313}, could be involved in Ca^{+2} binding (Matsouka

et al. 1995). Highly conserved regions exists in all bestrophin orthologous from

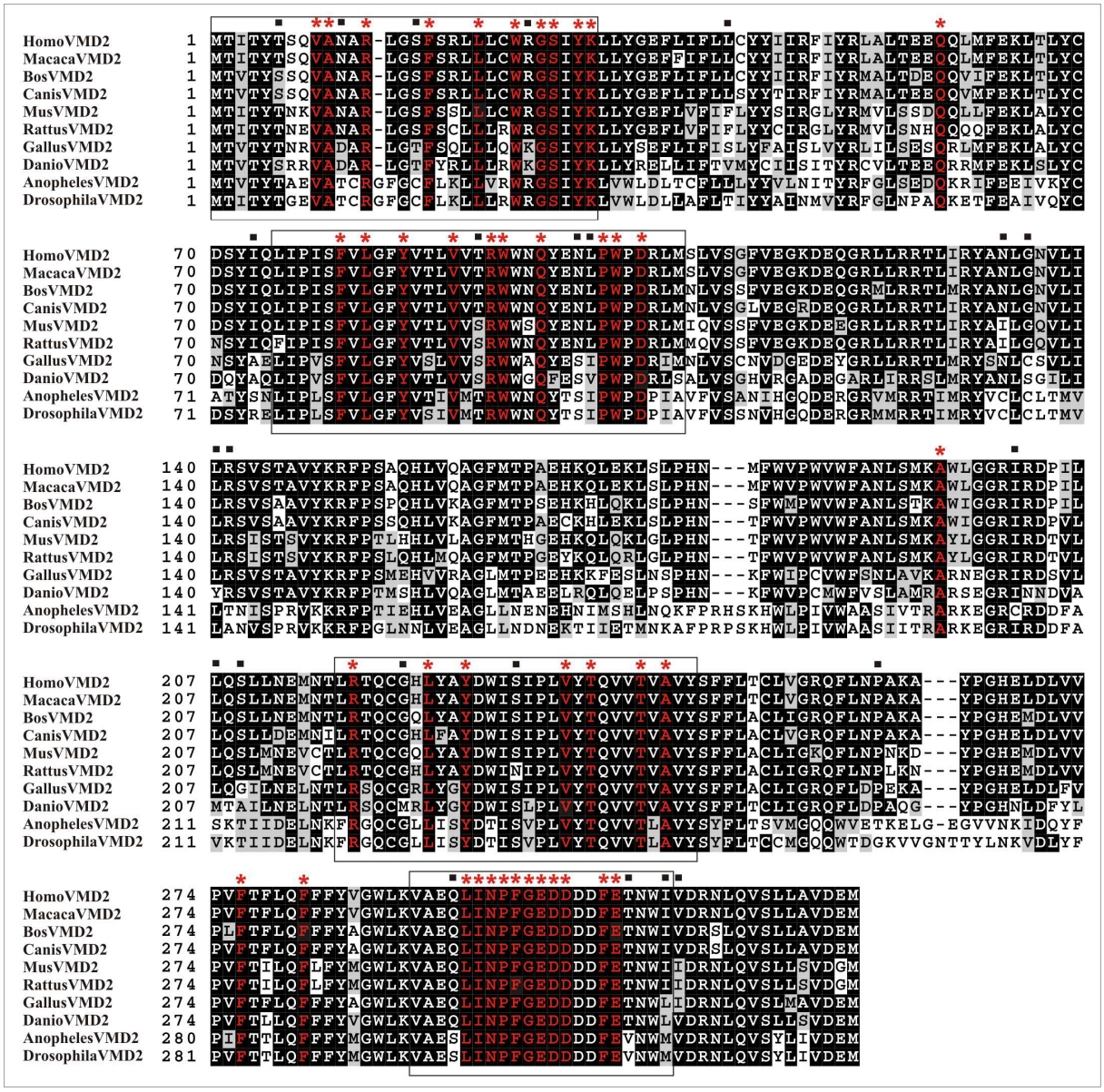

Figure 20 Multiple sequence alignment of the human bestrophin with representative orthologues. The alignment of the first 317 amino acid residues from the highly conserved N-terminus of the bestrophin was made with the Clustal W program. Hyphens correspond to gaps introduces to maintain the alignment. Identical residues between the sequences in the alignment are shown on a black background, and conservative amino acid substitutions are shaded. The black square above the aligned sequences indicate the locations of BMD associated mutations, and red asterisk denote conserved amino acid residues affected in BMD patients. Accession numbers for each protein sequence listed are as follows: HomoVMD2 (NP_004174), MacacaVMD2 (BAE02471), BosVMD2 (XP_585778), CanisVMD2 (XP_540912), MusVMD2 (NP_036043), RattusVMD2 (XP_574621), GallusVMD2 (XP_421055), DanioVMD2 (XP_689098), AnophelesVMD2 (EAA00042), and DrosophilaVMD2 (NP_652603).

amino acid 1 to 30 and from 217 to 245, but pattern searches using various online bioinformatics tools such as MotifScan (http://scansite.mit.edu/motifscan_seq.phtml) and InterProScan (http://www.ebi.ac.uk/InterProScan/) were unable to identify any known motifs. As a result of the present study, a number of conserved structural regions and motifs which

might be important for bestrophin function been identified. However, verification of the identified motifs awaits further investigations.

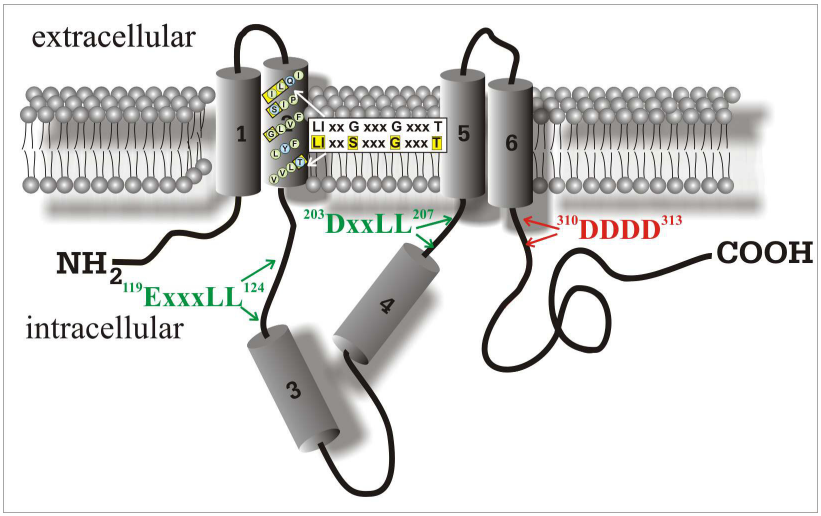

Fig. 21 Major structural features of the bestrophin
Different conserved domains and motifs of bestrophin are shown: gray cylinders represent putative TMD´s, potential dimerization motif located in the second TMD (white box), hypothetical dileucine lysosomal sorting signals (green letters) and putative Ca^{+2} binding motif (red letters).

3. Topology of normal and mutated bestrophin

Out of 89 different mutations which have been identified in BMD patients (www.uni-wuerzburg.de/humangenetics/vmd2.html, Stöhr et al. 2005) 85 are missense mutations, non-randomly distributed across the highly conserved N-terminal half of the bestrophin protein clustering near the predicted TMDs. The mechanism connecting putative Cl^- channel function to BMD pathology is not clear. Determination of the membrane topology of bestrophin may contribute to our understanding of the mechanism underlying the disease pathogenesis. Similarly, knowledge about the orientation of domains in the cytoplasm or the extracellular space could facilitate identification of cytoplasmic proteins that may interact with bestrophin using the Y2H system. Defining the positions of pathogenic mutations in correlation to the membrane topology can provide clues as to how these mutations may influence the function of the protein.

Previously, the membrane topology of bestrophin was studied using insertion of N-glycosylation and tobacco etch virus protease (TEVP) cleavage sites (Tsunenari et al. 2003). While hydropathy analysis of the primary amino acid sequence revealed that the protein contains 6 hydrophobic domains that might traverse the membrane, the experimental data suggest the presence of only 4 transmembrane domains with an additional hydrophobic domain dipped into the lipid bilayer (Tsunenari et al. 2003). Because of the uncertainty of how to interpret these data, we attempted to obtain independent evidence on topology of

bestrophin employing in vitro translation/translocation in the presence of dog pancreas microsomes. This method has been successfully used in resolving a membrane topology of several integral membrane proteins (Zhang and Ling 1991, Skach and Lingappa 1993, Shelness et al. 1993, Gafvelin et al. 1997, Lehmann et a. 1997, van Geest et al. 1997, Lu et al. 1998).

The goal of this part of the study was to first identify insertion signals of the bestrophin and then to determine whether interaction with downstream or upstream topogenic signals can affect their ability to insert into the membrane. Another objective was to analyze, possible effects of the 18 BMD mutations located within putative TMDs of bestrophin on the proper insertion into the membrane.

3.1 Potential transmembrane domains of bestrophin

The deduced amino acid sequence of human bestrophin was analyzed by using the algorithm of Kyte and Doolittle (Kyte and Doolittle 1982) and the TOPPRED II program developed by von Heijne (von Heijne 1992) (Fig 28).

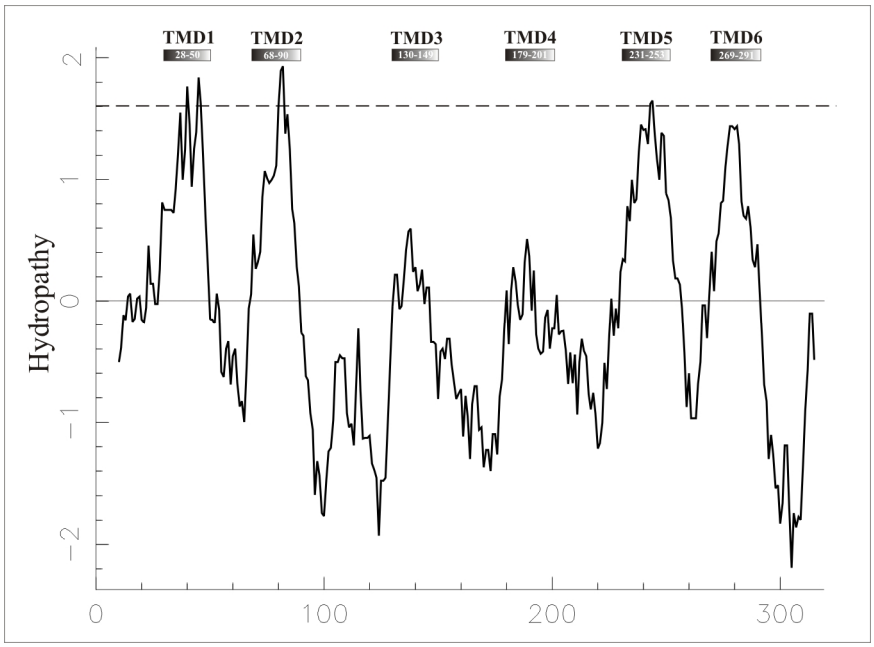

Fig 28 Kyte-Doolittle hydropathy plot of the N-terminal half of human bestrophin
Hydropathy plot was generated by the method of Kyte and Doolittle (Kyte and Doolittle 1982) with a window of 19 amino acids. Positive values indicate hydrophobic regions. Possible transmembrane segments (gray boxes) were determined by the TOPPRED II algorithm (von Heijne 1992) with the positions of the beginning and the ends of the segments indicated.

Both programs suggested that bestrophin contains 6 potential transmembrane domains. The putative transmembrane segments of human bestrophin and their average hydrophobicities are listed in Table 9. In addition average hydropathy plot (Fig.29), with four major and two minor hydrophobic peaks, derived from multiple alignment of 10 orthologous of bestrophin including sequences derived from *Homo*, *Macaca*, *Bos*, *Canis*, *Mus*, *Rattus*, *Gallus, Danio,*

Anopheles and Drosophila supports the assumption that the membrane topologies of all orthologous proteins are similar.

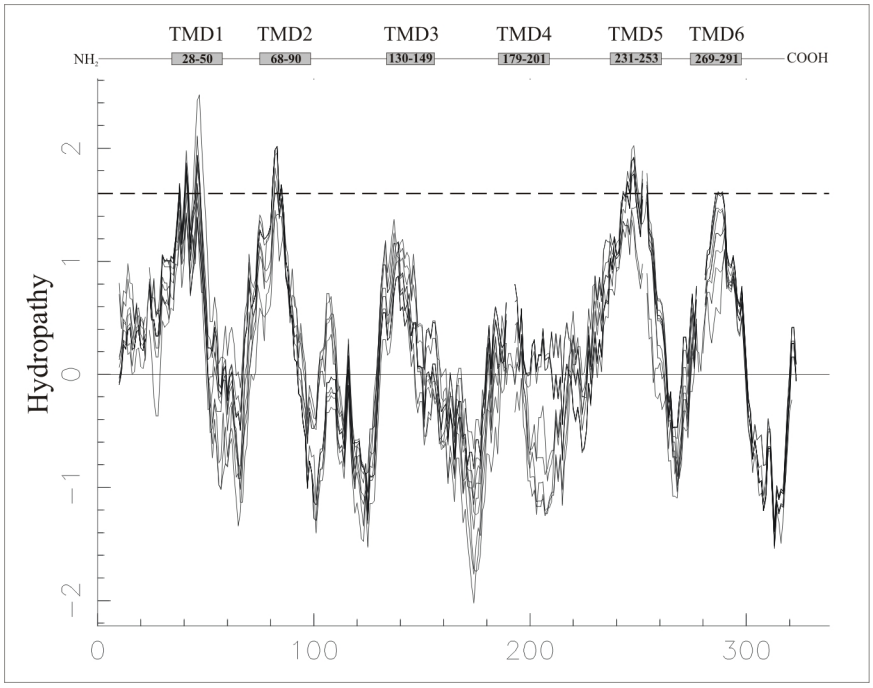

Figure 29 Average hydropathy plot for 10 bestrophin orthologues listed in the Fig. 2. Hydropathy plot was generated with PEPWINDOWALL program by the method of Kyte and Doolittle (Kyte and Doolittle 1982) with a window of 19 amino acids. Positive values indicate hydrophobic regions. Possible TMD´s (gray boxes) were determined by the TOPPRED II algorithm (von Heijne 1992) with the positions of the beginning and the ends of the segments indicated.

We first examined systematically the ability of the 6 predicted transmembrane segments to form individually a transmembrane α-helix in the ER membrane using an in vitro translation/translocation assay. Simplified, integration of polytopic membrane proteins into the membrane is thought to be directed by a series of alternating signal anchor (SA) and stop transfer (ST) sequences (Lingappa et al. 1979, Blobel 1980, Friedlander and Blobel 1985). A SA sequence is defined as a hydrophobic segment which can insert into the membrane with the N terminus in the cytoplasm and the C terminus in the lumen (N_{cyt}-C_{lum} orientation). The following hydrophobic region, the ST sequence, will be retained in the membrane with N_{lum}-C_{cyt} orientation, and the subsequent sequences will have cytoplasmic location, until the next SA sequence.

3.2 Leader peptidase as insertion vehicle

The well characterized *E. coli* membrane protein leader peptidase (Lep) (Johansson et al. 1993, Nilsson and von Heijne 1993) system was used as an insertion vehicle for the bestrophin fragments. Lep contains two NH_2-terminal transmembrane domains H1 and H2 which are linked by the P1 domain, and the catalytic P2 domain at the COOH-terminus (Fig 30).

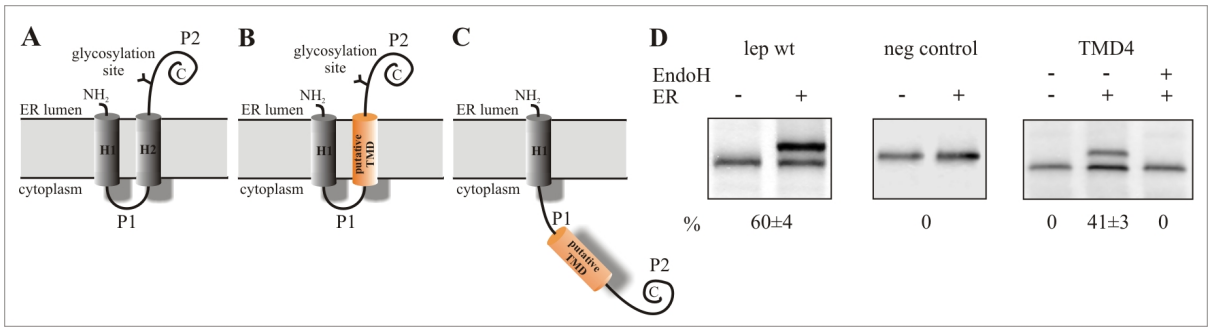

Fig. 30 Lep system A: Membrane topology of a Lep protein in the ER membrane. Replacement of the H2 domain by putative TMDs results in glycosylation **B**, and lack of glycosylation **C**, respectively. **D**, SDS-gel analysis of the control constructs: Lep wt, negative control (bestrophin construct containing amino acids 367-389), and Endo H treatment of construct TMD4, in vitro translated in the presence (+) or absence (-) of endoplasmic reticulum membranes (ER). The numbers bellow translated products presents glycosylation efficiencies from at least three independent experiments.

The H1 domain of Lep alone has the ability to target and to transverse the ER membrane with its N-terminus in the lumen. The transmembraneous H2 domain of Lep was replaced with various putative transmembrane fragments of bestrophin, and glycosylation of the P2 loop was utilized as an indicator of proper membrane insertion (Fig 31). The efficiency of glycosylation of Lep in our in vitro translation/translocation system was 60-70%, which was slightly below the glycosylation efficiency of 80-90% reported elsewhere (Johansson et al. 1993, Nilsson and von Heijne 1993, von Heijne 1994).

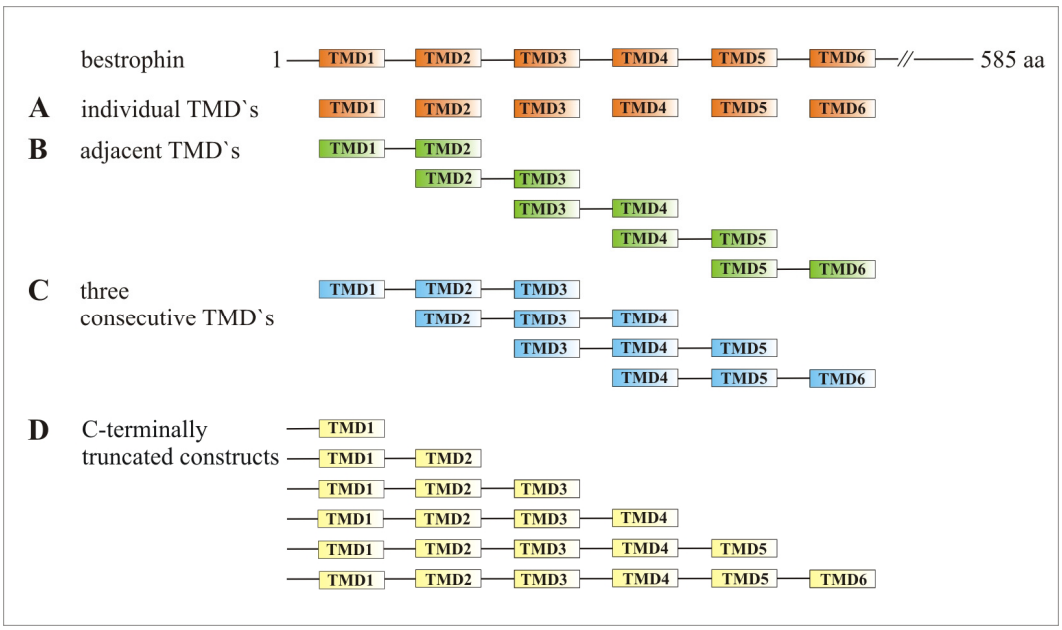

Fig. 31 Constructs of bestrophin used in this study
The transmembraneous H2 segment of Lep was exchanged by a series of putative **A,** individual, **B,** adjacent, **C,** three consecutive TMDs bestrophin fragments and **D,** C-terminally truncated constructs of bestrophin

3.3 SA (signal anchor) potential of individual putative TMDs of bestrophin

Based on the topological predictions, six constructs were made in which the H2 domain of Lep was replaced by different potential TMDs of bestrophin (Table 9). Following in vitro translation in the presence of canine microsomes, bestrophin segments with SA function will penetrate the membrane enabling glycosylation of the P2 domain in the luminal space, whereas a segment that lacks SA function will result in nonglycosylated molecules (Fig 32).

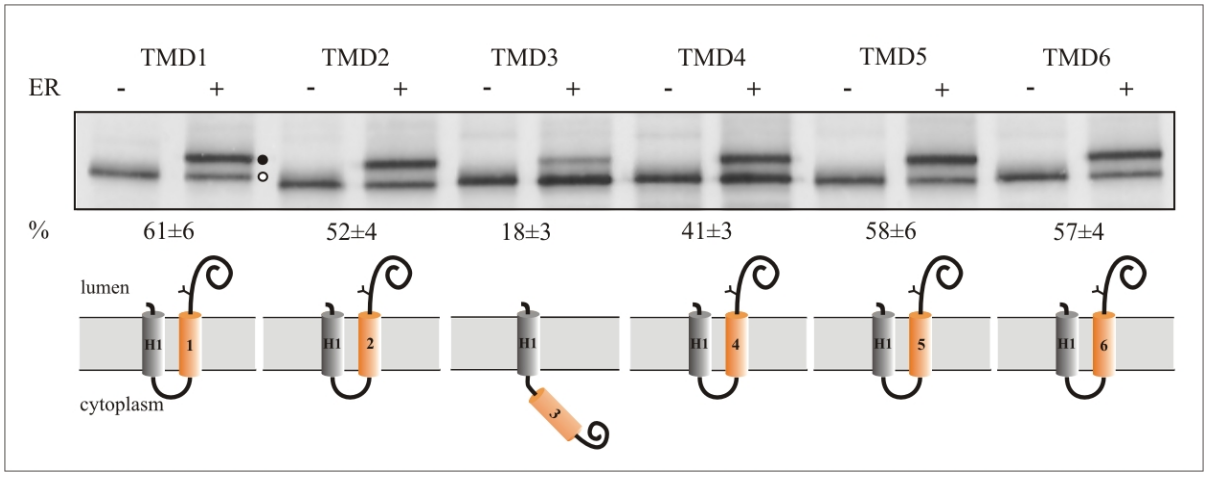

Figure 32 **Analysis of the predicted hydrophobic domains of bestrophin.** SDS-gel analysis of the in vitro translated individual transmembrane segments in the presence (+) or absence (-) of endoplasmic reticulum membranes (ER). The numbers bellow translated products presents glycosylation efficiencies from at least three independent experiments, and the possible orientation of each construct was elucidated on the bottom. The results are recapitulated in Table 9. Glycosylated and nonglycosylated products are indicated by black and white circles, respectively.

With the exception of the segment containing TMD3, all other constructs resulted in efficiently glycosylated products, approximately 3 kDa larger than that observed in the absence of microsomal components (Fig. 32 and Table 9). This indicates that TMD 1, 2, 4, 5 and 6 can potentially function as SA sequence in our in vitro system while TMD3 may not. It should be noted that TMD4 was not as efficiently glycosylated as expected from its average hydrophobicity (average glycosylation efficiency 41±3%) (Fig. 32).

Construct	Bestrophin residues	Average hydrophobicity	Glycosylation %
TMD1	**28-50**	0.79	61±6
Y29H			58±6
L41P			56±11
TMD2	**68-90**	0.81	52±4
I73N			44±3
Y85H			32±3
TMD3	**130-149**	0.69	18±3
L140R			1±1
A146K			13±5
TMD4	**179-201**	0.76	41±3
A195V			39±5

I201T			36±6
TMD5	**231-253**	0.79	58±6
S231R			56±5
T237R			58±7
TMD6	**269-291**	0.82	57±4
F276L			60±5
F281del			45±4
TMD6+9aa	**269-300**		57±4
Q293K			51±7
N296H			58±2
E300K			53±6

Table 9 **Insertion of normal and mutated individual TMDs of bestrophin in the ER**

3.4 SA and ST (stop transfer) function of adjacent bestrophin fragments

To further clarify the SA potential of TMD3 and 4, the H2 segment of Lep was replaced with fusions containing adjacent paired putative TMDs (Fig. 33 and Table 9 A). Constructs TMD1+2 and TMD5+6 each containing one SA and one ST sequence that cause retention of the P2 domain on the cytoplasmatic side yielded nonglycosylated products. Weak glycosylation efficiency noticed in the TMD1+2 construct can be considered as background signals (less than 20%). The fusion fragment TMD3+4 showed moderate glycosylation which was in agreement with some SA activity of the individual TMD4 segment. The P2 loop of the fusion proteins from constructs TMD2+3 and TMD4+5 were directed into the lumen of the ER thus resulting in glycosylated products.

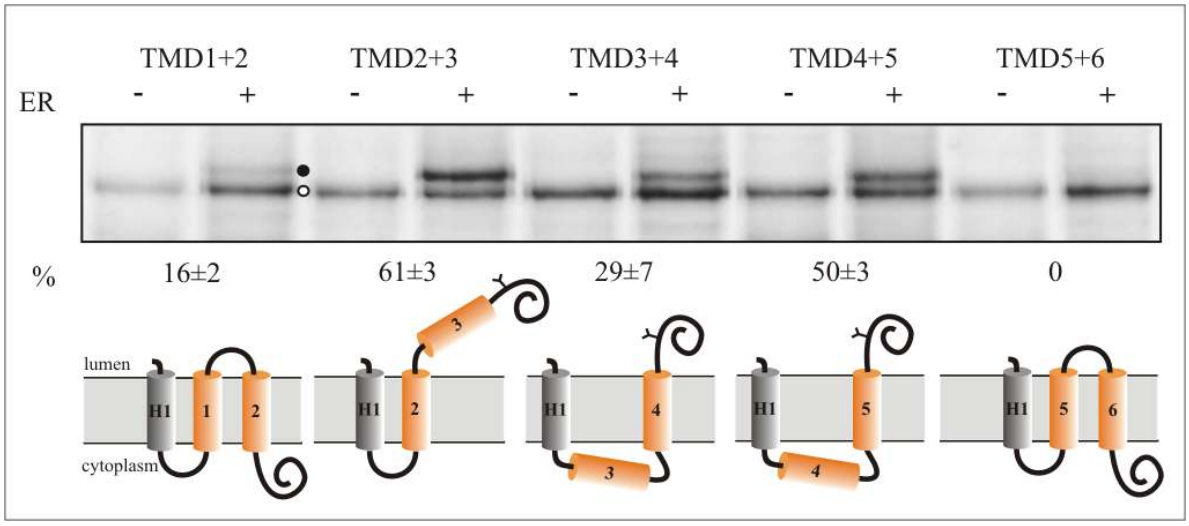

Fig. 33 Analysis of the predicted hydrophobic domains of bestrophin. SDS-gel analysis of the in vitro translated constructs containing adjacent pairs of putative TMDs in the presence (+) or absence (-) of endoplasmic reticulum membranes (ER). The numbers below the translated products represent glycosylation efficiencies from at least three independent experiments. A possible interpretation of experimental data shown in the upper panel are given at the bottom. The results are also given in Table 10. Glycosylated and nonglycosylated products are indicated by black and white circles, respectively.

Combined with the results obtained from the insertion experiments of the individual TMD segments, we conclude that TMD 1, 2, 5 and 6 represent functional SA sequences in vitro and therefore may be authentic transmembrane domains in vivo. In contrast, TMD4 appears not to function as an SA sequence probably as a consequence of the relatively low hydrophobicity of this fragment.

3.5 SA and ST function of three consecutive TMDs of bestrophin

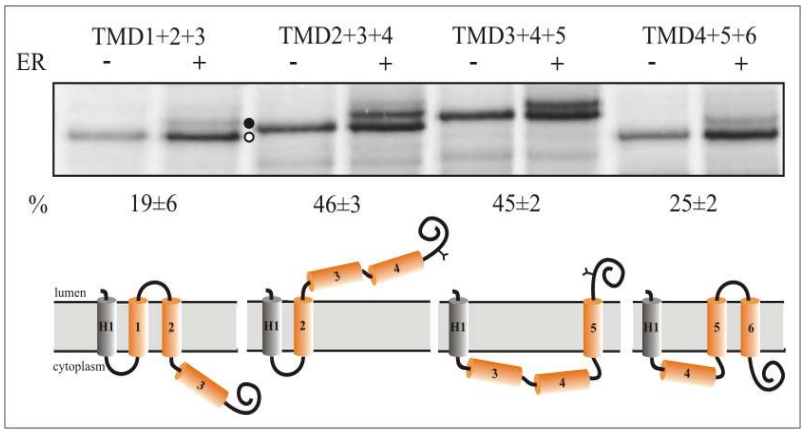

Fig. 34 Analysis of the predicted hydrophobic domains of bestrophin.
SDS-gel analysis of the in vitro translated constructs containing three consecutive putative TMD´s of bestrophin in the presence (+) or absence (-) of endoplasmic reticulum membranes (ER). bottom. A possible interpretation of experimental data shown in the upper panel are given at the bottom. The results are recapitulated in Table II.

Additionally, series of constructs containing three consecutive TMDs (Fig. 34 and Table 10 B) were generated and tested for its ability to integrate into the ER membrane. Fusions TMD1+2+3 and TMD4+5+6 were only slightly glycosylated as it would be expected from the even number of SA sequences. In contrast, constructs TMD2+3+4 and TMD3+4+5 yielded glycosylated products suggesting an odd number of SA sequences which agrees with results from the previous experiments.

3.6 SA and ST function of COOH-terminally truncated bestrophin fragments

In a further effort to resolve membrane topology of bestrophin, a series of COOH-terminally truncated constructs was generated. The H2 domain of Lep was replaced with constructs of bestrophin containing increasing numbers of putative TMDs (Table 10 C). Efficient glycosylation of the fusion protein with the first 55 amino acids of bestrophin again demonstrated high SA activity of TMD1 (Fig. 35 and Table 10 C).

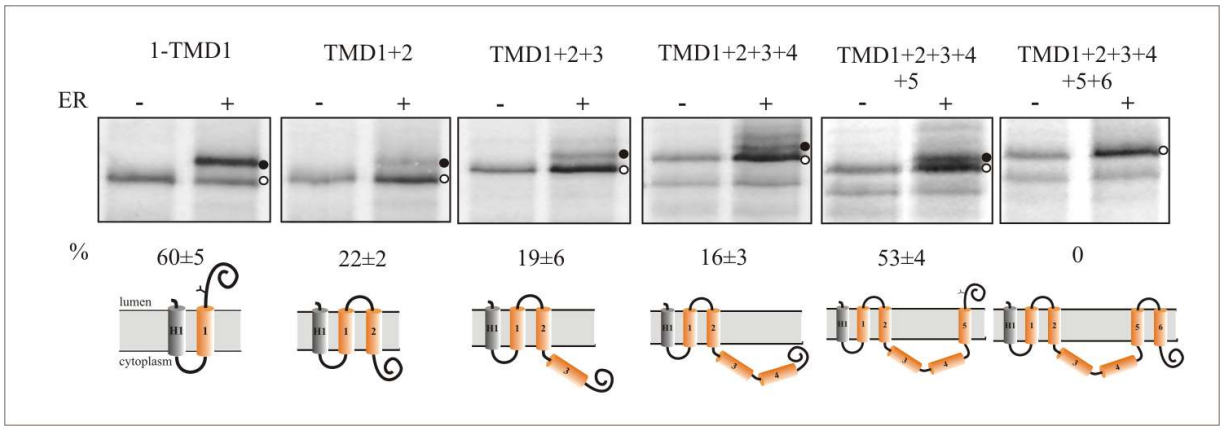

Fig. 35 Insertion of bestrophin COOH-terminally truncated constructs into the ER membrane. SDS-gel analysis of six constructs containing an increasing number of TMDs in the presence (+) or absence (-) of endoplasmic reticulum membranes (ER). The numbers bellow translated products represent glycosylation efficiencies from at least three independent experiments, and the possible topology of each construct was elucidated on the bottom. Glycosylated and nonglycosylated products are indicated by black and white circles, respectively.

The addition of the second putative TMD2 resulted in significantly reduced glycosylation of the fusion protein, suggesting a strong ability of TMD2 to act as ST sequence. Extension of the bestrophin fusion protein with the following putative transmembrane segment TMD3 resulted in non-glycosylation suggesting that the . putative TMD3 sequence lacks SA potential. This is also well supported by our results obtained from the previous experiments. Extending the bestrophin construct containing TMDs 1+2+3 with the following C-terminal hydrophobic segment, TMD4, again resulted in a non-glycosylated product. Obviously TMD4 does not have ability to insert into the membrane, and most likely

	Construct	Bestrophin residues	Glycosylation %
A	**TMD1-2**	**28-90**	16±2
	TMD2-3	**55-149**	61±3
	Y85H		37±2
	L140R		52±4
	TMD3-4	**130-201**	29±7
	L140R		30±3
	TMD4-5	**176-253**	50±3
	TMD5-6	**207-291**	0
	F281del		11±2
B	**TMD1-3**	**28-149**	19±6
	Y29H		27±8
	L41P		31±5
	I73N		29±12
	Y85H		31±8
	TMD2-4	**55-201**	46±3
	L140R		56±2
	TMD3-5	**91-253**	45±2

	A195V		42±8
	I201T		41±4
	TMD4-6	**176-291**	25±2
	S231R		18±4
	T237R		18±4
	F281del		17±2
C	**1-TMD1**	**1-55**	60±5
	W24C		59±6
	R25Q		61±3
	S27R		56±8
	TMD 1+2	**1-90**	27±5
	TMD 1+2+3	**1-149**	23±6
	TMD 1+2+3+4	**1-201**	16±3
	TMD 1+2+3+4+5	**1-253**	53±4
	TMD 1+2+3+4+5+6	**1-291**	0
	Lep wt	**f.l.**	60±4
	Neg. control	**367-389**	0

Table 10 Insertion of normal and mutated bestrophin constructs: **A**, adjacent, **B**, three consecutive and **C**, C-terminally truncated fragments in the ER

remains at the cytoplasmic side. This result clearly differs from topology data obtained by inserting N-glycosylation and protease cleavage sites (Tsunenari et al. 2003). Here, TMD4 was able to insert into the membrane, as evidenced by glycosylation of the loop between TMD4 and TMD5 (Tsunenari et al. 2003). Further addition of putative TMD5 to our clone fragment resulted in efficient glycosylation of the fusion protein. This may be expected from the construct TMD1+2+3+4 because TMDs 3 and 4 are probably not inserting into the membrane. Finally, extending the bestrophin construct containing TMD 1+2+3+4+5 with the final hydrophobic segment, TMD6, resulted in a nonglycosylated fusion protein, demonstrating ability of the TMD6 to insert into the membrane. Although unlikely, we cannot rule out that in constructs TMD 1+2+3+4, TMD 1+2+3+4+5 and TMD 1+2+3+4+5+6 both TMD3 and TMD4 may traverse the membrane, generating similar glycosylation profiles.

In conclusion, our in vitro translation/translocation data, suggest a topology model of bestrophin with four TMDs including TMD1, 2, 5 and 6. This would result in a large cytoplasmatic hydrophobic loop between TMD2 and TMD5 (Fig. 36).

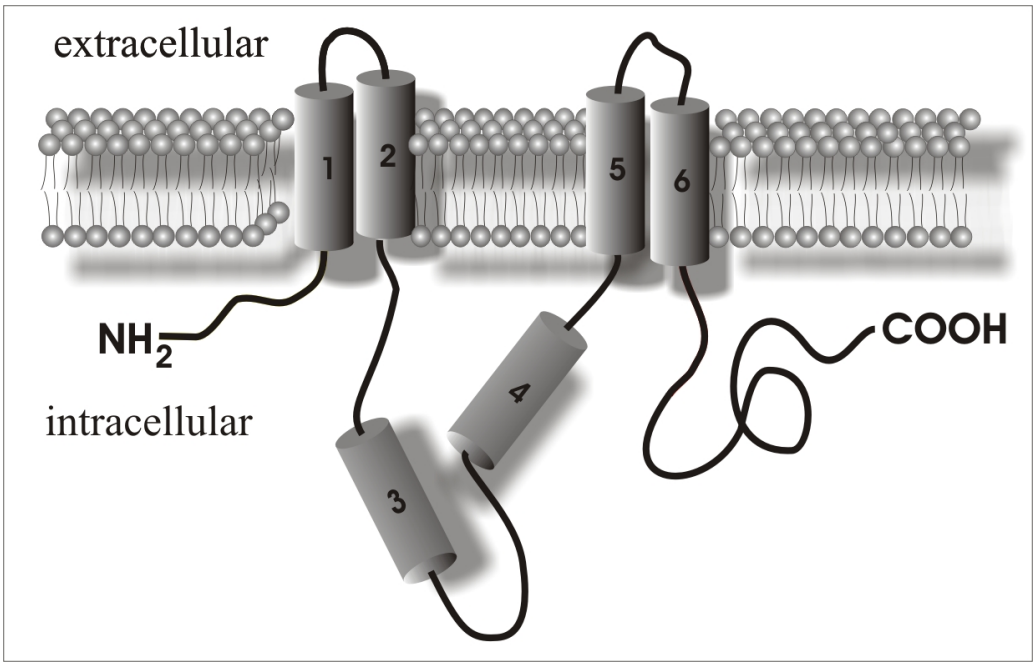

Fig. 36 Proposed membrane topology of human bestrophin. Hydrophobic domains are labeled 1 to 6 based on Kyte-Doolittle hydropathy analysis and TOPPRED II algorithm.

3.7 Effect of BMD-related mutations on bestrophin topology

The Best disease causing mutations are non-randomly distributed across the N-terminal half of the protein, and they tend to cluster near the predicted TMDs. The majority of the 65 amino acids affected in BMD (Kramer et al. 2000, White et al. 2000, Kramer et al. 2003), which can be mutated more then once are distributed in hydrophilic, solvent accessible regions of the protein. So far, 21 out of the 65 mutated codons are localized within the six hydrophobic regions of the bestrophin.

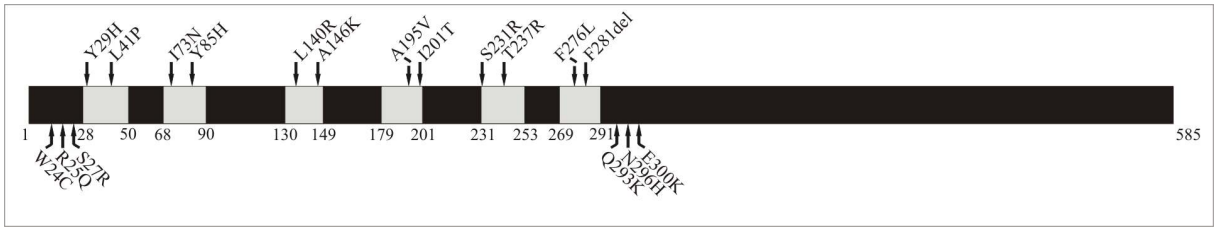

Fig.37 Schematic representation of bestrophin. Putative transmembrane domains are shown, along with the location of the BMD-related mutations characterized in this study.

In order to examine the effect of these mutations on membrane topology, 18 disease-associated mutations were generated by site directed mutagenesis (Fig. 37) and expressed in our in vitro translation/translocation system and their ability to insert into the ER membranes was assessed.

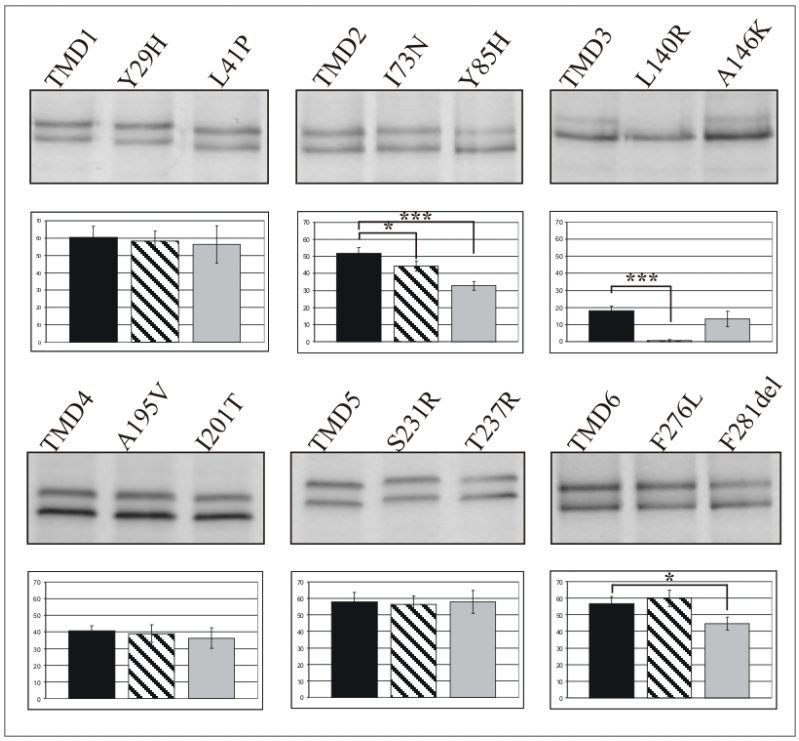

Fig. 38 Insertion of bestrophin constructs carrying BMD related mutations into the ER membrane.
SDS-gel analysis of individual TMD´s of bestrophin bearing mutation in the presence (+) or absence (-) of endoplasmic reticulum membranes (ER). The bars represent glycosylation efficiencies from at least three independent experiments. Values of significance were taken as *P<0.05, **P<0.01, and ***P<0.001.

A series of constructs in which the H2 domain of Lep was replaced by individual, mutated TMDs of bestrophin (Fig. 38, Table 9), were tested for its capacity to insert into the membrane. Insertion into the membrane of wild type and mutation bearing chimeric proteins, again was assayed by glycosylation of the Lep P2 domain. Missense mutations located in the transmembrane segments TMD1, TMD4 and TMD5 are apparently not influencing insertion of the fusion proteins into the membrane, as deduced from the unaffected glycosylation efficiency of the mutated proteins compared to the wt counterparts. In contrast, missense mutation I73N and Y85H in TMD2, L140R in TMD3 and the F281 deletion in TMD6 significantly abolished insertion of the respective mutated fusion proteins into the membrane. That is a somewhat unexpected result, as topological signals in membrane proteins tend to be generally robust and the topology of a protein is not so easily perturbed by a single point mutation. However, introduction of polar and charged residues into transmembrane segments seems to be more disrupting and may represent a potential mechanism for disease associated protein misassembly (Partridge et al. 2002).

Additionally, the mutations which demonstrated an effect on membrane topology were inserted into a construct containing adjacent and three consecutive TMDs of bestrophin, respectively, to test for their potential to integrate into the ER membrane (Fig. 39, Table 10 A, B). In this constellation the constructs including the I73N, L140R and F281del mutations did not significantly affect topology (Table 10 A, B). On the other hand, the construct with the

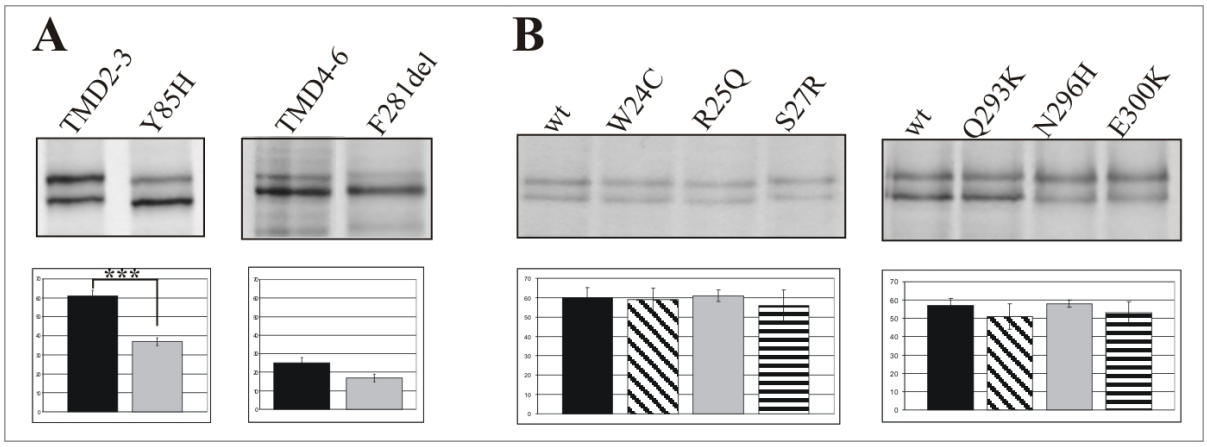

Fig. 39 Insertion of bestrophin constructs carrying BMD related mutations into the ER membrane. A, SDS-gel analysis of constructs containing adjacent (TMD2-3) and three consecutive (TMD3-5) TMDs of bestrophin. bearing mutation in the presence (+) or absence (-) of endoplasmic reticulum membranes (ER). **B,** in vitro translation/translocation of bestrophin constructs with mutations flanking the predicted TMD1 and 6.The bars represent glycosylation efficiencies from at least three independent experiments. Values of significance were taken as *P<0.05, **P<0.01, and ***P<0.001.

Y85H mutation containing adjacent transmembrane segments TMD2 and TMD3 was significantly less glycosylated than its corresponding wild type construct (Fig. 39. A). Finally, six additional mutations located in TMD1 and TMD6 flanking regions (Fig. 39. B), exhibited no effect on the insertion of the corresponding transmembrane segments.

3.8 Cysteine scanning mutagenesis

To gain additional information on membrane topology of bestrophin an extensive cysteine scanning mutagenesis was performed. In cysteine scanning mutagenesis, a series of constructs containing a single cysteine residue is generated and the membrane orientation is evaluated using membrane permeable and membrane impermeable sulfhydryl reagents. Cysteine-less bestrophin was created by mutating all five cysteine residues of human bestrophin at positions 23, 42, 69, 221 and 251, to a serine residue by five rounds of site directed mutagenesis (Fig. 40). All cysteine residues of bestrophin can be replaced without disrupting the function of the protein (Sun et al. 2002), thus enabling topology studies on complete and active protein.

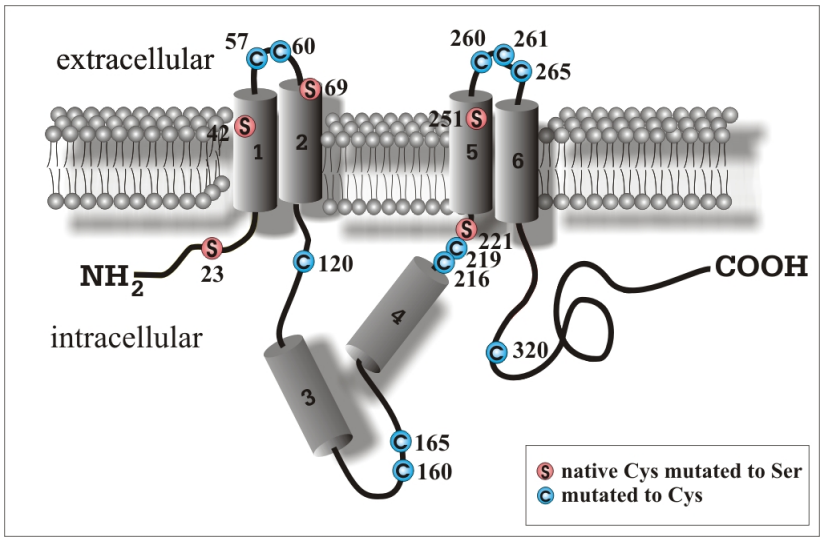

Fig. 40 Secondary structure model of bestrophin and the location of the cysteine insertions
All five native cysteine residues of bestrophin at positions 23, 42, 69, 221 and 251were replaced by serine residues (red circle). Single cysteine residues were introduced into the predicted extracellular or cytoplasmic loops of a cysteine-less bestrophin (blue circle). The membrane orientation of the substituted cysteine residues were evaluated by the treatment with sulfhydryl reagents.

For the topology studies, a series of bestrophin constructs tagged with Rho-1D4 tag at the C-terminus and with a single cysteine residue inserted into each of the putative extracellular or intracellular loops was created by site directed mutagenesis (Fig. 41, A). Thirty-six hours after transfection in EBNA-293, cells were treated for 30 min with the sulfhydryl reactive reagent, biotin maleimide (BM), with and without the membrane impermeable lucifer yellow iodacetamide (LYIA). Membrane proteins were solubilized and immunoprecipitated with anti-bestrophin polyclonal antibody. The immunoprecipitates were electrophoresed on SDS-PAGE gel, and the covalently bound biotin was labeled with HRP-conjugated streptavidin. Rho-1D4 tagged bestrophin proteins were detected with an anti Rho-1D4 monoclonal antibody (monoclonal anti-rhodopsin antibody was a gift from Dr. R. S. Molday, University of British Columbia, Vancouver, BC, Canada), after stripping the same membrane. Interestingly biotinylation of the bestrophin could occur only if combined with the cell permeabilizing reagent digitonin or saponin (Fig. 41, B), thus indicating intracellular localization of the heterologously expressed bestrophin constructs. Biotinylation experiments were performed in A-RPE19 and CHO-K1 cells expressing bestrophin constructs, but no biotinylation could be observed on the intact cells (data not shown).

Additional control biotinylation experiments were carried out using human anion exchange protein (AE1), a well characterized erythrocyte membrane protein (constructs kindly provided by Dr. J.R. Casey, Department of Physiology, University of Alberta, Edmonton, Canada). Biotinylation experiments were performed as described above, and the Rho-1D4 tagged hAE1 proteins (hAE1-Cless, hAE1-C555 and hAE1-C892) were immunoprecipitated with anti Rho-1D4 monoclonal antibody. Western blot analysis of the immunoprecipitates with anti-Rho-1D4 antibody demonstrates equal levels of expression of the hAE1 Rho-1D4 tagged constructs (Fig. 41, C, lower panel, ~109kDa band). Although a

substantial amount of hAE1-Cless protein was detected, no biotinylation signal could be visualized after striping and reprobing the membrane with streptavidin-HRP complex. Contrary to the cysteine-less construct of the hAE1, extracellular cysteine at position 555 of the hAE1-C555 was highly reactive towards BM and biotinylation was significantly reduced with membrane impermeable LYIA. On the other hand, inability of the LYIA to abolish biotinylation of the hAE1-C892, clearly demonstrate cytosolic orientation of the cysteine at position 892 (Casey et al. 1995). Conclusive results of the control experiments demonstrate a lack of biotinylation of the bestrophin constructs in intact cells. This may not be due to technical problems but could be due to an intracellular localization of bestrophin.

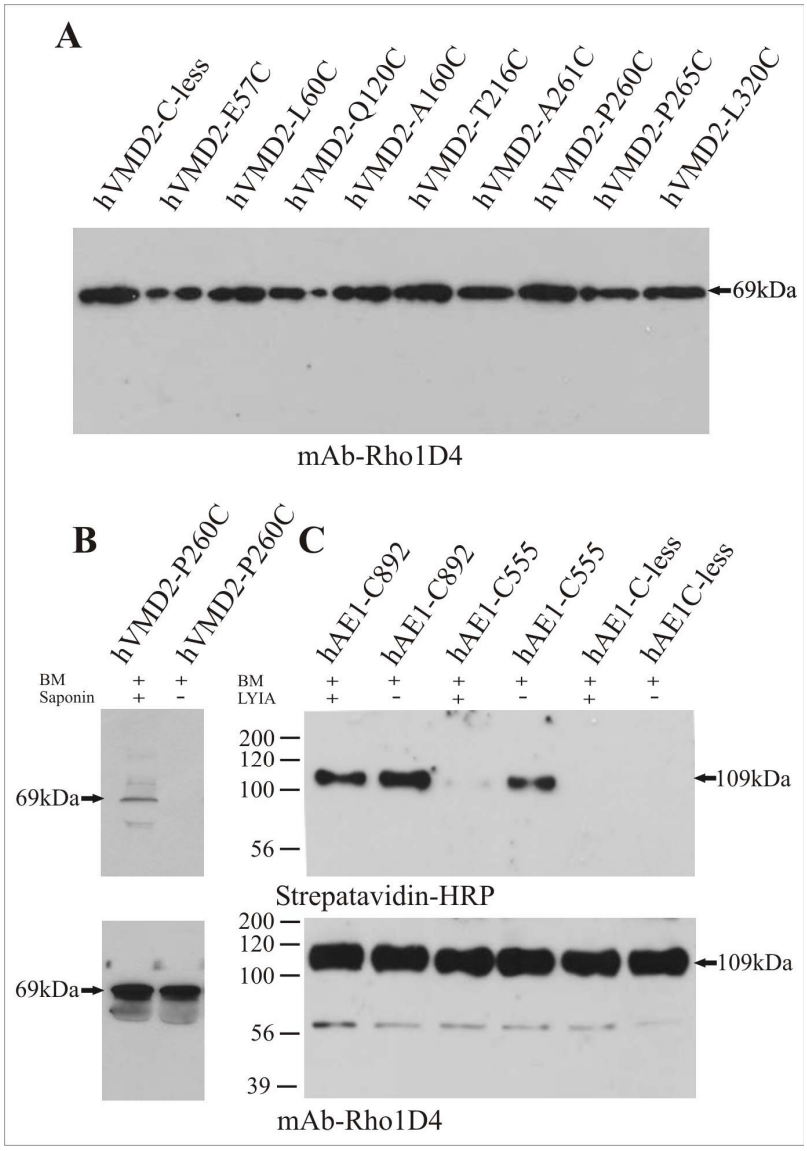

Fig. 41 Cysteine scanning mutagenesis
For the topology studies, individual cysteine residues are inserted into each of the predicted extracellular and intracellular loops of the cysteine-less bestrophin, and the orientation with respect to the membrane is evaluated using membrane permeable (BM) and membrane impermeable (LYIA) sulfhydryl reagents; **A,** immunoblot analysis of the Rho-1D4 tagged bestrophin constructs detected with anti-Rho-1D4 antibody; **B,** (upper panel), biotinylation of the bestrophin constructs (P260C shown) could take place only after the permeabilization of the cell by saponin or digitonin; **C,** (lower panel) Western blot analysis of the immunoprecipitates with anti-Rho-1D4 antibody demonstrates equal levels of expression of the Rho-1D4 tagged constructs of the hAE1; (upper panel), cysteine-less (hAE1-Cless) and single cysteine substituted hAE1 proteins (hAE1-C555 and hAE1-C892) were biotinylated in the presence or absence of the LYIA, immunoprecipitated with Rho-1D4 monoclonal antibody and biotinylation status of the protein was determined with streptavidin-peroxidase conjugate.

In conclusion, cysteine scanning mutagenesis was done to verify the topological model of bestrophin obtained by in vitro translation/translocation studies. One of the prerequisites of this assay is a plasma membrane localization of the protein, but in our

expression system the heterologously expressed constructs of bestrophin all localized to the intracellular membranes. This conclusion was supported by successful biotinylation of bestrophin after permeabilization of the plasma membranes. As a consequence, the cysteine scanning mutagenesis approach could not be used for characterization of the membrane topology of bestrophin.

6. Discussion

1. Search for interacting partners of bestrophin

Bestrophin is preferentially expressed in the retinal pigment epithelium (RPE) (Marquardt et al. 1998), where it is localized to the basolateral plasma membrane (Marmorstein et al. 2000, Bakall et al. 2003). The exact function of the bestrophin is not known although considerable evidence exists that supports bestrophin function as a Ca^{+2} activated Cl^- channel (Sun et al. 2002, Tsunenari et al. 2003, Qu et al. 2003, Qu and Hartzell 2004, Qu et al. 2004, Fischmeister and Hartzell 2005, Tsunenari et al. 2006). A causative relationship between chloride channel dysfunction and lipofuscin accumulation in BMD need to be clarified. As a first step, the identification of proteins that interact with bestrophin is essential for the elucidation of the regulation and the function of bestrophin. In the present study, we therefore sought to characterize interacting partners of bestrophin by using GAL4-based yeast two hybrid (Y2H) systems.

1.1 Advantages of the GAL4 based Y2H system

The GAL4-based Y2H system is an in vivo assay developed to detect protein-protein interaction in their native conformation (Fields and Song, 1989, Chien et al. 1991). In contrast to biochemical methods such as coimmunoprecipitation, pull down assays or cross-linking, this system is based on the reconstitution of a functional transcription activator in yeast. The yeast transcription factor GAL4 contains two physically and functionally separable domains, comprising a DNA-binding domain (DBD) and a transcription activation domain (AD). The DBD binds to specific promoter sequences (designated UAS for upstream activation sequence), whereas the AD recruits RNA polymerase II to transcribe downstream reporter genes. Two proteins which potentially interact with each other are expressed as fusions with the GAL4 DBD and AD domains. If the fusion protein interacts, a functional transcription factor will be reconstituted through noncovalent interaction of two hybrid proteins, and subsequent activation of the reporter genes facilitates the phenotypicall detection of the protein-protein interaction.

The Y2H system is a powerful and sensitive method for detecting protein-protein interaction. The sensitivity and the usefulness of the system has been continuously improved since first developments of the system in 1989, mainly by increasing the number of the reporter genes (Durfee et al. 1993), by creation of smaller vectors for increased transformation

efficiency and by introduction of reporter genes (HIS3) with variable sensitivities for refined selection stringencies . The high sensitivity of the Y2H assay is due to an amplification of the positive signal at the transcriptional, translational and enzymatic activity level, which suggests that protein-protein interactions with dissociation constants (Kd) above ~70 μM (Yang et al. 1995) can be detected. Additionally, some of the weak and transient protein-protein interactions may not be possible to be biochemically detectable, but may be important for the proper function of the cell (Guarente 1993, Estojak et al. 1995).

The GAL4 Two-Hybrid System 3 commercially available from BD Biosciences-Clontech further introduces a new yeast strain, AH109, which contains three reporter genes under the control of distinct GAL4 promotor elements. Nutritional selection of three reporter genes with distinct promoter sequences and the ability to control the stringency of selection, greatly reduce the number of false positive clones, allowing efficient screening of complex cDNA libraries.

1.2 Screening of the RPE cDNA library

Due to the expression of bestrophin in the RPE, a bovine RPE cDNA AD fusion library was constructed previously (Schulz et al. 2004) and was used to search for interacting partners of bestrophin. The full length bovine bestrophin was initially used as bait, but control experiments demonstrated autonomous activation of this construct. Therefore, a series of truncated bestrophin baits was constructed. Baits were designed to cover the entire protein, with the exception of the stretches of hydrophobic amino acids which were assumed to being capable of activating transcription of the reporter genes in the absence of a true protein-protein interaction (Abedi et al. 2001). From the five truncated bestrophin baits, only the baits coding for the N-terminal (from aa 1-30) and loop (from aa 91-234) regions were suitable for the Y2H experiments. Interestingly, all three C-terminal derived baits of bestrophin autonomously activated the reporter genes and thus were not suitable for the Y2H screen. Bioinformatic analysis of the protein sequences of the C-terminal baits reveals the existence of a cluster of acidic amino acids ^{310}DDDD^{313} which may be responsible for self activation (Ruden DM, 1992).

Screening of more than 4 million clones from the bovine RPE cDNA library, with the two soluble baits of bestrophin yielded 53 putative positive clones, which were subsequently verified for the specificity of the interaction. In spite of the fact that the screen reached a 2.6 (loop region derived baits) and 4.3 fold (N-terminal derived baits) coverage, respectively, no genuine interaction could be confirmed following a number of verification experiments. With

the exception of spermidine/spermine N1-acetyltransferase (SSAT), all other putative positive clones were able to activate transcription of the reporter genes by unspecific interaction with GAL4 DBD alone and/or GAL4 DBD fused to human lamin C (LamC) which served as a negative control. There are various reasons for the unspecific activation of the reporter genes. A common explanation is that fusion proteins posses a domain which is able to recruit endogenous yeast transcription factors or which directly interacts with the RNA polymerase II, causing the activation of the reporter genes in the absence of a protein-protein interaction. Additional verification experiments such as GST pull down assays or coimmunoprecipitation experiments failed to co-precipitate bestrophin and SSAT, strongly suggesting a lack of interaction between these two proteins. In addition, to our best knowledge, no physiological relevance could be possibly established between bestrophin and SSAT, given that SSAT is an enzyme ubiquitously expressed which catalyzes the N(1)-acetylation of spermine and spermidine which play important role in DNA synthesis and gene expression.

Our findings emphasize a general disadvantage of the yeast two hybrid system. In particular, sticky proteins with unspecific protein affinity may bind to the bait giving rise to false positives. Also, the fusion proteins used in the two hybrid system have to be transported to and properly folded in the nucleus. This may cause problems, because for a large variety of proteins, such as membrane-anchored proteins, the nucleus does not represent the appropriate organelle for the folding, stability, and interaction with other partners. Our results suggest that bestrophin may not be suitable for traditional Y2H screens, or that construction of the truncated baits caused disruption of some not yet known interacting domains important for proper bestrophin function.

To overcome these problems, an alternative Y2H system was used, named Sos recruitment system (SRS) based on the reconstitution of the Ras signaling pathway (Aronheim et al. 1997). An advantage of the SRS system is that protein-protein interactions occur in the cytoplasm instead of the nucleus. It is therefore primarily suitable for membrane proteins and proteins that depend on post-translational modifications in the cytoplasm. The bovine RPE cDNA library used in the conventional Y2H system was recloned into the SRS-specific pMyr prey vector and screened with loop and C-terminal fragments of bestrophin. Verification of the putative positive clones however indicated that all identified clones appear to be temperature revertants and therefore false positive. Because of the high incidence of the false positive rate in the SRS system (174 false positives resulted from the screening of the ~ 1 million clones), efficient screening of the cDNA library was not practicable.

1.3 Limitations of the Y2H system

Despite the fact that Y2H screens in general represent a powerful and flexible in vivo assay to identify new interacting partners, this method cannot be applied to all types of proteins. The sequencing of genomes from various organisms and their subsequent analysis demonstrate that approximately 40% of all proteins contain hydrophobic domains which can anchor in the lipid bilayer and are unlikely to enter the nucleus (Goffeau et al. 1996). Transmembrane proteins are very difficult to handle experimentally, and the conventional Y2H is not optimized for the study of these proteins, although it has been successfully applied in some limited number of cases for the study of membrane proteins (Chervitz et al. 1998, Kegan and Cooper 1996).

A number of other limitations are intrinsic to the Y2H systems: (i) the fusion proteins used in the Y2H system need to be transported and properly folded in the nucleus, (ii) non-nuclear proteins can be difficult to detect, (iii) hybrid proteins may not be expressed stably in yeast or may not efficiently move into the nucleus, (iv) the creation of hybrid proteins may slow down the natural folding patterns of the proteins and (vi) yeast cells lack complex post-translational modification mechanisms needed by many proteins for proper function. In addition, transmembrane proteins that require oligomerization via interactions between their respective TMDs cannot be used in the Y2H system. Even with these and other limitations, the Y2H system remains an effective tool for the identification of protein-protein interactions.

2. Functional analysis of bestrophin domains

Since the discovery of VMD2 as the gene responsible for juvenile onset, autosomal-dominant BMD (Marquardt et al. 1998, Petrukhin et al. 1998), an additional three paraloguous members (VMD2-L1 to L3) encoding proteins with highly conserved RFP domains have been identified in a large number of phylogenetically distant species (Stöhr et al. 2002, Tsunenari et al. 2003, Krämer et al. 2004). The bestrophin proteins are integral membrane proteins expressed in a variety of tissues, and have been suggested to function as Ca^{+2} activated Cl^{-}-channels (Sun et al. 2002, Tsunenari et al. 2003, Qu et al. 2003, Qu and Hartzell 2004, Qu et al. 2004, Fischmeister and Hartzell 2005, Tsunenari et al. 2006). In order to examine the phylogenetic relationship between the bestrophins, and to further analyze the similarities and differences between bestrophins at the protein level, a comprehensive bioinformatics/phylogenetic analysis of the bestrophin protein family was performed.

2.1 Phylogenetic analysis of the bestrophin family

Phylogenetic analysis of a protein family can be instrumental in determining regions highly conserved among family members, and can be useful for identification of the structurally and functionally important regions (Eisen 1998). A comprehensive analysis of the publicly accessible databases and unfinished genomic sequence projects reveals presence of bestrophin family members in nearly all organisms for which the appropriate information is available. Despite extensive genomic sequence information from prokaryotes, fungi and plants, the presence of bestrophin sequences appears restricted to the animal kingdom. Members of the bestrophin family were identified in invertebrates (insects, nematodes), and vertebrates (mammals, birds, amphibians and fishes). Most species contain three or four bestrophin paralogous proteins, with the exception of *Caenorhabditis elegans* which may carry up to 26 putative bestrophin homologous (Sonnhammer and Durbin, 1997). The occurrence of the bestrophins in species phylogenetically distant as insects and mammals likely indicates the general importance of this protein in eukaryotic cell physiology.

A phylogenetic tree from 41 selected sequences of bestrophins from phylogenetically diverse species was generated using the Neighbor-Joining (NJ) distance method with statistical confidence measured by bootstrap analysis (see also Fig. 19). Vertebrate and invertebrate homologues of bestrophin are clearly separated in two clusters in an unrooted dendrogram. Within the vertebrate cluster of bestrophin homologues, the four paralogous proteins (VMD2, VMD2-L1 to L3) form separate, monophyletic groups, all with very high bootstrap support for each group (Fig. 19). An exception to this is the paralogous proteins from *Xenopus laevis* which appear to be related to the VMD2-L1 proteins. Invertebrate homologues of bestrophin could not be associated to any of the four vertebrate paralogous groups, probably because of the noticeable divergence at the amino acid sequence level. Present phylogenetic study supports the hypothesis that all bestrophin homologous proteins have probably evolved about 700 Myr ago from a common protein sequence before the divergence of the ancestral vertebrate and invertebrate species (Ota and Saitou, 1999).

2.2 Bestrophin orthologous and paralogous

Phylogenetic analysis of the bestrophin protein family revealed existence of four paralogous proteins in mammals. The four paralogous proteins form separate clusters with their respective orthologues from other mammalian species, indicating that the divergence of bestrophin into subfamilies occurred before the divergence of individual mammalian species.

A high level of protein sequence identity between different species suggests that each of the paralogous proteins could have a distinct evolutionaryly conserved function. Expression of the bestrophin paralogues appears to be restricted to tissues with polarized epithelial cells (Stöhr et al. 2002, Krämer et al. 2004). Bestrophin-1 is preferentially expressed in the RPE where it localizes to the basolateral plasma membrane (Marmorstein et al. 2000, Bakall et al. 2003). The subcellular localization of other paralogues of bestrophin (bestrophin-1 to 4) remains to be determined, but the presence of the 4 to 6 conserved hydrophobic domains suggests membrane localization similar to bestrophin-1.

Electrophysiological evidence demonstrated that all four human bestrophins can induce Cl^- currents in experimental over-expression system (Sun et al. 2002, Tsunenari et al. 2003). Distinctive channel properties of the individual bestrophins are further supporting the hypothesis that the bestrophin paralogues could have different function in different cell types (Tsunenari et al. 2003, Tsunenari et al. 2006).

2.3 Conserved motifs of bestrophin

The similarity between sequences of bestrophin from evolutionary divergent organisms is generally not high at the nucleotide level, however protein sequence conservation is a distinctive feature. The amino acid sequence alignment of 10 selected orthologues of bestrophin (Fig. 20) revealed several novel regions and motifs of unknown function that are conserved across bestrophin orthologues. Bestrophin orthologues used for the multiple alignment were selected from phylogenetically divergent species such as Zebrafish and Drosophila, which allowed distinction of conserved regions from neutrally evolving elements in the protein sequence. Four highly conserved regions (1-30aa, 75-107aa, 217-245 and 290-310aa) identified in all bestrophins examined correlate well with the site of the mutations in Best disease patients, suggesting crucial importance of these regions for the structure and function of bestrophin-1.

In addition to the high conservation on the amino acid sequence level between orthologues of bestrophin, nearly identical hydrophobicity plots (Fig. 29), with four major and two minor hydrophobic peaks, indicate that the orthologous proteins share the same membrane topology. Six potential TMDs of bestrophin (TMD1 28-50aa, TMD2 68-90aa, TMD3 130-149aa, TMD4 179-201aa, TMD5 269-291, and TMD6 269-300aa) were functionally characterized in this study using various molecular and biochemical assays and alternative model of the membrane topology of bestrophin with four TMDs was proposed.

Further comprehensive bioinformatics analysis of the conserved regions identified putative glycophorin A like dimerization motif located in the second TMD of all bestrophin orthologues examined. Glycophorin A is a well characterized erythrocyte membrane protein which can homodimerize in the detergent solution (Lemmon et al. 1992, Brosig and Langosch 1998). Based on saturation and insertion mutagenesis (Lemmon et al. 1992), the motif (^{75}LIxxGxxxGxxxT^{87}) within the TMD of glycophorin A was proposed to comprise the helix-helix interface essential for the dimerization (Fig. 42). In view of the fact that the bestrophins can dimerize/oligomerize (Sun et al. 2002, Stanton et al. 2006) via the N-terminal half of the protein, the conserved amino acid sequences located in the second TMD can therefore be considered as a potential candidate for oligomerization of the bestrophins. In addition, the second TMD of the bestrophins seems to participate in formation of the selectivity filter and appears to be an important region for channel function (Qu and Hartzell 2004, Qu et al. 2004, Qu et al. 2006).

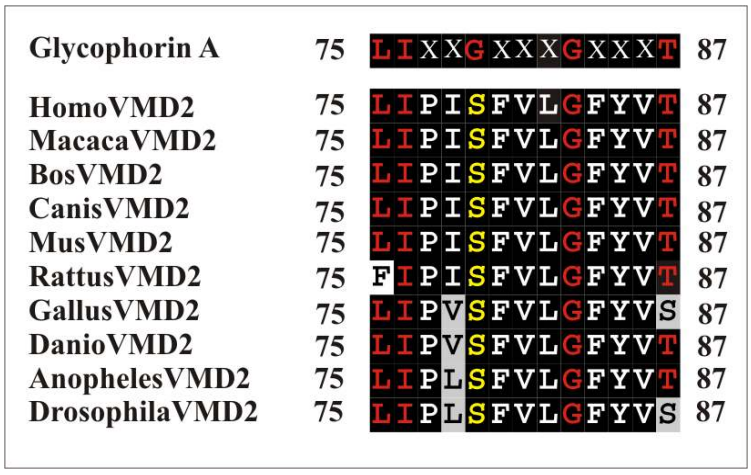

Fig. 42 Glycophorin A dimerization motif
The glycophorin A transmembrane segment homodimerizes to a right-handed pair of α-helices. The alignment of the TMD of glycophorin A with the second TMDs of bestrophin orthologous is shown. Identical residues implicated in self-asembly are in red letters, and simmilar sequences are in yellow letters.

Two putative dileucine lysosomal sorting signals conserved only in vertebrates were identified at positions ^{119}ExxxLL^{124} and ^{203}DxxLL^{207}. Dileucine and tyrosine based lysosomal sorting signals have a well established role in mediating lysosomal trafficking, endocytosis, and basolateral sorting in polarized epithelial cells (Kyttala et al. 2004). Although bestrophin localizes to the basolateral plasma membrane in RPE cells (Marmorstein et al. 2000) when overexpressed in HEK-293 cells, the vast majority of bestrophin-1 is found in intracellular compartments (Qu et al. 2003, Tsunenari et al. 2003). Intracellular distribution of bestrophin-1 can be caused by overexpression or it might suggest the intracellular function of bestrophin similar to the CLC-3 and CLC-7 chloride channels which have both plasma membrane and intracellular function (Jentsch et al. 2002). Existence of the potential dileucine lysosomal

sorting signals suggest lysosomal localization of the bestrophins, which may explain how a defect in the chloride channel could cause accumulation of the lipofuscin at the level of the RPE in the BMD patients. One possible explanation is that bestrophin act as a lysosomal Cl^- channel participating in proper acidification of the lysosomes. Since RPE cells phagocytose daily huge amounts of the shed disks of the photoreceptor outer segments (Young 1971), any dysfunction of Cl^- channels would result in disturbances of the lysosomal pH, which in turn would lead to impaired lysosomal function and consequently to the accumulation of undigested phagocytosed photoreceptor disks in the RPE cells. An increase in lysosomal pH has been associated with the accumulation of lipofuscin (Toimela et al. 1998, Shroyer et al. 2001), which makes a possible localization of the bestrophin to the lysosomal membranes an interesting research topic.

An additional well conserved site was identified in all bestrophin homologues and is composed of four consecutive aspartic acid residues ^{310}DDDD^{313}. Stretches of negatively charged aspartates can be involved in Ca^{+2} binding (Schreiber and Salkoff 1997, Tsunenari et al. 2006). The whole-cell, patch-clamp experiments imply that rise in intracellular Ca^{+2} concentrations can activate Cl^- conductance induced by heterologously expressed bestrophins (Sun et al. 2002). However it is not clear whether Ca^{+2} modulate Cl^- channel activity by directly binding to bestrophin or indirectly through protein phosphorylation cascade. Recent experiments on human bestrophin-4 protein in excised membrane patches (Tsunenari et al. 2006) indicate that Ca^{+2} is able to directly activate human bestrophin-4 in cell-free environment.

In addition to the conserved structural and functional features, various bioinformatics tools and pattern searches failed to identify known motifs in the two highly conserved regions of bestrophin from amino acid 1 to 30 and from 217 to 245. As a conclusion, in this study the phylogenetic relationship among members of the bestrophin family has been further clarified and additional conserved structural and functional motifs has been identified through sequence and phylogenetic analysis. Nevertheless, the exact function of newly identified motifs needs to be further investigated.

3. Topology of normal and mutant bestrophin

Bestrophin belongs to the RFP (arginine-phenylalanine-proline) family of integral membrane proteins (Stohr et al. 2002, Kramer et al. 2004) which appears to have four

paralogous proteins in mammals. Extensive electrophysiological evidence reported so far demonstrated that bestrophins can induce Cl^- currents when expressed heterologously (Sun et al. 2002, Tsunenari et al. 2003, Qu et al. 2003, Qu and Hartzell 2004, Qu et al. 2004, Tsunenari et al. 2006). The vast majority of known disease-associated alterations in bestrophin-1 are missense mutations which cluster near predicted TMDs. In order to assess consequences of point mutations on membrane integration and to further examine bestrophin topology, we have investigated its insertion into endoplasmic reticulum (ER) membrane.

3.1 Putative TMDs of bestrophin

Human bestrophin contains 6 hydrophobic segments which reveal hydrophobic profiles that can be considered as potential TMDs. The hydrophobicity profile of bestrophin with 4 major and two minor hydrophobicity peaks is well conserved between the bestrophin orthologues (Fig. 29), suggesting that all bestrophins share the same topology. The membrane topology of bestrophin based on hydropathy analysis and insertion of N-glycosylation and tobacco etch virus protease (TEVP) cleavage sites (Tsunenari et al. 2003), suggested that only 4 of these domains can traverse the membrane, with an additional hydrophobic domain dipped into the lipid bilayer, facing the extracellular space. Such complex topology indicates a mechanism of insertion in the membrane which is more complex than a simple sequential insertion of the hydrophobic domains.

3.2 Insertion of individual TMDs of bestrophin in the ER membrane

To systematically assess the membrane-spanning potential of the putative transmembrane segments of bestrophin, we applied an established *in vitro* translation/translocation Lep system. This method has been successfully applied for resolving the membrane topology of several integral membrane proteins (Zhang and Ling 1991, Skach and Lingappa 1993, Shelness et al. 1993, Gafvelin et al. 1997, Lehmann et a. 1997, van Geest et al. 1997, Lu et al. 1998). The signal anchor (SA) and stop transfer (ST) function of each potential TMD was assayed, both as an individual segment and in various truncated constructs of bestrophin.

Using Lep as insertion vehicle for bestrophin fragments, the H2 domain of Lep was replaced by six individual putative TMDs of bestrophin, and ability of the potential TMDs to insert into the membrane was assessed by the glycosylation status of the P2 domain. Four

potential TMDs with hydrophobicity values higher than the 1.6 threshold were able to insert into the ER membrane as evident by efficient glycosylation of the P2 domain. The lep construct containing the putative TMD4 was also able to insert into the membrane, although it was not as efficiently glycosylated as expected from its average hydrophobicity. The lep molecule containing the weakly hydrophobic TMD3 was inefficiently glycosylated suggesting lack of the SA activity in vitro. It is therefore unlikely that this hydrophobic segment can function as an authentic TMD in vivo. Analysis of the data from the insertion of the individual TMDs of bestrophin indicate that TMD1, -2, -4, -5 and -6 may function as SA sequences while TMD3 may not be integrated into the membrane of the ER microsomes.

3.3 Insertion of multiple TMDs of bestrophin into the ER membrane

To further clarify the SA potentials in particular of TMD3 and TMD4, the H2 segment of Lep was replaced with fusions containing paired adjacent putative TMDs, three consecutive putative TMDs and bestrophin fragments of increasing length. Consequently, the membrane topology was evaluated by glycosylation of the P2 domain of the fusion proteins.

In conclusion, from all putative TMDs examined only the marginally hydrophobic transmembrane segment TMD3 was not able to insert efficiently into the ER membrane as an individual segment. Further experiments involving adjacent and three consecutive TMDs of bestrophin clearly demonstrated inability of the TMD3 to act as a SA sequence in any of the constructs examined. On the other hand TMD4 exhibited moderate SA activity as an individual segment, but not in the neighbourhood of various truncated bestrophin constructs (Fig. 33-34). This may lead to an alternative explanation of our results with both TMD3 and TMD4 acting as transmembrane domains, and thus resulting likewise in an odd number of TMDs. However, such an interpretation would not be in agreement with the results from the glycosylation of constructs containing three consecutive TMDs (TMD1+2+3 and TMD4+5+6). Inability of the TMD4 to insert into the membrane in the context of the C-terminally truncated constructs indicates that the final topology of the bestrophin is not based solely on the hydrophobicity of its TMDs. Possibly, interaction of the putative TMDs and its flanking regions of the nascent polypeptide and translocon (Mothes et al. 1997, Monne et al. 2005) are crucial for acquiring proper topology of bestrophin in the ER membrane. Taking our *in vitro* translation/translocation data together, we suggest a topology model of bestrophin with four TMDs including TMD1, 2, 5 and 6 and a large cytoplasmatic hydrophobic loop between TMD2 and TMD5.

Contrary to our results, an alternative topological model of bestrophin, predicts that the marginally hydrophobic transmembrane segment, TMD4 is capable of inserting into the membrane, but that TMD5 not probably forming a reentrant loop (Tsunenari et al. 2003, Fig. 43). Possibly, both models are correct, since our in vitro translation/translocation system can not distinguish if TMD5 act as an authentic TMD or as a reentrant loop because of its high hydrophobicity. Although in both models TMDs 1, 2 and 6 are inserted into the membrane, our model is in better agreement with the hydrophobicity profile data, with two helical hairpins TMD1-2, and TMD5-6, which are the preferred structural element in membrane proteins (von Heijne 1999).

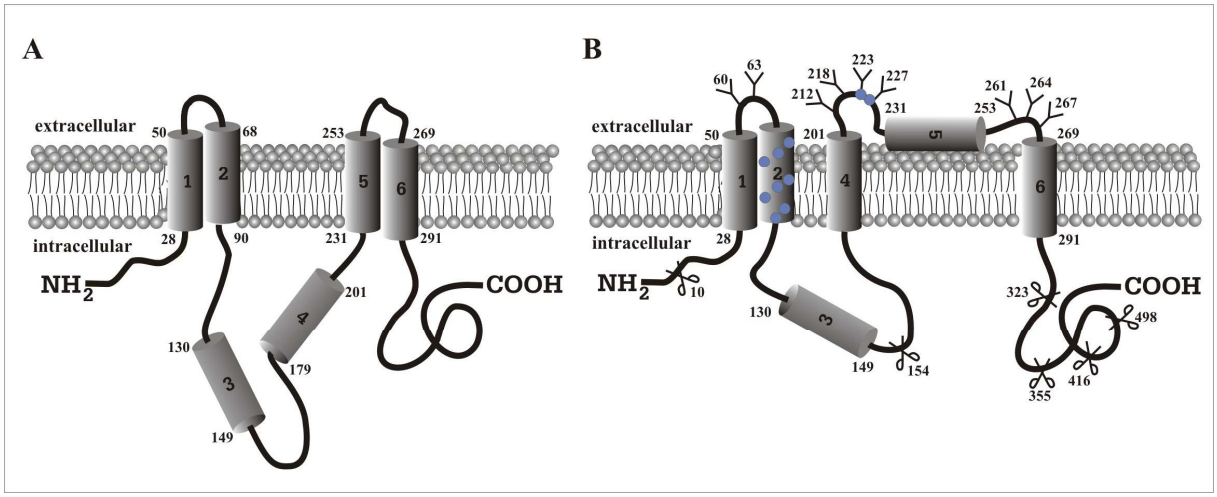

Fig. 43 Comparison between the two membrane topology models of bestrophin
A, model of the membrane topology of bestrophin in the ER membranes suggested by the in vitro transcription/translocation data obtained in this study. **B,** model of the bestrophin topology supported by experiments based on the: (i) insertion of the glycosylation sites (schematically depicted as a sugar chains on the extracellular side), (ii) insertion of the TEVP cleavage sites (represented with the scissors) and (iii) the introduction of the cysteine residues and subsequent treatment with MTSET (Tsunenari et al. 2003).

To resolve the disagreement between the two current topological models of bestrophin, cysteine scanning mutagenesis was employed. An important prerequisite for the cysteine scanning mutagenesis is the localization of the protein of interest in the plasma membrane. However, in our system the vast majority of the overexpressed bestrophin was localized to the intracellular membranes and not to the plasma membrane, in agreement with results from previous studies (Qu et al. 2003, Tsunenari et al. 2003). Additional studies on intact bestrophin are necessary to resolve the disagreement between the two topological models of bestrophin.

3.4 Effect of the BMD mutations on the topology of bestrophin

A considerable number of Best disease-causing mutations is located within 6 putative TMDs of bestrophin-1. To elucidate the mechanism by which single amino acid changes lead to disease phenotype, we tested the effect of disease-associated alterations on SA activity of various truncated constructs of bestrophin. Eighteen mutations located in the putative transmembrane segments and in the immediate flanking regions of TMD1 and TMD6 were examined. We found that mutations involving polar and charged residues were able to significantly diminish the ability of the TMDs to insert into the membrane. This results correlate with the finding that a high proportion of mutations occurring in TMDs of membrane proteins linked to human disease have been found to involve gain or loss of polar residues (Partridge et al. 2004). In turn, this may result in decreased folding efficiency and stability of the mutated proteins. Folding efficiency of the number of integral membrane proteins (Schubert et al. 2000, Turner and Varshavsky 2000) was found to be significantly lower than 100%, as for example cystic fibrosis transmembrane conductance regulator (CFTR) appears to be assembled with less then 50% efficiency (Kopito, 1999). For a protein with folding efficiency over 50% at body temperature, a single amino acid exchange which results in 1.5 kcal/mol change in free energy is sufficient to reduce the folding efficiency to less than 10% (Guerois et al. 2002). In summary, the present study suggests that the interaction between topogenic determinants encoded within transmembrane segments and their flanking residues are necessary for the successful folding of bestrophin. In addition, this study provides evidence that even subtle changes in protein sequence can substantially influence the topogenic behavior of mutated bestrophin.

7. References

[1]OMIM: http://www.ncbi.nlm.nih.gov/entrez/query.fcgi?db=OMIM

Abedi M, Caponigro G, Shen J, Hansen S, Sandrock T and Kamb A. 2001. Transcriptional transactivation by selected short random peptides attached to lexA-GFP fusion proteins. BMC Molecular Biology. 2:10.

Altschul SF, Madden TL, Schaffer AA, Zhang J, Zhang Z, Miller W, Lipman DJ. 1997. Gapped BLAST and PSI-BLAST: a new generation of protein database search programs. Nucleic Acids Res. 25(17):3389-402.

Arden GB, Barrada A and Kelsy JH. 1962. New clinical test of retinal function based on the standing potential of the eye. Brit J Ophthalmol. 46: 449-467.

Aronheim A, Zandi E, Hennemann H, Elledge SJ, Karin M. 1997. Isolation of an AP-1 repressor by a novel method for detecting protein-protein interactions. Mol Cell Biol. 17(6):3094-102.

Bakall B, Marmorstein LY, Hoppe G, Peachey NS, Wadelius C, Marmorstein AD. 2003. Expression and localization of bestrophin during normal mouse development. Invest Ophthalmol Vis Sci. 44(8):3622-8.

Bartel PL, Fields S. 1995. Analyzing protein-protein interactions using two-hybrid system. Methods Enzymol. 254:241-63.

Best F. 1905. Uber eine hereditare Maculaaffektion. Z Augenheilk. 13: 199-212

Blobel G. 1980. Intracellular protein topogenesis. Proc Natl Acad Sci USA. 77:1496-1500.

Bonifacino JS, Traub LM. 2003. Signals for sorting of transmembrane proteins to endosomes and lysosomes. Annu Rev Biochem. 72:395-447.

Brosig B, Langosch D. 1998. The dimerization motif of the glycophorin A transmembrane segment in membranes: importance of glycine residues. Protein Sci. 7(4):1052-6.

Casey JR., Ding Y , Kopito RR. 1995.The role of cysteine residues in the erythrocyte plasma membrane anion exchange protein, AE1. J Biol Chem, 270;15:8521-8527.

Chen C, Okayama H. 1987. High-efficiency transformation of mammalian cells by plasmid DNA. Mol Cell Biol. 7(8):2745-52.

Chervitz SA, Aravind L, Sherlock G, Ball CA, Koonin EV, Dwight SS, Harris MA, Dolinski K, Mohr S, Smith T, Weng S, Cherry JM, Botstein D. 1998. Comparison of the complete protein sets of worm and yeast: orthology and divergence. Science. 11;282(5396):2022-8.

Chien CT, Bartel PL, Sternglanz R, Fields S. 1991. The two-hybrid system: a method to identify and clone genes for proteins that interact with a protein of interest. Proc Natl Acad Sci USA.88(21):9578-82.

Deutmann AF. 1971. The hereditary dystrophies of the posterior pole of the eye. Assen, Van Gorcum; 198.

Dunn KC, Aotaki–Keen AE, Putkey FR, Hjelmeland LM. 1996. ARPE-19, a human retinal pigment epithelial cell line with differentiated properties. Exp Eye Res. 62.155-169.

Durfee T, Becherer K, Chen PL, Yeh SH, Yang Y, Kilburn AE, Lee WH, Elledge SJ. 1993. The retinoblastoma protein associates with the protein phosphatase type 1 catalytic subunit. Genes Dev. 7(4):555-69.

Eisen JA. 1998. Phylogenomics: improving functional predictions for uncharacterized genes by evolutionary analysis. Genome Res.8(3):163-7.

Estojak J, Brent R, Golemis EA. 1995. Correlation of two-hybrid affinity data with in vitro measurements. Mol Cell Biol. 15(10):5820-9.

Felsenstein J. 1988. Phylogenies from molecular sequences: inference and reliability. Ann Rev Genet. 22:521-565.

Felsenstein J. 1989. PHYLIP - Phylogeny Inference Package (Version 3.2). Cladistics 5: 164-166.

Fields S, Song O. 1989. A novel genetic system to detect protein-protein interactions. Nature. 20;340(6230):245-6.

Fischmeister R, and Hartzell HC. 2005. Volume sensitivity of the bestrophin family of chloride channels. J Physiol. 562. 477–491.

Forsman K, Graff C, Nordstrom S, Johansson K, Westermark E, Lundgren E, Gustavson K-H, Wadelius C, Holmgren G. 1992. The gene for Best's macular dystrophy is located at 11q13 in a Swedish family. Clin Genet. 42:156-159.

Freshney RI. 2000. Culture of animal cells, a manual of basic techniques. New York. John Wiley&Sons.

Friedlander M, and Blobel G. 1985. Nature. 318: 338-343.

Gafvelin G, Sakaguchi M, Andersson H, von Heijne G. 1997. Topological rules for membrane protein assembly in eukaryotic cells. J Biol Chem. 1997;272:6119-6127.

Gietz D, St Jean A, Woods RA and RH Schiestl. 1992. Improved method for high efficiency transformation of intact yeast cells. Nucl Acids Res. 20: 1425.

Godel V, Chaine G, Regenbogen L, Coscas G. 1986. Best's vitelliform macular dystrophy. Acta Ophthalmol Suppl. 175:1-31.

Goffeau A, Barrell BG, Bussey H, Davis RW, Dujon B, Feldmann H, Galibert F, Hoheisel JD, Jacq C, Johnston M, Louis EJ, Mewes HW, Murakami Y, Philippsen P, Tettelin H, Oliver SG. 1996. Life with 6000 genes. Science. 25;274(5287):546, 563-7.

Graff C, Forsman K, Larsson C, Nordstrom S, Lind L, Johansson K, Sandgren O, Weissenbach J, Holmgren G, Gustavson KH, Wadelius C. 1994. Fine mapping of Best's macular dystrophy localizes the gene in close proximity to but distinct from the D11S480/ROM1 loci. Genomics. 24: 425-434.

Graff C, Eriksson A, Forsman K, Sandgren O, Holmgren G, Wadelius C. 1997. Refined genetic localization of the Best disease gene in 11q13 and physical mapping of linked markers on radiation hybrids. Hum Genet. 101: 263-270.

Guarente L. 1993. Strategies for the identification of interacting proteins. Proc Natl Acad Sci USA. 1;90(5):1639-41.

Guerois R, Nielsen JE, Serrano L. 2002. Predicting changes in the stability of proteins and protein complexes: a study of more than 1000 mutations. J Mol Biol. 320(2):369-87.

Hedges SB. 2002. The origin and evolution of model organisms. Nature Rev. Genet. 3. 838-849.

Hou YC, Richards JE, Bingham EL, Pawar H, Scott K, Segal M, Lunetta KL, Boehnke M, Sieving PA. 1996. Linkage study of Best's vitelliform macular dystrophy (VMD2) in a large North American family. Hum Hered. 46: 211-220.

Jentsch TJ, Stein V, Weinreich F, and Zdebik AA. 2002. Molecular structure and physiological function of chloride channels. Physiol Rev 82: 503–568.

Johansson M, Nilsson I, and von Heijne G. 1993. Mol Gen Genet. 239. 251-256.

Keegan K, Cooper JA. 1996. Use of the two hybrid system to detect the association of the protein-tyrosine-phosphatase, SHPTP2, with another SH2-containing protein, Grb7. Oncogene. 4;12(7):1537-44.

Kopito RR. 1999. Biosynthesis and degradation of CFTR. Physiol Rev. 79(1 Suppl):S167-73.

Kramer F, White K, Pauleikhoff D, Gehrig A, Passmore LA, Rudolph G, Kellner U, Andrassi M, Lorenz B, Rohrschneider K, Blankenagel A, Jurklies B, Schilling H, Holz FG and Weber BH. 2000. Mutations in the VMD2 gene are associated with juvenile-onset vitelliform macular dystrophy (Best's disease) and adult vitelliform macular dystrophy but not age-related macular degeneration. Eur J Hum Genet. 8:286-292

Kramer F, Mohr N, Kellner U, Rudolph G, Weber BHF (2003) Ten novel mutations in the VMD2 gene associated with Best macular dystrophy (BMD). Hum Mut 22:418

Kramer F, Stohr H, Weber BH. 2004. Cloning and characterization of the murine Vmd2 RFP-TM gene family. Cytogenet Genome Res. 105(1):107-14.

Kyte J. and Doolittle RF. 1982. A simple method for displaying the hydropathic character of a protein. J Mol Biol. 157: 105-132.

Kyttala A, Ihrke G, Vesa J, Schell MJ, Luzio JP. 2004. Two motifs target Batten disease protein CLN3 to lysosomes in transfected nonneuronal and neuronal cells. Mol Biol Cell. 15(3):1313-23.

Lehmann S, Chiesa R, Harris DA. 1997. Evidence for a six-transmembrane domain structure of presenilin 1. J Biol Chem. 272:12047-12051.

Lemmon MA, Flanagan JM, Hunt JF, Adair BD, Bormann BJ, Dempsey CE, Engelman DM. 1992. Glycophorin A dimerization is driven by specific interactions between transmembrane alpha-helices. J Biol Chem.267(11):7683-9.

Lingappa VR, Lingappa J R, and Blobel G. 1979. Chicken ovalbumin contains an internal signal sequence. Nature. 281: 117-121.

Lu Y, Xiong X, Helm A, Kimani K, Bragin A, Skach WR. 1998. Co- and posttranslational translocation mechanisms direct cystic fibrosis transmembrane conductance regulator N terminus transmembrane assembly. J Biol Chem. 273:568-576.

Marmorstein AD, Marmorstein LY, Rayborn M, Wang X, Hollyfield JG, Petrukhin K. 2000. Bestrophin, the product of the Best vitelliform macular dystrophy gene (VMD2), localizes to the basolateral plasma membrane of the retinal pigment epithelium. Proc Natl Acad Sci USA. 97(23):12758-63.

Marquardt A, Stöhr H, Passmore LA, Krämer F, Rivera A and Weber BH. 1998. Mutations in a novel gene, VMD2, encoding a protein of unknown properties causejuvenile-onset vitelliform macular dystrophy (Best's disease). Hum Mol Genet. 7:1517-1525.

Matsuoka S, Nicoll DA, Hryshko LV, Levitsky DO, Weiss JN, Philipson KD. 1995. Regulation of the cardiac $Na^{(+)}$-Ca^{2+} exchanger by Ca^{2+}. Mutational analysis of the $Ca^{(2+)}$-binding domain. J Gen Physiol. 105(3):403-20.

Miller JH. 1972. Experiments in Molecular Genetics (Cold Spring Harbor Laboratory, Cold Spring Harbor, NY)

Mohler CW and Fine SL. 1981. Long-term evaluation of patients with Best's vitelliform dystrophy. Ophthalmology. 88: 688-92.

Monne M, Hessa T, Thissen L, von Heijne G. 2005. Competition between neighboring topogenic signals during membrane protein insertion into the ER. FEBS J. 272(1):28-36.

Mothes W, Heinrich SU, Graf R, Nilsson I, von Heijne G, Brunner J, Rapoport TA. 1997. Molecular mechanism of membrane protein integration into the endoplasmic reticulum. Cell. 89(4):523-33.

Nichols BE, Bascom R, Litt M, McInnes R, Sheffield VC, Stone EM. 1994. Refining the locus for Best vitelliform macular dystrophy and mutation analysis of the candidate gene ROM1. Am J Hum Genet. 54: 95-103.

Nilsson I, and von Heijne G. 1993. Determination of the distance between the oligosaccharyltransferase active site and the endoplasmic reticulum membrane. J Biol Chem. 268: 5798-580.

Nilsson I, Whitley P, von Heijne G. 1994. The COOH-terminal ends of internal signal and signal-anchor sequences are positioned differently in the ER translocase. J Cell Biol. 126 (5):1127-32.

Nordstrom S. 1974. Hereditary macular degeneration-a population survey in the country of Vsterbotten, Sweden. Hereditas. 78(1):41-62.

O'Gorman S, WA Flaherty, GA Fishman, and EL Berson. 1988. Histopathologic findings in Best's vitelliform macular dystrophy. Arch. Ophthalmol. 106: 1261-1268

Ota S, Saitou N. 1999. Phylogenetic relationship of muscle tissues deduced from superimposition of gene trees. Mol Biol Evol. 16(6):856-67.

Partridge AW, Therien AG, Deber CM. 2002. Polar mutations in membrane proteins as a biophysical basis for disease. Biopolymers. 66(5):350-8.

Partridge AW, Therien AG, Deber CM. 2004. Missense mutations in transmembrane domains of proteins: phenotypic propensity of polar residues for human disease. Proteins. 54(4):648-56.

Petrukhin K, Koisti MJ, Bakall B, Li W, Xie G, Marknell T, Sandgren O, Forsman K, Holmgren G, Andreasson S, Vujic M, Bergen AA, McGarty-Dugan V, Figueroa D, Austin CP, Metzker ML, Caskey CT, and Wadelius C. 1998. Identification of the gene responsible for Best macular dystrophy. Nature Genet. 19. 241-247.

Pinckers A, Cuypers MH, Aandekerk AL. 1996. The EOG in Best's disease and dominant cystoid macular dystrophy (DCMD). Ophthalmic Genet. 17:103-108

Puck TT, Cieciura SJ, and Robinson A. 1958. Genetics of somatic mammalian cells : III long-term cultivation of euploid cells from human and animal subjects. J Exp Med. 1958. 108: 945-956.

Qu Z, Wei RW, Mann W, and Hartzell HC. 2003. Two bestrophins cloned from Xenopus laevis oocytes express $Ca2^{+}$-activated Cl^{-} currents. J Biol Chem. 278. 49,563–49,572.

Qu Z, and Hartzell C. 2004. Determinants of anion permeation in the second transmembrane domain of the mouse bestrophin-2 chloride channel. J Gen Physiol. 124. 371–382.

Qu Z, Fischmeister R, and Hartzell C. 2004. Mouse bestrophin-2 is a bona fide Cl–channel: identification of a residue important in anion binding and conduction. J Gen Physiol. 123. 327–340.

Qu Z, Chien LT, Cui Y, Hartzell HC. 2006. The anion-selective pore of the bestrophins, a family of chloride channels associated with retinal degeneration. J Neurosci. 17;26(20):5411-9.

Ruden DM. 1992. Activating regions of yeast transcription factors must have both acidic and hydrophobic amino acids. Chromosoma. 101(5-6):342-8.

Saitou N, Nei M. 1987. The neighbor-joining method: a new method for reconstructing phylogenetic trees. Mol Biol Evol. (4):406-25.

Sambrook J, Fritsch EF and Maniatis T. 1989. Molecular cloning: A labarotory manual. 2nd Edition. Cold Spring Harbor, New York: Cold Spring Harbor Laboratory Press.

Scholl HP, Schuster AM, Vonthein R, Zrenner E. 2002. Mapping of retinal function in Best macular dystrophy using multifocal electroretinography. Vision Res. 42(8):1053-61.

Schulz HL, Rahman FA, Fadl El Moula FM, Stojic J, Gehrig A, Weber BH. 2004. Identifying differentially expressed genes in the mammalian retina and the retinal pigment epithelium by suppression subtractive hybridization. Cytogenet Genome Res. 106(1):74-81.

Schreiber M, and Salkoff L. 1997. A novel calcium-sensing domain in the BK channel. Biophys J. 73:1355-1363.

Shroyer NF, Lewis RA, and Lupski JR. 2001. Analysis of the ABCR (ABCA4) gene in 4-aminoquinoline retinopathy: is retinal toxicity by chloroquine and hydroxychloroquine related to Stargardt disease? Am J Ophthalmol 131: 761–766.

Schubert U, Anton LC, Gibbs J, Norbury CC, Yewdell JW, Bennink JR. 2000. Rapid degradation of a large fraction of newly synthesized proteins by proteasomes. Nature. 404(6779):770-4.

Shelness GS, Lin L, Nicchitta CV. 1993. Membrane topology and biogenesis of eukaryotic signal peptidase. J Biol Chem. 268:5201-5208.

Skach WR, Lingappa VR. 1993. Amino-terminal assembly of human P-glycoprotein at the endoplasmic reticulum is directed by cooperative actions of two internal sequences. J Biol Chem. 268:23552-23561.

Sonnhammer ELL and Durbin R. 1997. Analysis of protein domain families in Caenorhabditis elegans. Genomics. 46:200-216.

Stanton JB, Goldberg AF, Hoppe G, Marmorstein LY, Marmorstein AD. 2006. Hydrodynamic properties of porcine bestrophin-1 in Triton X-100. Biochim Biophys Acta. 1758(2):241-7.

Stöhr H, Weber BH. 1995. A recombination event excludes the ROM1 locus from the Best's vitelliform macular dystrophy region. Hum Genet. 95(2):219-22.

Stöhr H, Marquardt A, Rivera A, Cooper PR, Nowak NJ, Shows TB, Gerhard DS, Weber BH. 1998. A gene map of the Best's vitelliform macular dystrophy region in chromosome 11q12-q13.1. Genome Res. 8(1):48-56.

Stöhr H, Marquardt A, Nanda I, Schmid M, and Weber BH. 2002. Three novel human VMD2-like genes are members of the evolutionary highly conserved RFP-TM family. Eur J Hum Genet 10. 281–284.

Stöhr H, Milenkowic V, Weber BH. 2005. VMD2 and its role in Best's disease and other retinopathies. Ophthalmologe. 102(2):116-21.

Stone EM, Nichols BE, Streb LM, Kimura AE, Sheffield VC. 1992. Genetic linkage of vitelliform macular degeneration (Best's disease) to chromosome 11q13. Nature Genet. 1: 246-250.

Sun H, Tsunenari T, Yau KW, and Nathans J. 2002. The vitelliform macular dystrophy protein defines a new family of chloride channels. Proc Natl Acad Sci USA. 99. 4008–4013.

Thompson JD, Higgins DG, Gibson TJ. 1994. CLUSTAL W: improving the sensitivity of progressive multiple sequence alignment through sequence weighting, position-specific gap penalties and weight matrix choice. Nucleic Acids Res. 11; 22(22):4673-80.

Toimela T, Salminen L, and Tahti H. 1998. Effects of tamoxifen, toremifene and chloroquine on the lysosomal enzymes in cultured retinal pigment epithelial cells. Pharmacol Toxicol. 83: 246–251.

Tsunenari T, Sun H, Williams J, Cahill H, Smallwood P, Yau KW, and Nathans J. 2003. Structure-function analysis of the bestrophin family of anion channels. J Biol Chem. **278.** 41,114–41,125.

Tsunenari T, Nathans J, Yau KW. 2006. $Ca2^{+}$-activated Cl^{-} current from human bestrophin-4 in excised membrane patches. J Gen Physiol. 127(6):749-54.

Turner GC, Varshavsky A. 2000. Detecting and measuring cotranslational protein degradation in vivo. Science. 289(5487):2117-20.

Van de Peer Y, De Wachter R. 1994. TREECON for Windows: a software package for the construction and drawing of evolutionary trees for the Microsoft Windows environment. Comput Applic Biosci. 10. 569-570.

van Geest M, Nilsson I, von Heijne G, Lolkema JS. 1999. Insertion of a bacterial secondary transport protein in the endoplasmic reticulum membrane. J Biol Chem.274(5):2816-23.

von Heijne G. 1992. Membrane protein structure prediction- hydrophobicity analysis and the positive inside rule. J Mol Biol. 225: 487-494.

von Heijne G. 1994. Membrane proteins: from sequence to structure. Annu Rev Biophys Biomol Struct 23:167-192.

von Heijne G. 1999. Recent advances in the understanding of membrane protein assembly and structure. Q Rev Biophys. 32(4):285-307.
Weber BH, Stöhr H, Walker D. 1994a. A case of nonpenetrance in Best's disease. Am J Ophthalmol.118(3):398-9.

Weber BH, Vogt G, Stöhr H, Sander S, Walker D, Jones C. 1994b. High-resolution meiotic and physical mapping of the best vitelliform macular dystrophy (VMD2) locus to pericentromeric chromosome 11. Am J Hum Genet. 55:1182-7.

Weber BH, Walker D, Muller B, Mar L. 1994c. Best's vitelliform dystrophy (VMD2) maps between D11S903 and PYGM: no evidence for locus heterogeneity. Genomics. 20(2):267-74.

White K, Marquardt A and Weber BH. 2000. VMD2 mutations in vitelliform macular dystrophy (Best disease) and other maculopathies. Hum Mutat. 15:301-308

www.uni-wuerzburg.de/humangenetics/vmd2.html

Yang M, Wu Z, Fields S. 1995. Protein-peptide interactions analyzed with the yeast two-hybrid system. Nucleic Acids Res. 11;23(7):1152-6.

Young RW. 1971. The renewal of rod and cone outer segments in the rhesus monkey. J. Cell Biol. 49, 303-318.

Young JM, Cheadle C, Foulke JS Jr, Drohan WN, Sarver N. 1988. Utilization of an Epstein-Barr virus replicon as a eukaryotic expression vector. Gene. 62(2):171-85.

Zdobnov EM, von Mering C, Letunic I, Torrents D, Suyama M, Copley RR, Christophides GK, Thomasova D, Holt RA, Subramanian GM, Mueller HM, Dimopoulos G, Law JH, Wells MA, Birney E, Charlab R, Halpern AL, Kokoza E, Kraft CL, Lai Z, Lewis S, Louis C, Barillas-Mury C, Nusskern D, Rubin GM, Salzberg SL, Sutton GG, Topalis P, Wides R, Wincker P, Yandell M, Collins FH, Ribeiro J, Gelbart WM, Kafatos FC, Bork P. 2002. Comparative genome and proteome analysis of Anopheles gambiae and Drosophila melanogaster. Science. 298. 149-159.

Zhang JT, Ling V. 1991. Study of membrane orientation and glycosylated extracellular loops of mouse P-glycoprotein by in vitro translation. J Biol Chem. 266:18224-18232.

8. Appendix

List of abbreviations

3AT	3-amino-1,2,4-triazole
aa	amino acid
AD	activating domain
ADVIRC	autosomal dominant vitreo-retino-choroidopathy
AMD	age-related macular degeneration
APS	ammonium persulphate
AVMD	adult vitelliform macular dystrophy
BLAST	Basic Local Alignment Search Tool
BMD	Best´s macular dystrophy
bp	base pair
BSA	bovine serum albumine
cDNA	complementary DNA
cGMP	cyclic guanosine monophosphate
CMV	cytomegalovirus
DBD	DNA binding domain
ddH_20	double destiled water
DNA	double stranded DNA
dNTP	desoxynucleosidtriphosphate
DTT	dithiothreitol
EDTA	ethylenediaminetetraacetic acid
EOG	electro-oculography
ER	endoplasmatic reticulum
ERG	electro-retinography
EST	expressed sequenced tags
GST	gluthathione S-transferase
HEK	human embryonic kidney
IPTG	Isopropyl-β-D-thiogalactopyranoside
kb	kilo base pairs
kDa	kilo Dalton
LamC	lamin C
LAMP1	lysosomal associated membrane protein 1
LB	Luria Bertani media
LP	light peak
LYIA	lucifer yellow iodacetamide
M	molarity
MBP	maltose binding protein
MCS	multiple cloning site
min	minute
ml	mililiter
µ	micro-
MOPS	morpholinopropanesulfonic acid
MTSET	2-(Trimethylammonium) ethyl]methanethiosulfonate bromide
OD	optical density
OMIM	Online Mendelian Inheritance in Man
ONPG	o-nitrophenol β-D-galactopyranoside
PAA	polyacrylamid
pAB	polyclonal antibody
PBS	phosphate-buffered saline
PCR	polymerase chain reaction
PEG	polyethylenglycol
RFP-TM	arginine (R) phenylalanine (F) proline (P) transmembrane
RNA	ribonucleic acid
RPE	retinal pigment epithelium
rpm	rounds per minute
RT PCR	reverse trnscriptase PCR
s	seconds
SD	synthetic dextrose
SA	signal anchor
SDS	sodium dodecyl sulfate
SDS-PAGE	SDS-polyacrylamide gel electrophoresis
SSAT	spermidine/spermine N1-acetyltransferase
SRS	Sos recruitment system
ssDNA	single stranded DNA
SSH	suppression subtractive hybridization
ST	stop transfer
SV40	Simian virus 40
TEMED	N,N,N',N'-Tetramethylethylenediamine
TEVP	tobacco etch virus protease
TMD	transmembrane domain
Tris	Tris-(hydroxymethyl) aminomethane
U	units
VMD2	vitelliform macular dystrophy type 2
v/v	percentage volume to volume
w/v	percentage weight to volume
Y2H	yeast two hybrid

Table I General primers

Gene / Plasmid	Primer name	Primer sequence (5´-3´)
pCEP4	**pCEP-F**	AGCAGAGCTCGTTTAGTGAACCG
pCEP4	**EBV-R**	TGTGGTTTGTCCAAACTCATC
pcDNA3	**pcDNA3-F**	CTCGGATCCACTAGTAACGG
pcDNA3	**pcDNA3-R**	TAGGGCCCTCTAGATGCATG
pGADT7	**AD-T7-F**	CGATGATGAAGATACCCCAC
pGADT7	**3'AD-R**	AGATGGTGCACGATGCACAG
pGBKT7	**BD-T7-F**	CGGAAGAGAGTAGTAACAAAGG
pGBKT7	**3'BD-R**	TTTTCGTTTTAAAACCTAAGAGTC
pGEX	**pGEX-F**	GGGCTGGCAAGCCACGTTTGGTG
pGEX	**pGEX-R**	CCGGGAGCTGCATGTGTCAGAGG
pSOS	**Sos5´-F**	CCAAGACCAGGTACCATG
pSOS	**Sos3´-R**	GCCAGGGTTTTCCCAGT
pMyr	**Myr5`-F**	ACTACTAGCAGCTGTAATAC
pMyr	**Myr3`-R**	CGTGAATGTAAGCGTGACAT
GUSB	**GUS B3**	ACTATCGCCATCAACAACACACTGACC
GUSB	**GUS B5**	GTGACGGTGATGTCATCGAT
GUSB	**GUS B6**	GATCCACCTCTGATGTTCAC
GUSB	**GUS B7**	CCTTTAGTGTTCCCTGCTAG
G3PDH	**G3PDH-F**	ATCGTGGAAGGACTCATGACC
G3PDH	**G3PDH-R**	AGCGCCAGTAGAGGCAGGGAT
hAE1	**hAE1-5R**	CGGAACGCACGGTGGTGGCA
hAE1	**hAE1-1R**	TCTCCAGTGAGGAGTGTTGG
hAE1	**hAE1-2R**	TCAGGTAATAGGGGTAGCGG
hAE1	**hAE1-3R**	GGCTGTGTTGGGCAGGGGGC
hAE1	**hAE1-4F**	AGCCAGCACCCCAGGGGCTG
hAE1	**hAE1-4R**	CAGCCCCTGGGGTGCTGGCT
hAE1	**hAE1-HindIII-F**	CTAGAAGCTTATGGAGGAGCTGCAGGATGA
hAE1	**hAE1-XhoI-R**	CGGCCTCGAGCGCACAGGCATGGCCACTTCGTC
hSSAT	**hSSAT-KpnI-F**	CTAGGGTACCATGGCTAAATTCGTGATCCG
hSSAT	**hSSAT-SfiI-R**	TGGCCTTGCCGGCCTCTCCTCTGTTGCCATTTTTA
hTTR	**hTTR-KpnI-F**	TAGGGTACCATGGCTTCTATCGTCTGCT
hTTR	**hTTR-SfiI-R**	TGGCCTTGCCGGCCTTTCCTTGGGATTGGTGACGA
hVMD2	**hVMD2-HindIII-F**	CTAGAAGCTTATGACCATCACTTACACAAG
hVMD2	**hVMD2-o334-SfiI-R**	TGGCCTTGCCGGCCTGTGATCTTTGAGTGTAGTGT
hVMD2	**hVMD2-1-55-BamHI-R**	CATGGATCCCGTGAGGGCCAGCCTATAAAT
hVMD2	**hVMD2-1-95-BamHI-R**	CATGGATCCGTTCCACCAGCGGGTCACGAC
hVMD2	**hVMD2-1-150-BamHI-R**	CATGGATCCGCGCTTGTAGACTGCGGTGCT
hVMD2	**hVMD2-1-201-BamHI-R**	CATGGATCCGATTCGACCTCCAAGCCACGC
hVMD2	**hVMD2-1-255-BamHI-R**	CATGGATCCCCGCCCAACTAGACAAGTCAG
hVMD2	**hVMD2-368-BamHI-R**	CATGGATCCCAGGCTGATGTTGAAGGTGGA
hVMD2	**hVMD2-KpnI-F**	CTAGGGTACCATGACCATCACTTACACAAG
hVMD2	**hVMD2-SfiI-R**	TGGCCTTGCCGGCCTGGAATGTGCTTCATCCCTGT
pMyr	**pMyr-var1F**	AATTCCCGGGCTCGAGCGGCCG
pMyr	**pMyr-var1-R**	TCGACGGCCGCTCGAGCCCGGG
pMyr	**pMyr-var2-F**	AATTCCCCGGGCTCGAGCGGCCG
pMyr	**pMyr-var2-R**	TCGACGGCCGCTCGAGCCCGGGG
pMyr	**pMyr-var3-F**	AATTCCCCCGGGCTCGAGCGGCCG
pMyr	**pMyr-var3-R**	TCGACGGCCGCTCGAGCCCGGGGG
bVMD2	**bVMD2-CT-3-F**	AGCTGAATTCCTGGATAAGGAAGACATGGA
bVMD2	**bVMD2-CT-3-R**	CGATGGATCCTGTGCTTCATCCCTGTTTTC
pSos	**pSos-CT-1&2-F**	AGTCGGATCCCAGAGCAGCTCATCAACCCA
pSos	**pSos-loop-F**	AGTCGGATCCGATGGAACCAGTATGAGAACCT

pSos	**pSos-Nter-F**	AGTCGGATCCGAATGACCGTCACCTACTCGAGCCA
pSos	**pSos-CT-3-F**	AGTCGGATCCGACTGGATAAGGAAGACATGGA
bVMD2	**bVMD2-NT-EcoRI-F**	AGCTGAATTCATGACCGTCACCTACTCGAGCCA
bVMD2	**bVMD2-NT-BamHI-R**	CGATGGATCCATCCTTTGTAGATGCTGCCTCGCC
bVMD2	**bVMD2-loop-EcoRI-F**	ATCGGAATTCTGGAACCAGTATGAGAACCT
bVMD2	**bVMD2-loop-BamHI-R**	CGATGGATCCATCCGATCCAGTCGTAGGCATACA
bVMD2	**bVMD2-CT-EcoRI-F**	AGTCGAATTCGCAGAGCAGCTCATCAACCCA
bVMD2	**bVMD2-CT-BamHI-R**	CGATGGATCCATCCCTGATGTTGAAGGTGGAGCC

Table II Primers used for site directed mutagenesis

Primer name	Primer sequence (5′-3′)
ins-A-81-hVMD2-F	ATCCCCATTTCCTTCGCTGTGCTGGGCTTCTAC
ins-A-81-hVMD2-R	GTAGAAGCCCAGCACAGCGAAGGAAATGGGGAT
hVMD2-G83L-F	ATTTCCTTCGTGCTGCTCTTCTACGTGACGCTG
hVMD2-G83L-R	CAGCGTCACGTAGAAGAGCAGCACGAAGGAAAT
hVMD2-S79C-F	CAGCTCATCCCCATTTGCTTCGTGCTGGGCTTC
hVMD2-S79C-R	GAAGCCCAGCACGAAGCAAATGGGGATGAGCTG
hVMD2-Y29H_F	TGGCGGGGCAGCATCCACAAGCTGCTATATGGC
hVMD2-Y29H-R	GCCATATAGCAGCTTGTGGATGCTGCCCCGCCA
hVMD2-L41P-F	TTCTTAATCTTCCTGCCCTGCTACTACATCATC
hVMD2-L41P-R	GATGATGTAGTAGCAGGGCAGGAAGATTAAGAA
hVMD2-I73N-F	TATTGCGACAGCTACAACCAGCTCATCCCCATT
hVMD2-I73N-R	AATGGGGATGAGCTGGTTGTAGCTGTCGCAATA
hVMD2-L140R-F	GGCAACGTGCTCATCCGGCGCAGCGTCAGCACC
hVMD2-L140R-R	GGTGCTGACGCTGCGCCGGATGAGCACGTTGCC
hVMD2-A146K-F	CGCAGCGTCAGCACCAAAGTCTACAAGCGCTTC
hVMD2-A146K-R	GAAGCGCTTGTAGACTTTGGTGCTGACGCTGCG
hVMD2-A195V-F	AACCTGTCAATGAAGGTGTGGCTTGGAGGTCGA
hVMD2-A195V-R	TCGACCTCCAAGCCACACCTTCATTGACAGGTT
hVMD2-I201T-F	TGGCTTGGAGGTCGAACCCGGGACCCTATCCTG
hVMD2-I201T-R	CAGGATAGGGTCCCGGGTTCGACCTCCAAGCCA
hVMD2-S231R-F	GCCTACGACTGGATTAGGATCCCACTGGTGTAT
hVMD2-S231R-R	ATACACCAGTGGGATCCTAATCCAGTCGTAGGC
hVMD2-S27R-F	TGCTGGCGGGGCAGGATCTACAAGCTGCTA
hVMD2-S27R-R	TAGCAGCTTGTAGATCCTGCCCCGCCAGCA
hVMD2-K30R-F	GGGCAGCATCTACAGGCTGCTATATGGCGA
hVMD2-K30R-R	TCGCCATATAGCAGCCTGTAGATGCTGCCC
hVMD2-V89A-F	CTACGTGACGCTGGCCGTGACCCGCTGGTG
hVMD2-V89A-R	CACCAGCGGGTCACGGCCAGCGTCACGTAG
hVMD2-F80L-F	ATCCCCATTTCCTTAGTGCTGGGCTTCTAC
hVMD2-F80L-R	GTAGAAGCCCAGCACTAAGGAAATGGGGAT
hVMD2-W93C-F	GTCGTGACCCGCTGCTGGAACCAGTACGAG
hVMD2-W93C-R	CTCGTACTGGTTCCAGCAGCGGGTCACGAC
hVMD2-T91I-F	GACGCTGGTCGTGATCCGCTGGTGGAACCA
hVMD2-T91I-R	TGGTTCCACCAGCGGATCACGACCAGCGTC
hVMD2-L123A-F	GACGAGCAAGGCCGGGCGCTGCGGCGCACGCTC
hVMD2-L123A-R	GAGCGTGCGCCGCAGCGCCCGGCCTTGCTCGTC
hVMD2-L207A-F	CGGGACCCTATCCTGGCCCAGAGCCTGCTGAAC
hVMD2-L207A-R	GTTCAGCAGGCTCTGGGCCAGGATAGGGTCCCG
hVMD2-L207I-F	CGGGACCCTATCCTGATCCAGAGCCTGCTGAAC
hVMD2-L207I-R	GTTCAGCAGGCTCTGGATCAGGATAGGGTCCCG
hVMD2-Q96H-F	CGCTGGTGGAACCACTACGAGAACCTGCCG
hVMD2-Q96H-R	CGGCAGGTTCTCGTAGTGGTTCCACCAGCG

Table III Primers used for in vitro transcription/translation studies

Primer name	Primer sequence (5´-3´)
pGEM1-Lep-T7	CTTAATACGACTCACTATAGGGAGACCACCATGGC GAATATGTTTGCCCTG
TMD1-Bcl1-Nde1-F	GGAATGATCAAAATCTACAAGCTGCTATATGG
TMD1-Bcl1-Nde1-R	GAATTCCCATATGGATAAATAAAGCGGATGATGT
TMD2-Bcl1-Nde1-F	GGAATGATCAAATATTGCGACAGCTACATCCA
TMD2-Bcl1-Nde1-R	GAATTCCCATATGGCACGACCAGCGTCACGTAGA
TMD3-Bcl1-F	GGAATGATCAAACGCTACGCCAACCTGGGCAA
TMD3-Nde1-R	GAATTCCCATATGGCTTGTAGACTGCGGTGCTGA
TMD4-Bcl1-Nde1-F	GGAATGATCAAAAACATGTTCTGGGTGCCCTG
TMD4-Bcl1-Nde1-R	GAATTCCCATATGGGATTCGACCTCCAAGCCACG
TMD5-Bcl1-Nde1-F	GGAATGATCAAAAGTATCCCACTGGTGTATAC
TMD5-Bcl1-Nde1-R	GAATTCCCATATGGAACTAGACAAGTCAGGAAGA
TMD6-Bcl1-Nde1-F	GGAATGATCAAACTGGACCTCGTTGTGCCCGT
TMD6-Bcl1-Nde1-R	GAATTCCCATATGGTGCCACCTTCAGCCAGCCAA
TMD1-Bcl1-F	GGAATGATCAAAATGACCATCACTTACACAAG
TMD2-Bcl1-F	GGAATGATCAAAACGGAAGAACAACAGCTGAT
TMD3-Bcl1-F	GGAATGATCAAAACCCGCTGGTGGAACCAGTA
TMD4-Bcl1-F	GGAATGATCAAACTCCAGAGCCTGCTGAACGA
TMD5-Bcl1-F	GGAATGATCAAACTACCACACAACATGTTCTG
hVMD2-Y29H-Bcl1-F	GGAATGATCAAAATCCACAAGCTGCTATATGG
hVMD2-I73N-Bcl1-F	GGAATGATCAAATATTGCGACAGCTACAACCA
hVMD2-Y85H-Nde1-R	GAATTCCCATATGGCACGACCAGCGTCACGTGGA
hVMD2-A195V-Nde1-R	GAATTCCCATATGGGATTCGACCTCCAAGCCACA
hVMD2-I201T-Nde1-R	GAATTCCCATATGGGGTTCGACCTCCAAGCCACG
hVMD2-S231R-Bcl1-F	GGAATGATCAAAAGGATCCCACTGGTGTATAC
hVMD2-T237R-Bcl1-F	GGAATGATCAAAAGTATCCCACTGGTGTATAG
hVMD2-A146K-Nde1-R	GAATTCCCATATGGCTTGTAGACTTTGGTGCTGA

Table IV Primers used for cysteine scanning mutagenesis

Primer name	Primer sequence (5´-3´)
hVMD2-C23S-F	TCCCGCCTGCTGCTGAGCTGGCGGGGCAGC
hVMD2-C23S-R	GCTGCCCCGCCAGCTCAGCAGCAGGCGGGA
hVMD2-C42S-F	TTAATCTTCCTGCTCAGCTACTACATCATC
hVMD2-C42S-R	GATGATGTAGTAGCTGAGCAGGAAGATTAA
hVMD2-C69S-F	AAACTGACTCTGTATAGCGACAGCTACATC
hVMD2-C69S-R	GATGTAGCTGTCGCTATACAGAGTCAGTTT
hVMD2-C221S-F	ACCTTGCGTACTCAGAGTGGACACCTGTAT
hVMD2-C221S-R	ATACAGGTGTCCACTCTGAGTACGCAAGGT
hVMD2-C251S-F	AGCTTCTTCCTGACTAGTCTAGTTGGGCGG
hVMD2-C251S-R	CCGCCCAACTAGACTAGTCAGGAAGAAGCT
hVMD2-E57C-F	CTGGCCCTCACGGAATGTCAACAGCTGATGTTT
hVMD2-E57C-R	AAACATCAGCTGTTGACATTCCGTGAGGGCCAG
hVMD2-L60C-F	ACGGAAGAACAACAGTGTATGTTTGAGAAACTG

hVMD2-L60C-R	CAGTTTCTCAAACATACACTGTTGTTCTTCCGT
hVMD2-Q120C-F	GAAGGCAAGGACGAGTGTGGCCGGCTGCTGCGG
hVMD2-Q120C-R	CCGCAGCAGCCGGCCACACTCGTCCTTGCCTTC
hVMD2-A160C-F	CAGCACCTGGTGCAATGTGGCTTTATGACTCCG
hVMD2-A160C-R	CGGAGTCATAAAGCCACATTGCACCAGGTGCTG
hVMD2-P165C-F	GCAGGCTTTATGACTTGTGCAGAACACAAGCAG
hVMD2-P165C-R	CTGCTTGTGTTCTGCACAAGTCATAAAGCCTGC
hVMD2-V183C-F	CACAACATGTTCTGGTGTCCCTGGGTGTGGTTT
hVMD2-V183C-R	AAACCACACCCAGGGACACCAGAACATGTTGTG
hVMD2-A189C-F	CCCTGGGTGTGGTTTTGCAACCTGTCAATGAAG
hVMD2-A189C-R	CTTCATTGACAGGTTGCAAAACCACACCCAGGG
hVMD2-M193C-F	TTTGCCAACCTGTCATGTAAGGCGTGGCTTGGA
hVMD2-M193C-R	TCCAAGCCACGCCTTACATGACAGGTTGGCAAA
hVMD2-T216C-F	CTGAACGAGATGAACTGCTTGCGTACTCAGAGT
hVMD2-T216C-R	ACTCTGAGTACGCAAGCAGTTCATCTCGTTCAG
hVMD2-T219C-F	ATGAACACCTTGCGTTGCCAGAGTGGACACCTG
hVMD2-T219C-R	CAGGTGTCCACTCTGGCAACGCAAGGTGTTCAT
hVMD2-P260C-F	CGGCAGTTTCTGAACTGTGCCAAGGCCTACCCT
hVMD2-P260C-R	AGGGTAGGCCTTGGCACAGTTCAGAAACTGCCG
hVMD2-A261C-F	CAGTTTCTGAACCCATGCAAGGCCTACCCTGGC
hVMD2-A261C-R	GCCAGGGTAGGCCTTGCATGGGTTCAGAAACTG
hVMD2-P265C-F	CCAGCCAAGGCCTACTGTGGCCATGAGCTGGAC
hVMD2-P265C-R	GTCCAGCTCATGGCCACAGTAGGCCTTGGCTGG
hVMD2-L320C-F	TTGCAGGTGTCCCTGTGTGCTGTGGATGAGATG
hVMD2-L320C-R	CATCTCATCCACAGCACACAGGGACACCTGCAA

Table V List of homologues of bestrophin used for phylogenetic analysis

No.	Name	Organism	Identifier
1	HomoVMD2	*Homo sapiens*	NP_004174
2	HomoVMD2-L1	*Homo sapiens*	AAM76995
3	HomoVMD2-L2	*Homo sapiens*	AAI01824
4	HomoVMD2-L3	*Homo sapiens*	AAR99656
5	PanVMD2	*Pan troglodytes*	XP_522029
6	PanVMD2-L2	*Pan troglodytes*	*
7	PanVMD2-L3	*Pan troglodytes*	*
8	MacacaVMD2	*Macaca fascicularis*	BAE02471
9	MacacaVMD2-L2	*Macaca fascicularis*	*
10	MacacaVMD2-L3	*Macaca fascicularis*	*
11	BosVMD2	*Bos taurus*	XP_585778
12	BosVMD2-L1	*Bos taurus*	XP_607911
13	BosVMD2-L2	*Bos taurus*	XP_882882
14	BosVMD2-L3	*Bos taurus*	XP_613863
15	CanisVMD2	*Canis familiaris*	XP_540912
16	CanisVMD2-L1	*Canis familiaris*	XP_542045
17	CanisVMD2-L2	*Canis familiaris*	XP_539638
18	CanisVMD2-L3	*Canis familiaris*	XP_538279
19	MusVMD2	*Mus musculus*	NP_036043

20	MusVMD2-L1	*Mus musculus*	AAS09923
21	MusVMD2-L3	*Mus musculus*	AAS09921
22	RattusVMD2	*Rattus norvegicus*	XP_574621
23	RattusVMD2-L1	*Rattus norvegicus*	XP_344743
24	RattusVMD2-L2	*Rattus norvegicus*	*
25	RattusVMD2-L3	*Rattus norvegicus*	XP_235161
26	DrosophilaVMD2	*Drosophila melanogaster*	NP_652603
27	DrosophilaVMD2a	*Drosophila melanogaster*	NP_730039
28	DrosophilaVMD2b	*Drosophila melanogaster*	NP_729159
29	Xen2a	*Xenopus laevis*	AAP32199
30	Xen2b	*Xenopus laevis*	AAP32200
31	XenL1	*Xenopus laevis*	AAH84229
32	DanioVMD2	*Danio rerio*	XP_689098
33	DanioVMD2-L1	*Danio rerio*	XP_695597
34	DanioVMD2-L2	*Danio rerio*	XP_692160
35	StrongylocentrotusVMD2	*Strongylocentrotus purpuratus*	XP_786003
36	Ang1	*Anopheles gambiae*	EAA00042
37	Ang2	*Anopheles gambiae*	EAL40404
38	CelegansVMD2	*Caenorhabditis elegans*	NP_493632
39	CelegansVMD2a	*Caenorhabditis elegans*	NP_493631
40	CelegansVMD2b	*Caenorhabditis elegans*	NP_498717
41	GallusVMD2	*Gallus gallus*	XP_421055

Asterisks (*) indicate sequences deduced from the unfinished genome projects at the Human Genome Browser at the University of California, Santa Cruz (USCS Genome Browser at http://genome.ucsc.edu/).

Table VI Quality assessment of the bovine RPE cDNA library

No.	Name	Identifier	Description
1	ubi-d4	XM_881516.1	Apoptosis response zinc finger protein
2	RLBP1	NM_174451.2	Retinaldehyde-binding protein 1
3	PLA2G7	NM_174578.3	Phospholipase A2, group VII
4	ATP5G2	NM_176613.2	ATP synthase, H+ transporting, mitochondrial F0 complex, subunit c
5	pGADT7	-	empty vector
6	LRAT	NM_177503.2	Lecithin retinol acyltransferase (phosphatidylcholine-retinol O-acyltransferase)
7	ND1	AF493541	NADH dehydrogenase subunit 1
8	ATP6V0A1	NM_174754.2	ATPase, H+ transporting, lysosomal V0 subunit a isoform 1
9	CST3	BC109629.1	Cystatin C (amyloid angiopathy and cerebral hemorrhage)
10	SERPINF1	NM_174140.2	Serine (or cysteine) proteinase inhibitor, clade F (alpha-2 antiplasmin, pigment epithelium derived factor), member 1
11	LOC505283	XM_581547	Similar to abhydrolase domain containing 6, transcript variant 1
12	LARGE	XM_582913.2	Similar to like-glycosyltransferase
13	Bestrophin	XM_876870.1	Bestrophin
14	LOC616771	XM_868880.1	Similar to apoptosis related protein 3 isoform a
15	RLBP1	NM_174451.2	Retinaldehyde-binding protein 1
16	ATP1B2	NM_174677.2	ATPase, Na+/K+ transporting, beta 2 polypeptide
17	pGADT7	-	empty vector
18	LOC615567	XM_867416.1	Similar to WNK lysine deficient protein kinase 4
19	PGK1	BT021601.1	Phosphoglycerate kinase 1
20	RGR	NM_175775.2	Retinal G protein coupled receptor
21	Tspan-7	XM_867453.1	Similar to Tetraspanin-7
22	ACTB	AY141970.1	Beta-actin
23	PSMB4	BC102182.1	Proteasome (prosome, macropain) subunit, beta type, 4
24	RPE1	M81193.1	Bovine retinal pigment

25	PAICS	AY344127.1	Phosphoribosylaminoimidazole carboxylase
26	IDH	AF090322	NAD(+)-isocitrate dehydrogenase subunit 1
27	LOC516021	XM_594151.2	Similar to solute carrier family 5 (sodium-dependent vitamin transporter), member 6, transcript variant 1
28	LOC513445	XM_880350.1	Hypothetical LOC513445, transcript variant 2
29	LOC512034	XM_874336.1	Similar to neurotrypsin precursor, transcript variant 5
30	ED1	AJ278907	Ectodysplasin 1, isoform A1
31	SILV	XM_582778	Similar to Melanocyte protein Pmel 17 precursor
32	MDH1	BC102133.1	Similar to Malate dehydrogenase, cytoplasmic
33	Mimecan	AF105150	Keratan sulfate proteoglycan mimecan precursor
34	PDK2	BT025357.1	Pyruvate dehydrogenase kinase, isozyme 2
35	FZD3	XM_873410.1	Frizzled homolog 3 (Drosophila), transcript, variant 2
36	pGADT7	-	empty vector
37	TTR	BC103035	Transthyretin (prealbumin, amyloidosis type I)
38	CA14	XM_879868.1	Similar to carbonic anhydrase XIV precursor, transcript variant 3
39	M6b	XM_873129.1	Similar to Neuronal membrane glycoprotein M6-b
40	RCV1	NM_174165.2	Recoverin
41	RPE65	NM_174453	retinal pigment epithelium-specific protein (65kD)
42	LYPLA1	NM_001034688.1	Lysophospholipase I
43	pGADT7	-	empty vector
44	CTSD	XM_609913	Cathepsin D (lysosomal aspartyl protease), transcript variant 1
45	MARC 4	BE682154	MARC 4, Bos taurus cDNA
46	Bestrophin	XM_876870.1	Bestrophin
47	RDH5	X82262	11-cis retinol dehydrogenase
48	LOC505283	XM_873389.1	Similar to abhydrolase domain containing 6, transcript variant 3
49	TTR	BC103035	Transthyretin (prealbumin, amyloidosis type I)
50	LOC513445	XM_880350.1	Bos taurus hypothetical transcript variant 2

Table VII List of antibodies used in this study

Name	Raised in	Directed against
pAb334	rabbit	human/bovine bestrophin
mAbRho-1D4	mouse	rhodopsin
c-Myc	mouse	c-Myc tag in pGBKT7
mAb-LAMP1	mouse	LAMP1

9. Curriculum Vitae

Personal information

Vladimir Milija Milenkovic

Date of birth	July 31st, 1970
Place of birth	Belgrade, Yugoslavia
Nationality	Serbian
Marital status	Married

Education

Elementary school 1977-1985	**Belgrade, Yugoslavia**
Gymnasium 1985-1989	**Belgrade, Yugoslavia**
University studies 1990-1998	**M.Sc. in Molecular biology and Physiology**, Faculty of Biology, University of Belgrade, Yugoslavia. **Diploma thesis:** "Geographic variability within *Bombina variegata* (Anura, Discoglossidae): allozyme analysis"
Ph.D. thesis October 2000- December 2005	**Ph.D. studies in Human molecular genetics** **Title:** "Structural and Functional Analysis of Bestrophin" **Advisor:** Prof. Dr. Bernhard Weber, Institute of Human Genetics, University of Würzburg, Germany.

Professional experience

- **January 2006 - Present:** Postdoc, Institue of Physiology, University of Regensburg, Germany
- **October 2000 - December 2005:** PhD student, Institute of Human Genetics, University of Würzburg, Germany
- **July 1999-September 2000**: Research Associate, Toxoplasmosis Research Laboratory, Institute for Medical Research, Belgrade, Yugoslavia
- **November 1997-December 1998**: Department of Evolutionary Biology, Institute for Biological Research "Sinisa Stankovic", Belgrade, Yugoslavia

10. List of publications

Thesis related publications

- Stohr H, **Milenkowic V**, Weber BH 2005.VMD2 and its role in Best's disease and other retinopathies. *Ophthalmologe.* 102:116-21.

Thesis related publications – in preparation

- **Milenkovic V**, Rivera A, Horling F, von Heijne G, Casey JR, Weber BHF. Insertion and topology of normal and mutant bestrophin in the endoplasmic reticulum membrane

Further publications

- Djurkovic-Djakovic O, **Milenkovic V**, Nikolic A, Bobic B, Grujic J 2002. Efficacy of atovaquone combined with clindamycin against murine infection with a cystogenic (Me49) strain of Toxoplasma gondii. *J Antimicrob Chemother*. 50:981-7.

- Djurkovic-Djakovic O, **Milenkovic V**: 2001. Murine model of drug-induced reactivation of Toxoplasma gondii. *Acta Protozoologica.* 40:99-106

- Djurkovic-Djakovic O, **Milenkovic V**: 2000. Survival of Toxoplasma gondii tissue cysts at low temperatures. *Acta Veterinaria.* 50:375-380

List of poster presentations

- **Milenkovic V**, Rivera A, von Heijne G, Casey JR, Weber BHF. 2005. Insertion and topology of normal and mutant bestrophin in the endoplasmic reticulum membrane. The Association for Research in Vision and Ophthalmology (ARVO) Annual Meeting, Fort Lauderdale, USA

- **Milenkovic V**, F Krämer, Weber BHF. Structure-function analysis of the bestrophin. 2004. European Society of Human Genetics (ESHG) Conference, Munich, Germany

- **Milenkovic V**, Krämer F, Gehrig A and Weber BHF. 2002. The search of proteins interacting with bestrophin. 13. Jahrestagung der Deutschen und Österreichhischen Gesellschaft für Humangenetik, Leipzig, Germany

- Krämer F, **Milenkovic V**, Stöhr H and Weber BHF. 2001. Towards understanding the molecular pathology of vitelliform macular dystrophy (Best disease). 10th International Congress of Human Genetics, Vienna, Austria